The role of AMPK and CREB-1 in the regulation of mitochondrial biogenesis during muscle differentiation

Inaugural-Dissertation
zur
Erlangung des Doktorgrades
der Mathematisch-Naturwissenschaftlichen Fakultät
der Universität zu Köln

vorgelegt von
András Frankó
aus Budapest

Köln 2007

Berichterstatter: Prof. Dr. Rudolf J. Wiesner
Prof. Dr. Jens C. Brüning

Tag der mündlichen Prüfung: 11.07.2007

Nagyszüleimnek/To my grandparents

Contents

FIGURES AND TABLES ..... **IV**

ABBREVIATIONS ..... **V**

1 SUMMARY **1**

2 INTRODUCTION **4**

2.1 Mitochondria **4**

2.2 Biogenesis of mitochondria **5**

2.3 Rationale for studying AMPK and CREB-1 ..... **8**

2.4 The role of AMPK in mitochondrial biogenesis **10**

2.5 CREB-1 protein: a point of convergence **12**

2.6 Aim of the study **17**

3 MATERIALS AND METHODS **19**

3.1 Materials **19**
3.1.1 Chemicals 19
3.1.2 Equipment 19
3.1.3 Organisms 20
3.1.4 Materials for cell culture 20
3.1.5 Antibiotics 20
3.1.6 Materials for standard molecular biology 21
3.1.6.1 Oligonucleotides 21
3.1.6.2 Nucleic acids 21
3.1.6.3 Enzymes 21
3.1.6.4 Kits 22
3.1.6.5 Radiochemicals 22
3.1.6.6 Markers, dyes 22
3.1.6.7 Antibodies 22

3.2 Methods **24**
3.2.1 Standard molecular biology 24
3.2.1.1 E. coli cultivation 24
3.2.1.2 Preparation of transformation-competent *E. coli* 24
3.2.1.3 Plasmid DNA preparation 25
3.2.1.4 Transformation 25
3.2.1.5 Glycerol stock 25
3.2.1.6 Nucleic acid gel electrophoresis 25
3.2.2 Principle of Tet-Off system 25
3.2.3 Cloning of rat AMPKα1-CA into pTRE2-Hyg vector 26
3.2.3.1 Cultivation 27

3.2.3.2 Freezing and thawing of cells 27
3.2.3.3 Transfection 27
3.2.3.3.1 Stable transfection 27
3.2.3.3.2 Transient transfection 28
3.2.4 Nucleic acids 29
3.2.4.1 Total RNA preparation from C2F3 cells 29
3.2.4.2 PolyA$^+$ mRNA preparation from C2F3 cells 30
3.2.4.3 Random primed labeling of DNA 30
3.2.4.4 Northern Blot 30
3.2.5 Polymerase chain reaction (PCR) 31
3.2.5.1 Reverse transcription 31
3.2.5.2 PCR 32
3.2.6 Protein 32
3.2.6.1 Preparation of whole cell extracts 32
3.2.6.2 Nuclear and cytoplasmatic protein preparation 33
3.2.6.3 Protein gel electrophoresis 34
3.2.6.4 Western Blot 34
3.2.6.5 Immunoprecipitation 35
3.2.6.6 Kinase assay 36
3.2.6.7 Phosphatase treatment of nitrocellulose membrane 37
3.2.7 Reporter gene assay 37
3.2.8 Microscopy 38
3.2.8.1 Indirect immunofluorescence 38
3.2.8.2 Intracellular calcium measurement 39
3.2.9 Statistical analysis 40
3.2.10 Software tools 40

4 RESULTS 41

***4.1 In vitro* model for muscle differentiation and mitochondrial biogenesis 41**
4.1.1 Expression of differentiation markers during myogenesis 41
4.1.2 Intracellular calcium levels in myoblasts and myotubes 43
4.1.3 α-actinin4 localization during differentiation 47

4.2 The role of AMPK in cytochrome c promoter regulation 49
4.2.1 Cloning of AMPKα1-CA into pTRE2Hyg vector 49
4.2.2 Generation of stable cell lines expressing tTA transactivator 49
4.2.3 Transfection, isolation and selection of AMPKα1-CA clones 50
4.2.4 Analysis of AMPKα1-CA clones 51
4.2.5 Immunoprecipitation of AMPKα1-CA 53
4.2.6 AMPKα1 and AMPKα1-CA kinase assay 54
4.2.7 Analysis of cytochrome *c* promoter activity in AMPKα1-CA expressing cells 56

4.3 CREB-1 is involved in cytochrome *c* promoter regulation 58
4.3.1 CREB-1 and ATF-1 during myogenesis 58
4.3.2 CREB-1 isoforms in C2F3 cells 60
4.3.3 Knock-down of CREB-1 by siRNA technology 63
4.3.4 The effect of CREB-1 constructs on the cytochrome *c* promoter 65
4.3.5 Modulating the activity of PKA and PP2 phosphatases 66

5 DISCUSSION 70

5.1 Comparison of undifferentiated and differentiated muscle cells 70
5.1.1 Enhanced myogenic marker gene expression in differentiating muscle cells 70
5.1.2 Altered intracellular calcium levels during differentiation 70
5.1.3 α-actinin4 translocates to the nuclei of myotubes 72

5.2 Overexpression of AMPKα1-CA in C2C12 cells 73

5.3 CREB-1 regulates the cytochrome *c* promoter 75
5.3.1 CREB-1 isoforms are present in different tissues 76
5.3.2 CREB-1 activates the cytochrome *c* promoter 79
5.3.3 CREB-1 regulating upstream signals 81

6 APPENDIX 85

7 REFERENCES 88

8 ACKNOWLEDGEMENTS 99

Figures and Tables

Figure 1. A scheme of mitochondrial biogenesis in muscle, fusion/fission and apoptosis [18] 6
Figure 2. Schematic structure and expression of the gene of cytochrome *c* 9
Figure 3. The structure of CREB-1 isoforms [48] 13
Figure 4. The CREB-1 signal transduction pathway 14
Figure 5. The principle of Tet-Off system 26
Figure 6. C2F3 cells during differentiation 41
Figure 7. MHC expression of differentiated C2C12 myotubes 42
Figure 8. Myogenin expression in differentiating C2F3 cells 43
Figure 9. Calcium concentration in C2C12 cells during the differentiation process 44
Figure 10. Calcium concentration of C2C12 cells during the loading procedure 45
Figure 11. Calcium concentration in confluent C2C12 cells 46
Figure 12. Expression of α-actinin4 in nuclear and cytoplasmic fractions of C2F3 cells 48
Figure 13. TRE promoter activity in TRE transactivator (tTA) expressing cells 50
Figure 14. AMPKα1-CA clones using anti-c-myc antibody 51
Figure 15. Western blot of AMPKα1-CA clones using anti-AMPKα antibody (showed partially) 52
Figure 16. Immunoprecipitation of AMPKα1-CA by AMPKα or c-myc antibodies 54
Figure 17. Endogenous AMPKα1 and AMPKα1-CA kinase assays 55
Figure 18. AMPKα1-CA protein expression level in AMPKα1-CA clones 56
Figure 19. Cytochrome *c* promoter activity in *(A)* AMPKα1-CA stablely transfected cell lines or *(B)* transiently transfected cells 57
Figure 20. Protein expression of CREB-1 family members during muscle differentiation 59
Figure 21. Phosphatase treatment of CREB-1 immunoreactive bands 60
Figure 22. Identification of CREB-1α and CREB-1Δ protein isoforms by Western blot 61
Figure 23. Determining the log phase for semiquantitative RT-PCR 61
Figure 24. Distribution of CREB-1α and CREB-1Δ mRNA isoforms during myogenesis 62
Figure 25. CREB-1 gene expression detected by Northern hybridization 63
Figure 26. siRNA against CREB-1 decreases CREB-1 protein 64
Figure 27. Cytochrome *c* promoter activity upon siRNA cotransfections 65
Figure 28. Cytochrome *c* and α-inhibin promoter activities modulated by CREB-1 66
Figure 29. PKA and PP2 phosphatases influences the phosphorylation status of CREB-1 67
Figure 30. Quantitation of phospho133-CREB-1 intensities upon treatment with phosphatase and PKA inhibitor or PKA activator 68
Figure 31. Cytochrome *c* promoter activity in the presence of phosphatase and PKA inhibitors or PKA activator 69
Figure 32. TRE promoter activity in muscle cell lines 74
Figure 33. A model for a transcriptosomal complex on mitochondrial genes 76
Figure 34. An interaction model of CREB-1 and cytochrome *c* promoter 80
Appendix Figure 1. Cloning procedures of AMPKα1-CA into pTRE2Hyg vector 85
Appendix Figure 2. Western blot analysis of AMPKα1-CA clones 86

Table 1. Examples of AMPK substrates and their biological effects [34] 11
Table 2. Summary of the AMPKα1-CA clones[1] 53

Abbreviations

AICAR	5-aminoimidazol-4-carboxamid-ribonucleosid
AMP	adenosine 5’-monophosphate
AMPK	AMP activated kinase
APS	ammonium persulfate
ATF	activating transcription factor
ATP	adenosine 5’-triphosphate
BSA	bovine serum albumine
bp	base pair
CA	constitutively active
cDNA	complementary DNA
CMV	Cytomegalovirus
COX	cytochrome oxidase, complex IV
cpm	counts per minute
CREB	cyclic AMP-response element binding protein
dCTP	deoxycytidine triphosphate
DMEM	Dulbecco's Modified Eagle Medium
DMSO	dimethyl sulfoxide
DNA	deoxyribonucleic acid
dNTP	deoxyribonucleotide triphosphate
DTT	dithiothreitol
Dox	doxycycline
E. coli	*Eschericia coli*
ECL	enhanced chemiluminescence
EDTA	ethylenediaminetetraacetic acid
EGTA	glycol-bis(2-aminoethylether)-N,N,N',N'-tetraacetic acid
EMSA	electrophoretic mobility shift assay
FCS	fetal calf serum
HB	hypotonic buffer
HBS	Hepes-buffered saline
HEPES	4-(2-hydroxyethyl)-1-piperazineethanesulfonic acid
HRP	Horseradish peroxidase
Hyg	Hygromycin
IgG	immunoglobulin G
IP	immunoprecipitation

kb	kilobase
kDa	kilodalton (1,000 Dalton)
LB	Luria broth or Luria-Bertani broth
mM	millimolar (mmol/l)
mRNA	messenger RNA
MHC	myosin heavy chain
MOPS	3-(N-morpholino) propanesulfonic acid
OD	optical density
PAGE	polyacrylamide gel electrophoresis
PBS	phosphate buffer saline
PCR	polymerase chain reaction
pH	negative logarithm of the proton concentration
PKA	protein kinase A
PMSF	phenylmethylsulfonyl fluoride
PP2	protein phosphatase 2
PSS	physiological salt solution
RLU	relative light units
RNA	ribonucleic acid
rpm	rounds per minute
SAMS peptide	substrate for AMPK
SDS	sodium dodecylsulfate
TAE	Tris (40 mM), acetate (20 mM), EDTA (1mM)
Taq	*Thermus aquaticus*
Tet	tetracycline
TRE	Tet-responsive element
Tris	Tris(hydroxymethyl) aminomethane
UV	ultraviolet
V	Volt
WB	Western blot

1 Summary

The aim of the study was to identify main regulators of mitochondrial biogenesis in a skeletal muscle differentiation model. To investigate candidate factors we used the cytochrome *c* promoter as a representative promoter since cytochrome *c* levels correlate well with respiratory chain complexes. We chose the AMP activated kinase (AMPK) and cyclic AMP-response element binding protein 1 (CREB-1) as promising candidates, which could control the process of mitochondrial proliferation.

To analyze whether AMPK regulates the cytochrome *c* promoter, a cell line stably expressing a constitutively active AMPKα1-CA was generated. Indeed, AMPKα1-CA kinase activity was found to be increased in these clones. However, AMPKα1-CA and dominant negative AMPKα constructs did not change cytochrome *c* promoter activity in reporter gene assays, total AMPK activity was unchanged during muscle differentiation suggesting that it is not involved in the regulation of mitochondrial biogenesis in this model. In contrast, the constitutively active CREB construct, C2/CREB, elevated cytochrome *c* promoter activity. This increased promoter activity was diminished in the presence of a dominant negative CREB (A-CREB) construct showing that CREB-1 directly activates the cytochrome *c* promoter. Western blot analysis revealed two different CREB-1 isoforms: CREB-1α and CREB-1Δ. Myoblasts contain predominantly CREB-1Δ, while myotubes have preferably the CREB-1α isoform. The phosphorylation state of these isoforms changed in parallel with their protein levels suggesting a functional isoform switch during differentiation. Two appropriate, alternatively spliced isoforms of CREB-1 mRNA were found but their ratio did not change during differentiation. This suggests that posttranslational modifications and/or recruitment of the CREB-1 isoforms by other factors of the transcriptional complex play a dominant role in determining their cellular levels. To elucidate, which upstream factors regulate the activity of CREB-1, kinase and phosphatase inhibitors were used. A PKA activator and two phosphatase inhibitors increased the phosphorylation of CREB-1 at Ser-133, which is thought to be necessary for its activation. Furthermore, Cyclosporin A not only enhanced phosphorylation of CREB-1, but also the cytochrome *c* promoter activity. Therefore, it is likely that PP2B (calcineurin) regulates the phosphorylation of CREB-1 during muscle differentiation. Intracellular resting calcium levels were found to be smaller in myotubes compared to myoblasts, thus changes in steady-state calcium levels seem not to be a key regulator of mitochondrial biogenesis in muscle cells.

In summary, these data indicate that phosphorylation and an isoform switch of CREB-1 could play a major role in the regulation of cytochrome *c* promoter and thus mitochondrial biogenesis during muscle differentiation. ***

Das Ziel der vorliegenden Arbeit war es, wichtige Regulatoren der mitochondrialen Biogenese in einem Skelettmuskel-Differenzierungsmodell zu identifizieren. Zur Untersuchung relevanter Faktoren wurde repräsentativ der Cytochrom c-Promotor verwendet, da der Cytochrom c-Gehalt mit dem Gehalt der Atmungskettenkomplexe korreliert. Das Enzym AMPK (*AMP activated kinase*) und CREB-1 (*cyclic AMP-response element binding protein 1*) wurden als vielversprechende Kandidaten bei der Regulation der mitochondrialen Proliferation ausgewählt.

Zur Untersuchung des regulatorischen Einflusses von AMPK auf den Cytochrom c-Promotor wurde eine Zelllinie generiert, die stabil eine konstitutiv aktive AMPKα1-CA exprimiert. Tatsächlich zeigten diese Klone eine erhöhte konstitutiv aktive Kinase-Aktivität. In Reporter-Genassays wurde dennoch keine durch AMPKα1-CA oder dominant negativen AMPKα-Konstrukts veränderte Cytochrom c-Promotor-Aktivität beobachtet, die gesamte Kinase-Aktivität ist während der Differenzierung unverändert geblieben, was darauf hindeutet, dass AMPKα1 nicht an der Regulation der mitochondrialen Biogenese in diesem Modell beteiligt ist. Im Gegensatz dazu erhöhte der konstitutiv aktive CREB-Konstrukt, C2/CREB, die Cytochrom c-Promotor-Aktivität. Diese erhöhte Promotor-Aktivität wurde in Gegenwart eines dominant negativen CREB-Konstrukts (A-CREB) vermindert und weist damit auf eine direkte Aktivierung des Cytochrom c Promotors durch CREB-1 hin. Zwei unterschiedliche CREB-Isoformen konnten mittels Western Blot-Analysen gefunden werden: CREB-1α und CREB-1Δ. Myoblasten enthalten vorrangig CREB-1Δ, während Myotuben hauptsächlich die CREB-1α Isoform exprimieren. Der Phosphorylierungsstatus der beiden Isoformen veränderte sich entsprechend ihrer Proteinexpression. Dies deutet auf einen funktionellen Wechsel der Isoformen im Zuge der Differenzierung hin. Zwei entsprechende, alternativ gespleißte Isoformen der CREB mRNA werden nachgewiesen, deren Verhältnis sich jedoch während des Differenzierungsprozesses zueinander nicht änderte. Dies lässt vermuten, dass posttranslationale Modifikationen und/oder die Rekrutierung der CREB-1 Isoformen durch andere Faktoren des Transkriptionsapparates eine große Rolle bei der Regulation ihres zellulären Gehalts einnehmen. Um aufzuklären, welche vorgeschalteten Faktoren die Aktivität von CREB-1 aktivieren, wurden Kinase- und Phosphatase-Inhibitoren eingesetzt. Die Phosphorylierung von CREB-1 an der Position Ser-133, die für dessen Aktivierung wichtig ist, wurde durch einen PKA-Aktivator und zwei Phosphatase-Inhibitoren erhöht. Des Weiteren steigerte Cyclosporin A nicht nur die Phosphorylierung von CREB-1, sondern auch die Cytochrom c Promotor-Aktivität. Daher ist es wahrscheinlich, dass PP2B (Calcineurin) die Phosphorylierung von CREB-1 während der Muskeldifferenzierung reguliert. In Vergleich zu Myoblasten waren aber die basalen intrazellulären Kalziumlevels bei Myotuben geringer. Demnach scheinen Veränderungen des

basalen Kalziumlevels in Muskelzellen keine Schlüsselfunktion während der mitochondrialen Biogenese zu haben.

Zusammengefasst weisen diese Daten darauf hin, dass die Phosphorylierung und der Wechsel zwischen den CREB-1 Isoformen eine wichtige Rolle bei der Regulierung des Cytochrom c-Promotors und somit der mitochondrialen Biogenese bei der Muskeldifferenzierung einnehmen können.

2 Introduction

The aim of the present work was to understand the regulation of mitochondrial biogenesis, which we define as an increase in mitochondrial number and/or mass [1]. The main questions in this field are i) how a cell can sense the need for enhanced mitochondrial mass and ii) what are the regulatory pathways involved in the resulting proliferation of mitochondria. To address this issue we chose a cell culture model: satellite mouse muscle myoblasts were differentiated to multinucleated myotubes, because the amount of mitochondria increases during this process [2]. Based on former results of our laboratory [3] we analyzed the AMP-activated kinase (AMPK) and the cyclic AMP response element binding protein 1 (CREB-1), since it was suggested that these proteins participate in the process of mitochondrial proliferation [4,5].

2.1 Mitochondria

Mitochondria are thought to have evolved from a symbiotic relationship between aerobic bacteria (α-proteobacteria) and primordial anaerobic eukaryotic cells [6,7]. As the site of oxidative phosphorylation, these double-membrane organelles provide a highly efficient route for eukaryotic cells to generate ATP from energy-rich molecules. Electrons from oxidized substrates are transferred to oxygen, via a series of redox reactions, to generate water. In this process, protons are pumped from the matrix across the mitochondrial inner membrane by respiratory complexes I, III, and IV. When protons return to the mitochondrial matrix down their electrochemical gradient, ATP is synthesized via complex V (ATP synthase) [8]. Although the vast majority of the (1000 to 1500) mitochondrial proteins are encoded by the nuclear genome and imported into the mitochondria, mitochondria also maintain a genome that is essential for their respiratory function [9]. The 16 kilobase circular mitochondrial DNA (mtDNA) genome contains 37 genes. Thirteen of these genes encode protein subunits of respiratory complexes I, III, IV, and V; only complex II is solely composed of proteins encoded by nuclear genes. mtDNA also encodes 22 mitochondrial tRNAs and 2 rRNAs that are essential for translation of mitochondrial transcripts [8]. When mitochondria were discovered, ATP synthesis and Krebs (citric acid) cycle were claimed to be their most important function. But besides this, mitochondria form the compartment for other essential metabolic pathways such as β-oxidation of fatty acids, urea cycle and biosynthesis of pyrimidines, amino acids, phospholipids, Fe-S clusters and heme [10]. In the beginning, mitochondria were thought to have a rigid morphology, however in the past 10 years it became clear that they form a functional reticulum whose steady-state morphology is regulated by dynamic fission, fusion and motility events [11]. The

mitochondrial fusion and fission processes are controlled by a growing set of 'mitochondria-shaping' proteins, which also appear to influence mitochondrial pathways of cell death, but the underlying mechanisms are largely unknown [12]. As mitochondria play a central role in the "usual daily" physiology of the cell, an increasing number of degenerative diseases are recognized to be produced by a failure of mitochondrial functions mentioned above [10].

In contrast to their vital function, several organisms are known to lack classical mitochondria. These include Microsporidia (e.g. *Encephalitozoon cuniculi*), Apicomplexa (e.g. *Cryptosporidium parvum*), Diplomonads (e.g. *Giardia intestinalis*), Entamoeba (e.g. *Entamoeba histolytica*) and Trichomonads (e.g. *Trichomonas vaginalis*). However, these organisms have two alternative forms of mitochondria-like organelles to carry out essential functions: the so-called hydrogenosomes in Trichomonads, fungi and anaerobic ciliates and mitosomes in Microsporidia, Diplomonads, Apicomplexa and Entamoeba [6,13].

2.2 Biogenesis of mitochondria

The most energy demanding organs contain the highest amount of mitochondria including brain, heart, skeletal muscle, brown adipose tissue (BAT) and liver. The amount of mitochondria changes during tissue differentiation and adaptation processes. These processes of controlled mitochondrial biogenesis are well studied in skeletal muscle and BAT. BAT in contrast to white adipose tissue (WAT) contains high numbers of mitochondria in order to perform non-shivering thermogenesis, which are uncoupled due to the presence of the brown-fat-specific uncoupling protein-1 (UCP-1). When brown adipocytes differentiate during late fetal development, they accumulate lipid in smaller, several vacuoles and acquire a high content of mitochondria compared to WAT. This mitochondrial differentiation takes place in the absence of an environmental thermogenic stress, and can be modeled with precursor cells differentiating into brown adipocytes in cell culture [14]. During cold exposure of small rodent a massive mitochondrial proliferation occurs in brown adipose tissue [15]. The mitochondrial mass in skeletal muscle increases during embryonic muscle differentiation, following the repair of adult muscle after injury and during endurance training [16,17]. Since the latter processes have been extensively investigated for decades we decided to further analyze the question how mitochondrial biogenesis is regulated in muscle cells.

Mitochondrial proliferation is a unique, precisely controlled mechanism including the expression of nuclear encoded mitochondrial genes (NEM or NUGEM) and mtDNA encoded mitochondrial genes (MEM) (Figure 1). Calcium plays a crucial role in this process especially in muscle. When action potentials are evoked at the neuromuscular junction, muscle action potentials open the calcium channels of sarcoplasmatic reticulum (SR) and calcium ions bind to

troponin, thus actin filaments can interact with myosin. Besides activating contraction, calcium can also directly trigger the calcium/calmodulin dependent protein kinases (CaMKs) and probably indirectly induces AMPK, which are postulated to the activate the peroxisome proliferator-activated receptor (PPAR) γ coactivator 1α (PGC-1α), believed to be a master coactivator of MEM genes (Figure 1 and [18]).

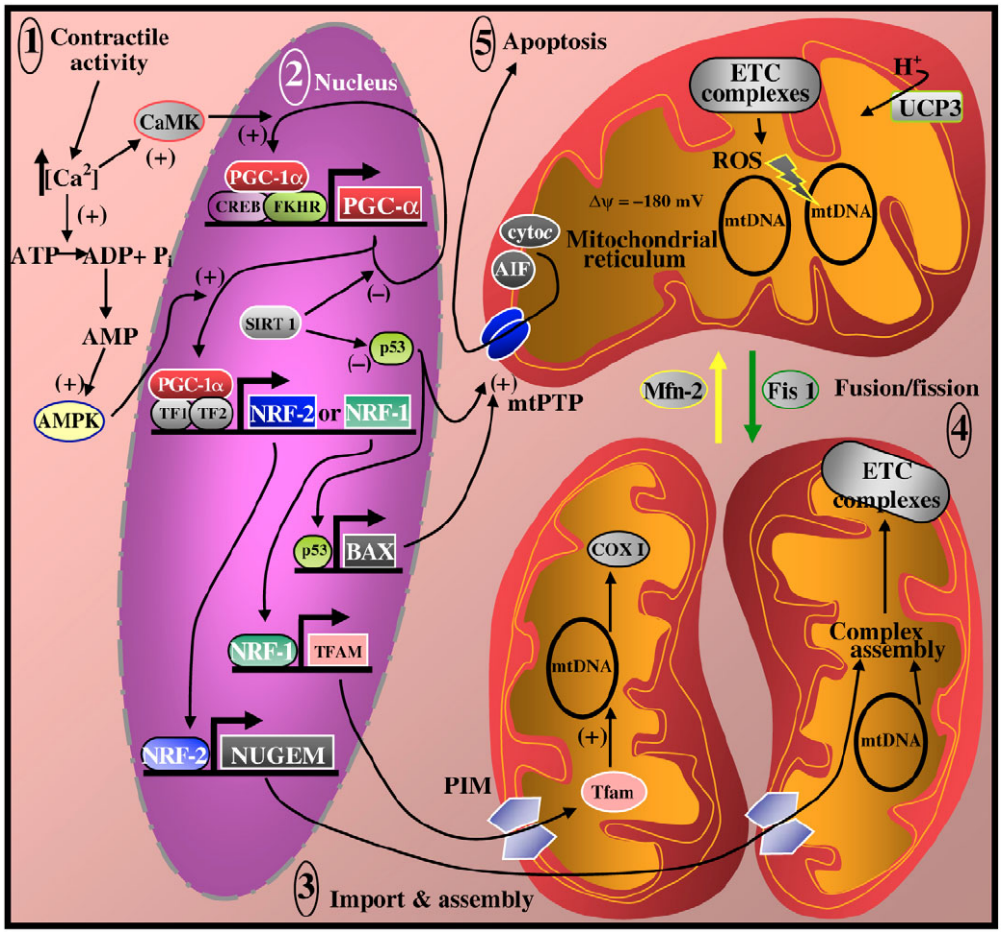

Figure 1. A scheme of mitochondrial biogenesis in muscle, fusion/fission and apoptosis [18]

For details see text below.

Changes of the cytoplasmatic calcium concentration were shown to be very important for the expression of genes regulating the muscle differentiation program. The upregulation of the structural muscle protein α-actin was completely absent in the presence of L-type calcium channel inhibitors in cultivated muscle cells [19]. Intermittent exposure to the calcium ionophore ionomycin, or to the SR calcium channel activator caffein elevated the protein expression of δ-aminolevulinic acid synthase (ALAS), a mitochondrial key enzyme of heme synthesis and COXI, the mitochondrial encoded subunit I of cytochrome oxidase complex IV. EGTA, suppressing the effect of ionomycin or dantrolene, which blocks the calcium channels of SR, hence counteracting with caffeine, strongly prevented the calcium induced expression of mitochondrial enzymes [20]. In addition, caffeine was shown to activate the expression of PGC-

1α and mitochondrial transcription factor A (TFAM), which is crucial for mtDNA replication and transcription as well as the DNA binding activity of nuclear respiratory factor-1 and 2 (NRF-1, NRF-2), and these effects were completely inhibited with dantrolene. The elevated intracellular calcium concentration was thought to activate CaMKs, which could also be involved in the regulation of mitochondrial proliferation, since the CaMK inhibitor KN93 diminished the caffeine induced expression of mitochondrial enzymes [21]. Cytochrome *c* mRNA levels as well as the cytochrome *c* promoter activity was also shown to be regulated by calcium mediated signals, since both were elevated with the calcium ionophore A23187 treatment, while EGTA preincubation diminished these effects. In these studies PKC but not CaMKII, IV or PKA was identified as the calcium activated kinase [22]. These results suggest that calcium besides regulating myogenesis is necessary for the execution of mitochondrial biogenesis. On the other hand, Gros and colleagues showed that calcium is responsible for MHC (myosin heavy chain) II to MHC I fiber transition but not for altered mitochondrial enzyme activities upon fast to slow twitch fiber type transformation [23,24]. The authors observed a moderately elevated resting, intracellular calcium concentration in primary muscle cells upon electrostimulation [24].

Upon muscle contraction ATP:ADP ratio may decrease, which could increase AMP levels via the myokinase reaction: 2 ADP↔AMP+ATP. AMP-activated protein kinase has been described as an AMP-sensing signal transducer. A rise of AMP levels leads to allosteric activation of AMPK and it phosphorylates its substrates (e.g. acetyl-CoA carboxylase, HMG-CoA reductase) but may also trigger the function of the transcriptional co-activator PGC-1α (Figure 1). PGC-1α also autoregulates its own gene along with the expression of NRF-1 and NRF-2. These are factors activating the transcription of many nuclear genes encoding mitochondrial proteins. NRF-1 also induces the expression of TFAM that, along with other nuclear-encoded mitochondrial proteins, is imported into mitochondria by the protein import machinery (PIM). TFAM regulates the expression of the 13 mtDNA encoded genes of the respiratory chain complexes [25]. Mitochondrial proteins encoded by the nucleus as well as by the mtDNA are assembled to form the multi-subunit enzyme complexes performing oxygen consumption and ATP synthesis. CREB-1 is proposed to activate PGC-1α, as Figure 1 shows, CREB-1 with PGC-1α is involved in the transcription of the *PGC-1α* gene.

The figure also shows that the mitochondrial phenotype is altered through fusion and fission events. Mitofusion-2 (Mfn-2) influences the fusion of discrete populations of mitochondria into a larger mitochondrial reticulum, whereas Fis 1 is a protein involved in organelle fission. A high mitochondrial membrane potential ($\Delta\psi$) is also associated with the production of reactive oxygen species (ROS) from the electron transport chain complexes

(ETCs). Elevated ROS levels can trigger the opening of the mitochondrial permeability transition pore (mtPTP) and the release of pro-apoptotic factors such as cytochrome *c* and apoptosis-inducing factor (AIF). Liberation of these proteins is the primary step in the mitochondrially mediated apoptotic program [18].

2.3 Rationale for studying AMPK and CREB-1

Former experiments in our laboratory suggested a role of AMPK and CREB-1 proteins regulating the proliferation of mitochondria. In these studies, luciferase reporter gene assays were performed in the murine muscle cell line C2F3. The promoters of three different nuclear encoded mitochondrial genes (cytochrome c, TFAM, COXIV) were tested to identify sequence elements and proteins influencing their expression. The activities of all three promoters were highly increased upon differentiation comparing myoblasts with differentiated myotubes, respectively [3]. Site directed mutagenesis of the upstream CREB-1 binding site abolished the activation of the cytochrome *c* promoter during myogenesis [3]. Cytochrome *c* is used as a marker of mitochondrial density [26,27] because the amount of cytochrome *c* protein correlates well with the mitochondrial respiratory chain protein levels [28]. The rat somatic cytochrome *c* promoter has several binding sites for transcription factors e.g. NRF-1, CREB-1/ATF-1 and Sp1 (Figure 2). Sp1 sites were found to responsible for the cytochrome c promoter activity in mammalian cells transfected with cytochrome *c* reporter constructs [29]. In addition, both CRE sequences contributed to the cytochrome *c* promoter activation upon increased cAMP level [30]. Furthermore, serum induction also enhanced cytochrome *c* promoter activity, and mutating the CREB-1 or NRF-1 binding *cis*-elements disturbed upregulation of promoter activity, so phosphorylated CREB-1 and NRF-1 are suggested to be involved in this process [5].

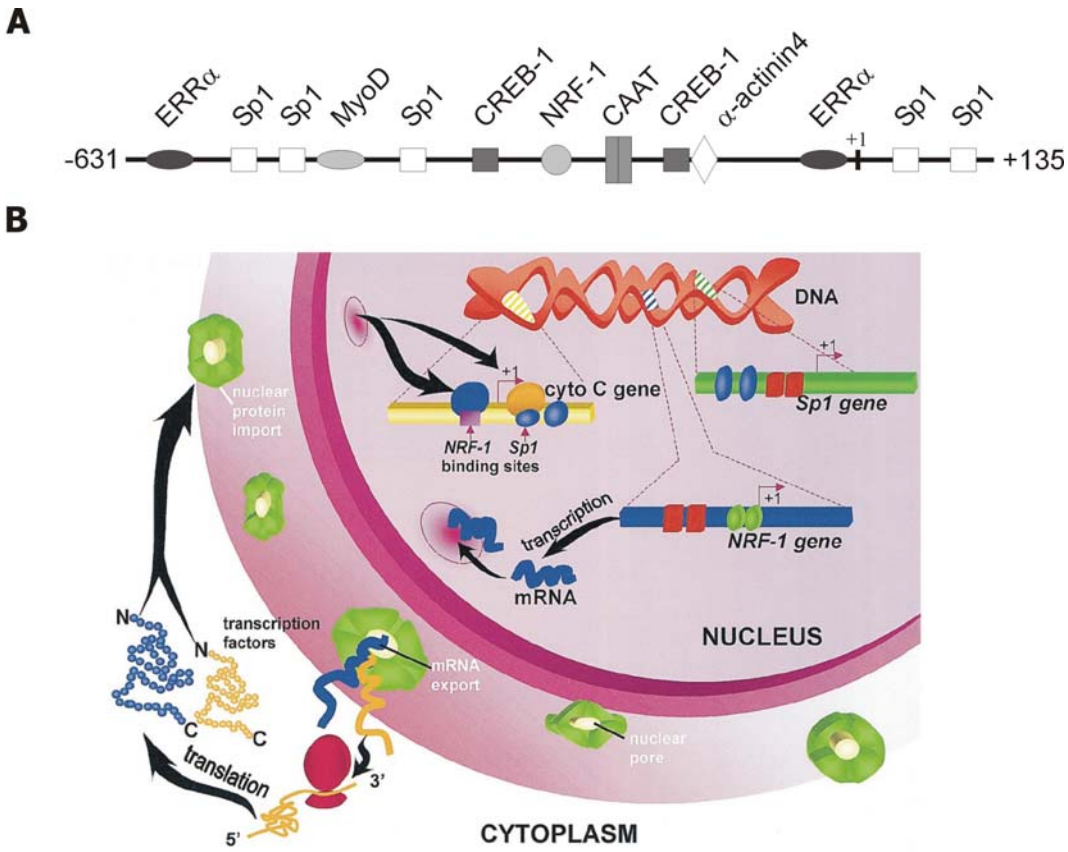

Figure 2. Schematic structure and expression of the gene of cytochrome *c*

A The promoter structure of rat somatic cytochrome *c* is shown with the transcription factor binding sites thought to be important for its regulation in muscle. The *cis*-acting element analysis was performed by the Genomatix MatInspector tool [31] and those, which had matrix similarity higher than 0.8 were chosen. One should note that the functionality of every single element was not verified. ***B*** A simplified scheme of expression of cytochrome *c* during contractile activity in muscle cells [16].

Based on our own [3] and these results [5,30], cytochrome *c* was chosen as a model promoter to search for candidate transcription factors and their regulators, which could play a role in mitochondrial biogenesis during muscle differentiation.

Gopalakrishnan and Herzig *et al.* investigated the *in vitro* promoter activation upon cAMP as well as serum induction in COS and fibroblast cells, respectively [5,30]. In contrast, we have chosen a more physiological model of muscle differentiation, which we believe may be closer to the *in vivo* situation of mitochondrial biogenesis. The cytochrome *c* promoter activity was increased upon treatment with AICAR, a well-known activator of AMPK in myoblasts as well as in myotubes [3]. In addition, comparing the metabolite profiles between myoblasts, confluent cells and myotubes, it was found that the AMP concentration increased strikingly during the differentiation program [3]. These results suggested an important role of AMPK in this myogenic process and thus we further studied the role of AMPK. The cytochrome *c* promoter was shown to be strongly stimulated during myogenesis, since myotubes showed highly elevated

cytochrome *c* promoter activity. In order to find the *cis*-elements controlling the promoter during muscle differentiation, several deleted cytochrome *c* promoter constructs were analyzed in promoter assays. A single point mutation in the downstream CRE element abolished the basal promoter activity in myoblasts, but more importantly the upregulation during differentiation as well [3]. Nuclear proteins prepared from myoblasts and myotubes bound to the sequence of the downstream CRE element and anti-CREB as well as anti-P-CREB antibodies bound to this complex performed a supershift in myotubes [32]. As these results suggested that CREB-1 directly activates the cytochrome *c* promoter, we further clarified its role in mitochondrial biogenesis.

2.4 The role of AMPK in mitochondrial biogenesis

The evolutionary conserved AMP activated kinase belongs to the Ser/Thr protein kinase family. It forms a heterotrimeric complex consisting of the α (63 kDa), β (38 kDa) and γ (35 kDa) subunits [33]. In mammals, each subunit is encoded by multiple genes (α1, α2, β1, β2, γ1, γ2, γ3) with additional splice variants. AMP activates the kinase activity by three different mechanisms; it allosterically activates AMPK, triggers the upstream kinase (LKB1) to phosphorylate the important Thr-172 site in the α subunit of AMPK, and inhibits the dephosphorylation of this site by blocking a protein phosphatase. All effects of AMP are antagonized by high amounts of ATP emphasizing the role of AMPK as an energy sensor. Briefly, the major function of the kinase is to activate the catabolic, energy producing pathways, such as fatty acid oxidation, glycolysis, etc and inhibit anabolic, ATP consuming pathways, such as fatty acid synthesis or gluconeogenesis. In addition to its acute metabolic role, it is also believed to participate in the regulation of proteins involved in mitochondrial biogenesis, e.g. by upregulating the gene for NRF-1 and PGC-1α (Table 1) [34].

Table 1. Examples of AMPK substrates and their biological effects [34]

Organ/cell type		Immediate outcome	Biologic end result
Glucose homeostasis — Primary targets			
Muscle	glycogen synthase	enzyme activity ↓	glycogen synthesis ↓
Heart	6-phosphofructo-2-kinase	enzyme activity ↑	glycolysis ↑
C2C12 cells	insulin receptor substrate-1	PI-3-kinase binding ↑	insulin sensitivity ↑?
Liver	transcription factor ChREBP	DNA binding ↓	pyruvate kinase expression ↓
Lipid metabolism — Primary targets			
Liver	acetyl-CoA carboxylase-1/α	enzyme activity ↓	fatty acid synthesis ↓
Muscle	acetyl-CoA carboxylase-2/β	enzyme activity ↓	fatty acid oxidation ↑
Liver	HMG-CoA reductase	enzyme activity ↓	cholesterol synthesis ↓
Adipose tissue	hormone-sensitive lipase	activation by PKA ↓	lipolysis ↓
Mitochondrial biogenesis/function — No known primary targets. Secondary targets include:			
Muscle	transcription factor NRF1	DNA binding ↑	mitochondrial biogenesis ↑
Muscle	UCP3	expression↑	mitochondrial proton leak ↑
Muscle	co-activator PGC-1α	expression ↑	mitochondrial biogenesis ↑
Other (examples) — Primary targets			
Epithelia	CFTR	channel activity ↓	Cl-/fluid secretion ↓
Heart	endothelial NO synthase	enzyme activity ↑	NO production ↑
Cultured cells	TSC2	inhibition of TOR ↑	protein synthesis/cell growth ↓
Cultured cells	TOR	phosphorylation of S6 kinase ↓	protein synthesis/cell growth ↓?
Cultured cells	co-activator p300	coactivator-receptor binding ↓	gene expression ↓

"Primary targets" are direct targets for AMPK where the phosphorylation site(s) have been identified. "Secondary targets" are either regulated indirectly or the direct target remains unclear.

AICAR is a widely used AMPK activator. Upon chronic AICAR treatment in rats, mRNA and protein levels of UCP-3 (uncoupling protein 3) as well as enzyme activities of citrate synthase and hydroxyacyl-CoA-dehydrogenase (HADH), which are known to increase in proportion to mitochondrial volume, were increased in muscle [4,35], but the MHC based fiber type transition did not occur [4]. In another study, chronic AICAR treatment increased the activity of the mitochondrial enzymes citrate synthase, succinate dehydrogenase, and malate dehydrogenase as well as the cytochrome *c* and ALAS protein levels in white quadriceps [36]. β-guanidinopropionic acid (β-GPA; 1% enriched diet), a creatine analog that is known to induce mitochondrial proliferation similar as in exercise training was used to activate AMPK in rat muscle. β-GPA treatment results in an energetic deficit with increased levels of ALAS mRNA and enhanced NRF-1 binding activity to the ALAS promoter sequence. Cytochrome *c* protein and mitochondrial density were also elevated upon β-GPA treatment [37].

AICAR and β-GPA are not specific activators of AMPK, but also could activate other AMP-binding proteins [38] and other programs and their efficiency and specificity depends on their uptake [39], which restrict their usage in experiments. For this reason constitutively active (CA) and dominant negative (DN) AMPK constructs were created to modulate the kinase activity more specifically [40]. Overexpression of the AMPKα1-CA construct and AICAR were shown to enhance glucose transport in a rat liver epithelial cell line [41]. In addition, in H-2K^b mouse muscle cells, ectopic AMPKα1-CA expression increased glucose uptake and the

expression of the glucose transporters GLUT-1 and GLUT-4, which are suggested to regulate glucose transport in this cells [42].

Silencing AMPK expression by siRNA showed that it is also involved in GLUT-3 mediated glucose uptake [43]. Furthermore, muscle specific transgenic mice showed that a dominant AMPKα2 inhibitory mutant completely blocked the hypoxia or AICAR activated glucose uptake in skeletal muscle, while the contraction stimulated glucose uptake was only partially inhibited [44]. Analyzing skeletal muscle of these mice showed that AMPKα2 participates in the induction of CaMKIV, PGC-1α, cytochrome *c* [45]. Deletion of both catalytic subunits (α1 and α2) in mouse resulted an embryonic lethal phenotype [34]. However, $\alpha1^{-/-}$ KO showed no defect in glucose homeostasis, while $\alpha2^{-/-}$ KO exhibited high plasma glucose level, low plasma insulin level, reduced muscle glycogen synthesis and insulin resistance [46]. AICAR induced glucose uptake was abolished in skeletal muscle of $\alpha2^{-/-}$ KO mice, which was not visible in mice deficient in the subunit α1, although in none of the knock-out mice, glucose uptake induced by the contraction was affected [47]. In conclusion, the function of AMPK *in vivo* is not clear yet and there are many unsolved details how this kinase regulates cell metabolism, especially the process of mitochondrial biogenesis.

2.5 CREB-1 protein: a point of convergence

The cyclic AMP (cAMP) response element (CRE)-binding protein 1 (CREB-1) belongs to the bZIP (basic leucine zipper) transcription factor superfamily and comprises a subcategory including CREB-1, CREM (cAMP response element modulator) and ATF-1 (activating transcription factor 1) [48]. CREB-2 (ATF-4) [49], CREB-3 (Luman) [50], CREB-4 [51] and CREB-5 (CRE-BPa) [52] have also been identified but they do not belong to the classical CREB-1 family. The CREB-1 protein contains two glutamine rich domains called Q1 and Q2/CAD (constitutive active domain) (Figure 3). The Q2/CAD domain interacts with the basal transcription factor TAF130, a component of TFIID complex and TFIIB. The KID (kinase inducible domain) lies between these domains containing Ser-133, the phosphorylation of which is a prerequisite for the transcriptional activity of CREB-1. This domain has other amino acids (e.g. Ser-142), which could be also phosphorylated but their functions are not clear yet. The C-terminal bZIP domain is rich in the positively charged basic amino acids lysine, arginine and leucine. The heptad repeat of leucine forms the so-called Leucine zipper motif connecting two monomers. The CREB-1 family members can form homo- or heterodimers, but in the latter case they are restricted to heterodimerize with each other and not with other bZIP transcription factors, with the exception of C/EBPβ.

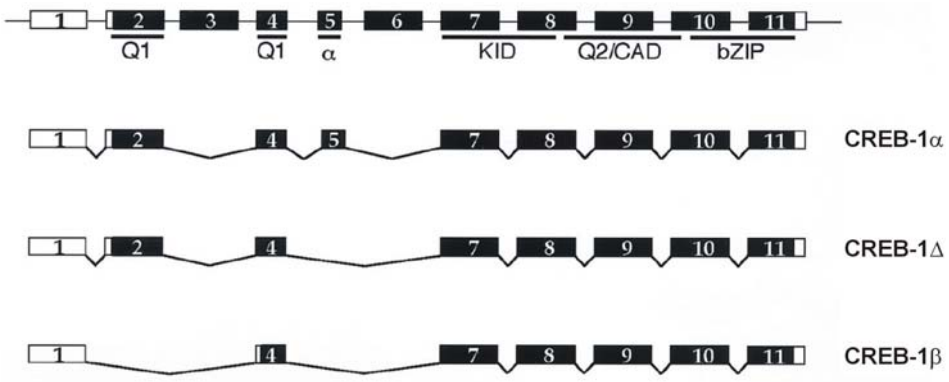

Figure 3. The structure of CREB-1 isoforms [48]

Exon organization of the CREB-1 gene is shown by the upper graphic, exon 5 is spliced out to form CREB-1Δ mRNA and exon 2 is spliced out to form CREB-1β mRNA. Black boxes indicate the translated regions. Q1 and Q2: glutamine rich regions, α: exon 5, KID: kinase inducible domain, CAD: constitutive active domain, bZIP: basic leucine zipper domain.

The CREB-1 gene contains 11 exons (Figure 3). By alternative splicing several isoforms of CREB-1 are produced; the full length CREB-1 isoform is called CREB-1 α (coding 341 amino acid), if the 5th (α) exon is spliced out CREB-1 Δ (coding 327 amino acid) is formed, and if the 2nd exon is also missing, CREB-1 β is generated (Figure 3). They are the best known CREB-1 isoforms but their detailed function remains obscure. Alternative splicing of the gene of CREM creates transcriptional activators (CREM α and τ) or the repressors ICER (inducible early cAMP repressor) or S-CREM, while ATF-1 derived from a third gene serves as an activator of transcription [48].

To increase the complexity of CREB-1 effects, it is known that the "CREB-1-transcriptosome" differs dramatically from cell type to cell type according to the presence of other transcription factors, transcriptional coactivators, enhancers and silencers [53]. CREB-1 is localized in the nucleus and got its name due to its binding to the octamer, *cis*-acting CRE element 5′-TGACGTCA-3′, which is responsible for the reaction to increased levels of cAMP. The G protein coupled catecholamine receptors (GPCRs) start a signal cascade on the cell membrane (Figure 4). After a ligand (e.g. dopamine or norepinephrine) binds to the receptor, adenylate cyclase (AC) is stimulated to increase the level of cAMP, which activates protein kinase A (PKA), so that its catalytic subunits translocate to the nucleus and phosphorylate Ser-133 of the CREB-1 protein. Upon Ser-133 phosphorylation, CREB-1 is activated as it recruits the CREB binding protein (CBP) or its paralogue p300, which are transcriptional coactivators with histone acetyl transferase (HAT) activity. CBP or p300 serves as a molecular bridge that allows transcription factors to stabilize the RNA polymerase II transcription initiation complex. The CREB-1-CBP/p300 complex binds to the basal transcription factors (TFIIB, TFIID) and to

the RNA helicase A (RHA), completing the initiation of transcription and transcriptional elongation can start [48].

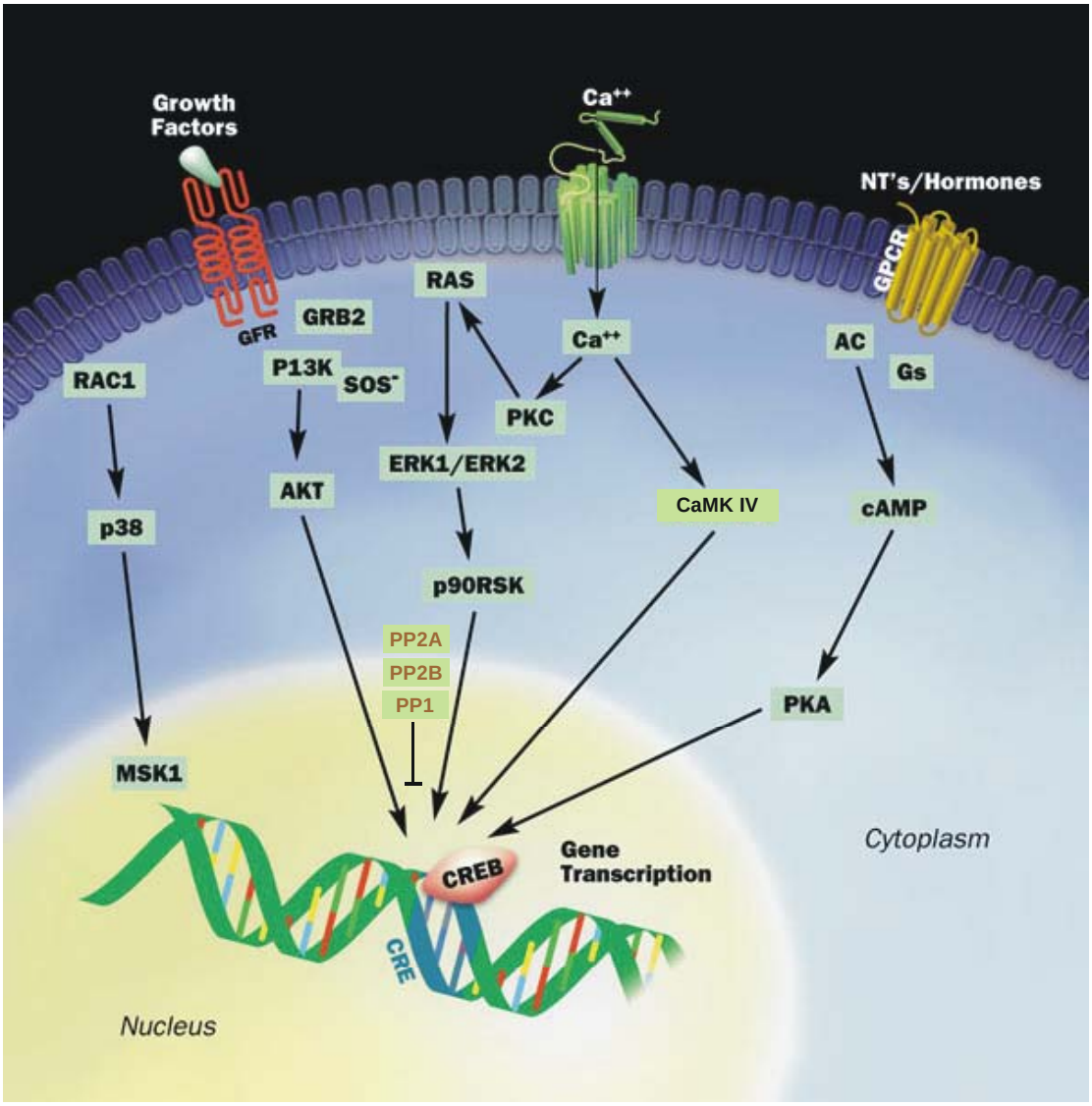

Figure 4. The CREB-1 signal transduction pathway

For details see text above.

GPCRs are not the only receptors transmitting the signal for CREB-1 activation; Ca^{2+} channels, growth factor receptors (GFRs), activated RAC1 (Rho GTPase) are first sensors of cells to induce the transcription of genes activated by CREB-1. Other known CREB-1 phosphorylating kinases besides PKA are the MSK1 (Mitogen and stress activated protein kinase 1), AKT (Protein kinase B α), RSK (Ribosomal protein S6 kinase) and CaMK IV (Figure 4). Beside protein kinases, protein phosphatases are also contributing to modify the activity of CREB-1. Protein phosphatase 1 (PP1), 2A and 2B (calcineurin) dephosphorylate Ser-133, thus preventing its interaction with CPB/p300 and inhibit CREB-1 activated gene expression (Figure 4) [48].

CREB-1 is one of the best-characterized stimulus-induced transcription factors. CREB-1 has pleiotropic functions as it is critical for many distinct cellular processes and it is puzzling how such a widely expressed transcription factor activated in many situations can facilitate so diverse but still so specific functions [54]. It plays a role in the control of memory, cell proliferation, differentiation, adaptive responses, glucose and lipid metabolism.

Brain seems to be the best studied organ to clarify the function of CREB-1 and the protein is involved in the process of learning and memory, addiction, depression, anxiety [55] and even was reported to be modulated in suicide behavior [56]. Complete CREB-1 KO is lethal in mice, but not during embryogenesis but rather immediately after birth. The main cause of death is respiratory distress with strong reduction of nerve cell mass in corpus callosum and the anterior commissures but also impaired T-cell development [57]. In order to investigate the function of CREB-1 in the absence of CREM, which may compensate the effect of CREB-1, neuronal CREB-1 KO mice were crossed with CREM KO mice. The descendent animals neither have CREB-1 nor CREM in their brains. During development of neurons in the central nervous system, extensive apoptosis was found and in postnatal forebrain the hippocampus showed progressive neurodegeneration [58]. These results suggest that CREB-1 is essential for neuronal survival signal pathways.

Besides neuronal tissue, CREB-1 is also involved in transcriptional processes in adipocytes, hepatocytes and muscle. In adipocyte differentiation, it binds the promoter of several adipocyte specific genes such as phosphoenolpyruvate carboxykinase (PEPCK), fatty acid binding protein (FABP), CCAAT-enhancer binding protein β (C/EBP β) and activates the expression of PPAR-γ2 [59]. Upon the insulin induced differentiation of adipocytes, CREB-1 becomes activated and, besides PPAR-γ2 and FABP, also induces the expression of GLUT-4 and leptin [60]. In mature adipocytes, CREB-1 regulates both the survival and apoptotic pathways and seems to be important as an anti-apoptotic protein [61]. In addition, CREB-1 coordinates hepatic lipid and glucose metabolism during fasting through induction of PGC-1α [62] and inhibition of PPAR-γ [63].

In skeletal muscle, CREB-1 is associated with MyoD in C2.7 cells and targeted to the retinoblastoma (RB) gene promoter to enhance its transcription. The elevated level of RB protein is essential for myoblast cell cycle arrest, therefore for terminal differentiation and for survival of myocytes [64]. Recently it was shown that CREB-1 is also required for Wnt-directed myogenic gene expression and Wnt proteins could also stimulate CREB-1 mediated transcription [65].

Muscle differentiation is strictly dependent on the function of mitochondria [66]. CREB-1 also controls the expression of several genes involved in the function of mitochondria. Mitochondrial dysfunction, i.e. complete absence of mtDNA in rho^0 cells or depleting the

mtDNA with ethidium bromide (rho$^-$ cells) was found to activate CRE sequence containing promoters (c-Fos and α-inhibin). This induction was blocked by expressing CREB-1 dominant negative constructs suggesting a role of CREB-1 in the proliferation defects observed in these cells. Phosphorylation of CREB-1 at Ser-133 was increased in the presence of disturbed mitochondrial function and CaMKIV was identified as the CREB-1 phosphorylating upstream kinase [67]. The amount of cytochrome *c* protein was elevated and promoter activity of cytochrome *c* was increased in rho^0 cells, which was again blocked by the expression of CREB-1 dominant negative constructs. Interestingly, the authors detected an increased mitochondrial amount in rho^0 cells and concluded that the depletion of mtDNA causes a counteracting stimulation of mitochondrial biogenesis [68]. In addition, mitochondrial dysfunction in adipocytes caused by blocking complex III induced elevated levels of triglycerides (TG) and CREB-1 activation was needed for this TG accumulation, which was shown to be due to the induction of several adipogenetic genes [69]. Taken together, mitochondrial dysfunction seems to cause a kind of retrograde stimulation of mitochondrial biogenesis, in which CREB-1 is also a key regulator.

In hepatocytes, CREB-1 stimulates the promoter of liver carnitine palmitoyltransferase I, which is the rate limiting enzyme in mitochondrial fatty acid oxidation, shown by treatment with a cAMP analogue and PGC-1α coactivates this effect of CREB-1 [70]. PGC-1α was originally identified as a coactivator of PPAR-γ and a regulator of brown fat differentiation, but it turned out that together with PGC-1β, it is also a main regulator of mitochondrial biogenesis in muscle [9].

Recently a new CREB-1 coactivator family was identified called transducers of regulated CREB activity (TORCs). TORC-1, 2 and 3 proteins are considered to bind the bZIP domain of CREB-1 and recruit it to TAFII 130, independently of the phosphorylation state of Ser-133 [71]. TORC function is essential for CRE-mediated gene expression induced by cAMP, calcium, GPCRs and the nuclear transport of TORC1 was sufficient to activate CRE dependent transcription [72]. TORC1 was the most potent PGC-1α activator from 10,000 screened human cDNAs. TORC2 and 3 also elevate PGC-1α transcription in a CREB-1 dependent manner. Overexpression of all the TORCs enhanced mitochondrial oxidative capacity in muscle cells, and all of them increased the level of cytochrome *c* mRNA [73].

Cytochrome *c* was the first mitochondrial gene to be studied intensively and shown to be a target promoter regulated by CREB-1. In quiescent fibroblasts, serum induced proliferation elevates mitochondrial respiration as well as the level of mRNA, protein and promoter activity of cytochrome c [5]. The serum induced proliferation activates the cytochrome *c* promoter through

the PGC-1 related coactivator (PRC) [74]. CREB-1 and NRF-1 bind to the PRC promoter but they are also required for the stimulation of the cytochrome *c* promoter by PRC [75].

Against the dogma, which says that CREB-1 resides exclusively in the nucleus, extranucleic CREB-1 was found associated to mitochondria. Mitochondrial CREB-1 and phospho-CREB-1 were detected in rat forebrain and the authors suggest that they are localized in the mitochondrial matrix or in the inner membrane. Increased calcium levels decreased the phosphorylation state of mitochondrial CREB-1 meaning that calcium could regulate mitochondrial CREB-1 function [76]. In brain, CREB-1 and phospho-CREB-1 were partially colocalized with cytochrome *c* and in CREB-1 KO mice the phospho-CREB-1 immunoreactivity was completely diminished. Three different CRE elements were detected in the sequence of the regulatory D-loop region of mouse mtDNA and all of them were able to bind CREB-1. CREB-1 was also shown to slightly increase ND2 and ND4 transcripts of complex I, while the dominant negative A-CREB protein decreased transcripts of ND5 and ND6 of complex I as well as its enzyme activity. The mitochondrial CREB-1 appears to regulate neuronal pro-survival effects because upon treatment with a mitochondrial toxin 3-nitropropionic acid, A-CREB stimulated the cell death and the release of cytochrome *c* caused by the toxin [77]. However, a more recent study suggests that phospho-CREB-1 immunoreactivity in neurons is the phospho-pyruvate dehydrogenase E1 α subunit, due to crossreactivity with the antibody against phospho-CREB-1 [78]. Although in the latter study a mitochondrial CRE binding activity could not be shown, the former study found a clear CRE binding activity supershifted with an anti-CREB-1 antibody and even shown an *in vivo* interaction between the mtDNA D-loop region and CREB-1 by chromatin immunoprecipitation (ChIP) [77]. In conclusion, while CREB-1 involvement in the regulation of mtDNA is still controversial, it upregulates the promoter of cytochrome *c* and many other mitochondrial genes encoded in the nucleus directly and via enhancing coactivators, and could be a key factor for mitochondrial biogenesis.

2.6 Aim of the study

In spite of intensive investigations, many questions concerning the regulation of mitochondrial biogenesis have not been solved yet. Our main question was, which factors activate the cytochrome *c* promoter and thus may be involved in stimulation of mitochondrial proliferation. If the factors were identified, how do they control the complex process of mitochondrial biogenesis, where hundreds of genes have to be coordinated. Which upstream signals are involved in controlling these “regulator” proteins? To study these questions, muscle precursor cells were differentiated to multinucleated myotubes, which is accompanied by a marked increase of mitochondrial enzymes.

AMPK was the first studied candidate and cell lines expressing constitutively active AMPKα1 were created to investigate its role. CREB-1 and its isoform was the second factor of choice and its expression was analyzed at the levels of mRNA and protein, together with investigation of its phosphorylation status. This was followed by assessment of its activity by using siRNA knock-down, constitutively active and dominant negative constructs in reporter gene assays.

3 Materials and Methods

3.1 Materials

3.1.1 Chemicals

All chemicals were purchased from the companies Merck, Sigma-Aldrich or Roth, unless otherwise specified.

Coelenterazine	Biotium
D-Luciferin	Biotium
ExGen	Fermentas
Fura-2 AM	TEFLabs
Lipofectamine 2000	Invitrogen
Metafectene	Biontex
Mini complete® Proteaseinhibitor-Cocktail (EDTA free)	Roche
Rp-8-CPT-cAMPS	BioLog
Sp-5,6-DCI-cBIMPS	BioLog
Trizol	Invitrogen

3.1.2 Equipment

Agarose gel chamber	Easycast	Owl Scientific
Cell counter	CASY®1 Modell TT	Schärfe System
Centrifuge		Eppendorf
Hybridisation oven		Amersham Pharmacia
Fluorescence microscope	Axiovert 100	Zeiss
Fluorescence microscope	Axiophot	Zeiss
Incubators	HeraCell	Heraeus
Liquid Scintillation Counter	LS 6500	Beckman
Luminometer	Sirius-1	Berthold Detection Systems
Medical X-Ray Film	Super RX	Fuji
Microplate Reader	µQuant	BioTek Instruments
PCR-Thermocycler	PTC-100	MJ Research Inc.
SDS-PAGE chamber	Tall Mighty Small	Hoefer
Spectrophotometer		Beckman
UV-Crosslinker	UVC500	Hoefer

3.1.3 Organisms

Bacterial organism *Escherichia coli* DH5α [79]

F^- gyrA96 (Nal^r) recA1 relA1 endA1 thi-1 hsdR17 ($r_k^- m_k^+$) glnV44 deoR Δ(lacZYA-argF) U169 [ϕ80dΔ(lacZ)M15]

Mammalian cell lines

C2F3	mouse muscle cell line [80]
C2C12	mouse muscle cell line (ATTC Number: CRL-1772) [80]

3.1.4 Materials for cell culture

Cell culture dishes	TPP, Costar Corning
DMEM with Glutamax I, 4.5 g/l Glucose	Gibco BRL Cat.No. 61965-026
DMSO, cell culture tested	Sigma Cat.No. D-4540
FCS	PAA Cat.No. A15-043
Horse serum	Sigma Cat.No. H 1270
MEM Nonessential Amino Acids 100x	Gibco BRL Cat.No. 11140-035
Na-Pyruvate 100 mM (sterile filtered)	Gibco BRL Cat.No. 11840-048
OptiMEM	Gibco BRL Cat.No. 51985-026
PBS	Gibco BRL Cat.No. 18912-014
Trypsin-EDTA 0.05 % in HBSS	Gibco BRL Cat.No. 25300-054

Additives to the media:

1 mM sodium pyruvate

1x nonessential amino acids

1 % penicillin streptomycin

10 % FCS for cultivating the cells, or 2 % horse serum for differentiation media

3.1.5 Antibiotics

		End concentration
Ampicillin	Sigma	50 µg/ml
Carbenicillin	Sigma	50 µg/ml
G418	PAA	700 µg/ml
Hygromycin B	PAA/InvivoGen	700 µg/ml
Penicillin	Gibco BRL	1 %

Streptomycin	Gibco BRL	1 %

3.1.6 Materials for standard molecular biology

3.1.6.1 Oligonucleotides

mCREB-103-5′	5′-ACATTAGCCCAGGTATCCATGCCAG-3′
mCREB-396-3′	5′-GGCCTCCTTGAAAGGATTTCCCTTCG-3′
mCREB 418 5′	5′-GACTTATCTTCTGATGCACCAGG-3′
mCREB 962 3′	5′-GGTTTTCAAGCACTGCCACTC-3′

Oligonucleotides were synthetised by Sigma-Genosys or by Operon.

3.1.6.2 Nucleic acids

Vectors

pcDNA-AMPKα1-CA	gift from Dr. Carling
pGL3-cytochrome *c*-Firefly	made by Dr. Goffart
pRL-CMV	Promega
pRL-SV40	Promega
pTRE2-Hyg	Clontech
pRSETA	gift from Dr. Goffart
pCMV	gift from Dr. Thiel
pTRE2-Firefly	gift from Prof. Brüning
pCMV-Flag-C2/CREB	gift from Dr. Thiel
pEBGN-CREB	gift from Dr. Thiel
pEBGN-K-CREB	gift from Dr. Thiel
pCMV-A-CREB	gift from Dr. Thiel
α-inhibin-Firefly	gift from Dr. Arnould

siRNAs

siRNA SMART pool against CREB-1 NM 133828	Dharmacon
siCONTROL negative #1	Dharmacon
siCONTROL negative pool	Dharmacon
siCONTROL TOX	Dharmacon

3.1.6.3 Enzymes

Taq-Polymerase	Fermentas
Klenow-Fragment	Fermentas
T4-DNA-Ligase	Fermentas

Shrimp alkaline phosphatase	Amersham
Lambda protein phosphatase	Upstate
Restriction enzymes	New England Biolabs/Fermentas

3.1.6.4 Kits

Chroma spin columns (for DNA purification)	Clontech
Dynabeads mRNA DIRECT Kit	Invitrogen
ECL-Kit	PerkinElmer
GenElute Plasmid Maxiprep Kit	Sigma
QIAamp DNA Mini Kit	Qiagen
QIAGEN Plasmid Midi Kit	Qiagen
QIAEX II Gel Extraction Kit	Qiagen
QuantiTect Reverse Transcription Kit	Qiagen
QIAquick PCR Purification Kit	Qiagen
Random Primed DNA-Labeling Kit	Roche
5x Passive lysis buffer	Promega

3.1.6.5 Radiochemicals

α^{32}P-ATP	5,000 Ci/mmol	Hartmann Analytics
γ^{32}P-dCTP	5,000 Ci/mmol	Hartmann Analytics

3.1.6.6 Markers, dyes

1kb-Ladder	Gibco BRL
GeneRuler 100 bp Marker	Fermentas
PageRuler Prestained Protein Ladder	Fermentas
6x DNA loading dye	Fermentas
RiboRuler RNA ladder, High range	Fermentas

3.1.6.7 Antibodies

First antibodies		Cat.No.	Working dilution
Monoclonal anti-β-actin	Sigma-Aldrich	A 1978	1:5,000
Monoclonal anti-β-tubulin	Sigma-Aldrich	T 4026	1:1,000
Monoclonal anti-c-myc	Santa Cruz B.	sc-40	1:1,000
Monoclonal anti-Histone H1	Santa Cruz B.	sc-8030	1:1,000
Monoclonal anti-Myogenin (F5D)	Santa Cruz B.	sc-12732	1:400
Monoclonal anti-MHC (1F11)	gift from Dr. F. Pons		1:2 (IHC)

Polyclonal anti-α-actinin 4	ImmunoGlobe	0042-05	1:1,000-1:3,000
Polyclonal anti-AMPKα	Cell Signaling T.	2532	1:1,000(WB)
			1:100 (IP)
Polyclonal anti-AMPKα1	gift from Dr. Carling		1:50 (IP)
Polyclonal anti-CREB-1	Cell Signaling T.	9192	1:500-1:1,000
Polyclonal anti-CREB-1α	Santa Cruz B.	sc-58	1:1,000
Polyclonal anti-CREB-1	Upstate	06-863	1:2,000
Polyclonal anti-Phospho-CREB-1	Cell Signaling T.	9191	1:1,000

Secondary antibodies		Cat.No.	Working dilution
Donkey-anti-rabbit IgG-HRP	Dianova	711-035-152	1:1,000
Goat-anti-mouse IgG-HRP	Dianova	115-035-062	1:5,000-1:10,000
Goat-anti-mouse IgG-Cy3			1:50

3.2 Methods

3.2.1 Standard molecular biology

3.2.1.1 *E. coli* cultivation

Eschericia coli DH5α strain was used as a tool for plasmid DNA amplification. Bacteria were inoculated from an LB-agar plate (complemented with the appropriate antibiotic) into LB medium (with the antibiotic) for overnight incubation with shaking at 37°C. Plasmid preparation was made from overnight bacterial cultures.

LB-Medium/Agar 1 % NaCl
1 % bacto trypton
0.5 % yeast extract
pH 8.0
(1.5 % bacto agar)

3.2.1.2 Preparation of transformation-competent *E. coli*

Eschericia coli strain DH5α was streaked from −80°C frozen stock on a fresh LB plate and grown overnight at 37°C. A single colony was inoculated into 10 ml LB. It was grown overnight with shaking at 37°C. 1 ml was inoculated into 200 ml LB and shaken at 37°C until OD_{600}=0.5. The flask was chilled on ice for 5 minutes and the bacteria were centrifuged for 5 minutes at 5,500 x g. The pellet was resuspended in 80 ml ice cold Buffer 1 and incubated in ice for 5 minutes. It was centrifuged for 5 minutes at 5,500 x g again, the pellet was resuspended in 8 ml ice cold Buffer 2 and chilled on ice for 15 minutes. 200 µl aliquots were made in 1.5 ml tubes, flash-frozen in liquid nitrogen and then stored at −80°C.

Buffer 1 30 mM potassium acetate pH 5.8
100 mM $RbC1_2$
10 mM $CaCl_2$
50 mM $MnC1_2$
15 % glycerol

Buffer 2 10 mM MOPS/KOH pH 6.5
75 mM $CaC1_2$
10 mM $RbC1_2$
15 % glycerol

3.2.1.3 Plasmid DNA preparation

Plasmid preparations were made from transformed *E. coli* overnight culture according to the manual of the Kits used. The plasmid DNA was eluted with H_2O or with 10 mM Tris pH 8.0 and the concentration was measured spectrophotometrically at 260 nm.

3.2.1.4 Transformation

A 200 µl aliquot of *E. coli* competent bacteria was thawed on ice. Plasmid DNA was added and mixed gently. They were incubated on ice for 10 minutes followed by a heat shock for 1 minute at 42°C. The bacteria were incubated for 5 minutes on ice, 1 ml LB was added and shaken for 1 hour at 37°C. The whole bacterial supernatant or a part of it was plated on LB-agar (with antibiotic) and incubated overnight at 37°C.

3.2.1.5 Glycerol stock

For long time storage of transformed bacteria, 15 % glycerol stocks were made in LB medium and stored at –80°C. After storage the bacteria were scraped with a sterile loop onto LB-agar completed with the appropiate antibiotic and incubated overnight at 37°C.

3.2.1.6 Nucleic acid gel electrophoresis

The separation of DNA fragments were analyzed in 1-2 % agarose gels in 1x TAE buffer with 0.5 µg/ml ethidium bromide. 6x DNA loading dye (Fermentas) or 10x DNA loading dye was added to the probes. A molecular weight marker was also loaded to determine the molecular size of the fragments. The samples were run at 80-90 V for 30-40 minutes and were documented using a CCD video camera.

50x TAE	2 M Tris
	1 M acetic acid
	50 mM EDTA pH 8.0
10x DNA loading dye	0.06 % bromophenol blue
	0.06 % xylene cyanol
	50 % glycerol
	20 mM Na-EDTA pH 8.0
	180 mM Tris pH 7.5

3.2.2 Principle of Tet-Off system

In the Tet-Off system, the transactivator protein (tTA) consists of a tetracycline repressor (tetR) and a VP16 activation domain, working as a tetracycline sensitive activator [81] (Figure 5). It binds on the TRE sequence of the second plasmid with the gene of interest and activates its

transcription. In the presence of tetracycline (Tet) or its derivative doxycycline (Dox), the transactivator protein binds the ligand resulting in the inhibition of transcription. The system got its name since in the presence of Tet, the transcription of the gene of interest is "switched off". The ligand is present in the phase of creating stable cell lines and removing it induces the expression of the gene of interest.

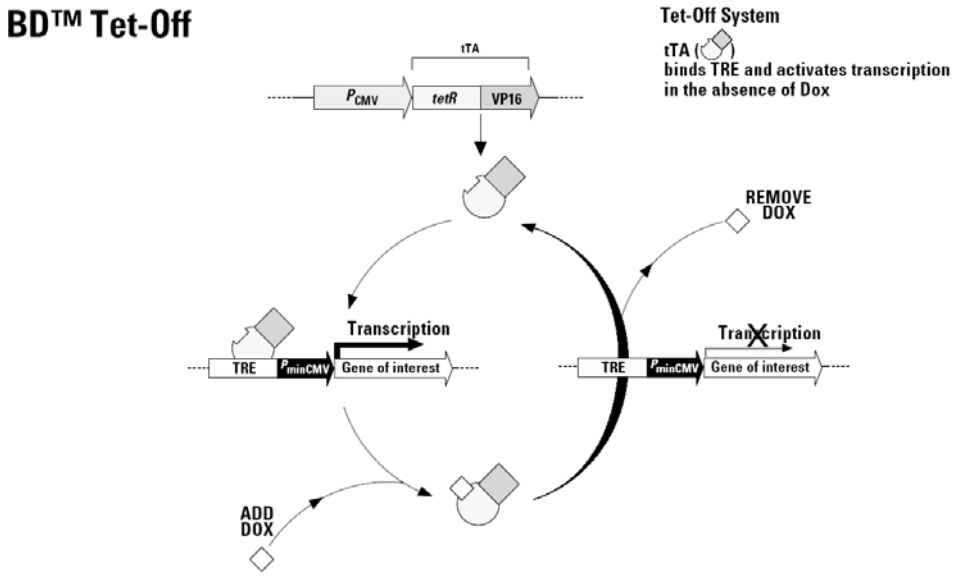

Figure 5. The principle of Tet-Off system

The transactivator (tTA) protein is continuously expressed driven by the CMV promoter. It binds to the TRE sequence of the plasmid containing the gene of interest and enhances the transcription of the gene in the absence of Tetracycline or Doxycycline. In the presence of Tet or Dox the tTA protein is inhibited to bind to the TRE sequence, which causes the lack of transcription.

3.2.3 Cloning of rat AMPKα1-CA into pTRE2-Hyg vector

The DNA sequence of the AMPKα1-CA was cloned into the mammalian expression vector pTRE2Hyg, which has a Tetracycline response (TRE) promoter and resistance genes against Ampicillin and Hygromycin B. The pTRE2Hyg vector was digested with PvuII, purified with the QIAquick PCR Purification Kit and digested with SalI enzymes (Appendix Figure 1 A and B). To diminish self-ligation the free phosphate group was dephosphorylated by SAP phosphatase and the vector was purified from agarose gel. The pcDNA3-AMPKα1-CA construct was digested first with KpnI enzyme cutting out AMPKα1-CA from the pcDNA3 vector, purified with the QIAquick PCR Purification Kit (Appendix Figure 1A) and the overhanging nucleotides were filled up using Klenow enzyme to generate blunt ends. The AMPKα1-CA blunt ended fragment was purified from agarose gel and digested with XhoI enzyme (Appendix Figure 1B)

followed by a gel purification by QIAEX II Gel Extraction Kit. The PvuII/SalI cut pTRE2Hyg vector and the XhoI/blunt ended AMPKα1-CA fragments were ligated with T4 DNA ligase for 1 hour at 22°C according to the blunt ends (PvuII and filled KpnI) and the compatible sticky ends (SalI and XhoI). The ligation mixture was transformed into competent *E. coli* DH5α bacteria and several growing colonies were checked with restriction digestion. Test digestions verified that AMPKα1-CA was integrated into the pTRE2Hyg vector. The sequence was verified by sequencing the AMPKα1-CA region starting from the commercially available pTRE2-Hyg primers. PstI enzyme cut the pTRE2Hyg-AMPKα1-CA construct into two fragments, which are 4324 bp and 1988 bp (Appendix Figure 1C) in contrast to the empty vector, which is linearized having only one PstI site. The cloned AMPKα1-CA insert contains two HindIII restriction sites. HindIII digestion of the pTRE2Hyg-AMPKα1-CA construct resulted in three fragments with the length of 5205, 876 and 231 bp (Appendix Figure 1D).

3.2.3.1 Cultivation

The murine muscle cell lines (C2C12 and C2F3) were cultivated at 37°C, 5 % CO_2 and in humidified air on cell culture plates or flasks. Both cell lines were routinely cultivated in DMEM+10 % FCS. The cells were split on every second or third day (cells should have not been more confluent than 85 %) and seeded 2-3 x 10^5 cells on a 10 cm cell culture dish for two days. Cells were detached with trypsin, centrifuged at 200 x g and resuspended in PBS for counting. Differentiation was induced by growning the myoblasts to 100 % confluency followed by changing growing medium (DMEM+10 % FCS) to differentiation medium (DMEM+2 % horse serum). For the myotubes, the medium was changed every day and experiments were done with myotubes, which had been cultivated in DMEM+2 % horse serum for 3-7 days.

3.2.3.2 Freezing and thawing of cells

For long time storage about 10^6 cells were centrifuged at 200 x g, the cell pellet was resuspended in 1 ml FCS+10 % DMSO, cooled down in an isopropanol filled box to −80°C and latter transfered to liquid N_2. For thawing, the cells were warmed up quickly at 37°C and were seeded out into a 10 cm cell culture dish.

3.2.3.3 Transfection

3.2.3.3.1 Stable transfection

In order to transfect the constitutively active form of AMPKα1 into mammalian cells, C2C12 myoblasts were transfected with purified pTRE2-Hyg-AMPKα1-CA vector. To analyze, which transfection method is suitable to reach high transfection efficiency using C2C12 cells, three

different transfection approaches were applied: Metafectene, ExGen or calcium phosphate-based transfections were performed.

Metafectene

15-15 µg plasmid DNA was transfected with 30-30 µl Metafectene into cells seeded on two 10 cm dishes according to the manual of the manufacturer.

ExGen

8 µg plasmid DNA was transfected with 53 µl ExGen into cells seeded on a 10 cm dish according to the manual of the manufacturer.

Calcium phosphate

Cells were transferred to 6 % CO_2 for 30 minutes before and after transfection. 30 µg pTRE2-Hyg-AMPKα1-CA plasmid DNA was mixed with 24 µg pRSETA in 1 ml 0.22 M $CaCl_2$ solution. They were incubated for 20 minutes and then mixed in small amounts with 1 ml 2x HBS. The calcium phosphate-DNA solution was incubated for 20 minutes, vortexed well and 2 ml solution was given to two 10 cm dishes (1 ml solution/10 cm dish). Next day the calcium phosphate precipitate was discarded by washing the cells three times with PBS.

2x HBS (Hepes-buffered saline)	280 mM NaCl
	10 mM KCl
	1.5 mM Na_2HPO_4
	12 mM α-D-glucose
	50 mM HEPES
	pH 7.05

3.2.3.3.2 Transient transfection

Plasmid DNA transfection

In order to perform reporter gene assays myoblasts were transfected at the stage of 30-50 % confluency. Usually 2-3 x 10^4 cells were seeded per one well of a 12-well plate one day before transfection. Metafectene was used as transfection reagent and was applied according to the manual of the manufacturer. Briefly, plasmid DNAs were mixed with OptiMEM and Metafectene was separately mixed with OptiMEM. Then the two solutions were combined and incubated at room temperature for 20 minutes. 100 or 200 µl plasmid DNA–Metafectene complex in OptiMEM was given to a well of a 12-well plate or a well of a 6-well plate. 0.5-1 µg DNA was transfected in a 1:3.33 ratio with Metafectene or in a 1:5 ratio with Lipofectamine 2000 per one well of a 12-well plate. Non-confluent myoblasts were analyzed 24 hours,

confluent myoblasts 48-72 hours after transfection, myotubes were analyzed 96-144 hours after transfection.

siRNA transfection

In order to knock-down the mRNA of CREB-1 siRNA against the CREB-1 mRNA was transfected with Lipofectamine 2000 into 30-50 % confluency C2F3 cells. 9x 10^4 cells were seeded per one well of a 6-well plate one day before transfection. 5-100 nM siRNA was transfected with 4-15 µl Lipofectamine 2000 per well of a 6-well plate. Medium was changed 6-24 hours after transfection.

siRNA and plasmid DNA cotransfection

In order to analyze the effect of CREB-1 acting on the cytochrome *c* promoter pGL3-cytochrome *c*-Firefly+pRL-CMV and siRNA SMARTpool against CREB-1 (NM 133828) or the appropiate siCONTROL siRNAs were cotransfected into 30-50 % confluency C2F3 cells. Usually 2-3 x 10^4 cells were seeded per one well of a 12-well plate one day before transfection. 0.3 µg plasmid DNAs were cotransfected with 5 nM, 20 nM, 50 nM, 100 nM siRNAs and 1 µl, 1 µl, 2.5 µl and 5 µl Lipofectamine 2000 per well, respectively. Promoter activity was analyzed 24 hours after transfection.

3.2.4 Nucleic acids

3.2.4.1 Total RNA preparation from C2F3 cells

C2F3 myoblasts were seeded on 10 cm dishes and cultivated to 70-80 % confluency (non-confluent myoblasts), to 100 % confluency (confluent myoblasts) or after myotube formation had been induced by a change to differentiation medium. Cells were harvested with trypsine, centrifuged (at 200 x g for 5 min at 4°C) and washed two times with ice cold PBS. After the last washing step the pellet was lysed in Trizol for 5 minutes. 0.2 ml chloroform was added, and the mixture was shaken vigorously for 15 seconds followed by a three minutes incubation. The tubes were centrifuged at 12,000 x g for 15 minutes at 4°C. The mixtures were separated to a lower red phenol-chloroform phase (proteins, DNA), an interphase (DNA) and a colourless upper aqueous phase (RNA). The RNA (aqueous) phase was transferred into a fresh tube and precipitated overnight by addition of 0.5 ml isopropanol at −80°C. The tubes were centrifuged at 12,000 x g at 4°C for 10 minutes, the supernatants were removed and the pellets were washed first with 100 % ethanol (centrifuged at 7,500 x g for 5 minutes at 4°C) and then two times with 75 % ethanol. Then the pellets were air-dried for 20 minutes at room temperature and resuspended in 15-30 µl RNAse-free DEPC-water. The RNA concentration was measured at 260 nm and 1 µg

RNA was loaded onto a 1 % agarose gel to check the integrity of the RNAs (without RNAse) stained with ethidium bromide.

3.2.4.2 PolyA$^+$ mRNA preparation from C2F3 cells

C2F3 myoblasts were seeded on 10 cm dishes and cultivated to 70-80 % confluency (non-confluent myoblasts) or to 100 % confluency (confluent myoblasts) or after at 100 % confluency myotube formation was induced by a change to differentiation medium (myotubes). Cells were harvested with trypsine, centrifuged (at 200 x g for 5 min at 4°C) and washed two times with ice cold PBS. After the last washing step the pellet was lysed in 1250 µl Lysis/Binding buffer and the protocol was continued according to the instructions of the Invitrogen Direct mRNA isolation kit. Briefly, the polyA-mRNAs were bound to Oligo(dT) Dynabeads, collected with a Dynal MPC-S magnetic bar, the unspecifically bound nucleic acids were washed off and the polyA-mRNAs bound to the beads were eluted in 40 µl RNA loading buffer (see 3.2.4.4). Usually 20 µl from the eluate was used for Northern blot analysis.

3.2.4.3 Random primed labeling of DNA

The mouse CREB DNA sequence from 418 till 962 basepairs was amplified by PCR to generate a CREB probe (see 3.2.5.2). The PCR product was purified with PCR purification kit to discard the primer dimers and eluted in 30 µl 10 mM Tris (pH 8.0). 50 ng double stranded DNA was denatured by boiling at 100°C for 5 minutes. 40 µCi αP^{32}-dCTP was used for the labeling by Klenow fragment with Random Primed DNA-Labeling Kit. The reaction was incubated for one hour at 37°C and the unincorporated αP^{32}-dCTP was discarded by Chroma spin columns. The eluted radioactive probe was boiled at 100°C for 5 minutes and after a short centrifugation it was placed to ice before adding it to the hybridisation buffer.

3.2.4.4 Northern Blot

10 µg total RNA or 20 µl of polyA-mRNA samples in RNA loading buffer (without RNA loading dye) were heated to 65°C for 15 minutes, spin centrifuged, directly put on ice and completed with the RNA loading dye. Then they were loaded onto a 1.2 % denaturing agarose gel (with 1x MOPS buffer+ 6.5 % formaldehyd) and electrophoretically separated at 80 V for 5-6 hours untill the bromphenol blue was migrated 10.5 cm from the top of the gel. The RNA was capillary transfered overnight in 10x SSC to a Gene Screen Plus Hybridization transfer nylon membrane and was crosslinked with 0.12 J/cm^2 UV-light (wavelength 254 nm) for 1 min. The membrane was prehybridised at 50°C overnight in dextran sulfate hybridisation buffer then hybridised with the radioactively labelled mouse CREB probe in hybridisation buffer at 50°C for 24 hours. The unspecifically bound, radioactively labelled probe was washed away with low

stringency buffer (usually two times for 7 minutes) and optionally with high stringency buffer (one to two times for 7 minutes). Fuji medical X-ray film (Super RX) was used to detect the specific mRNA signals and was usually exposed at −80°C for 24-48 hours.

10x formaldehyde RNA loading dye	1 mM EDTA, pH 8.0
	0.25 % bromphenol blue
	0.25 % xylene cyanol
	50 % glycerol
RNA loading buffer	10 µg total RNA in 4.5 µl RNAse free water
	1x MOPS
	6.5 % formaldehyde
	50 % formamide
	2x RNA loading dye
10x MOPS	0.4 M MOPS
	0.1 M sodium acetate
	0.01 M EDTA pH 8.0
dextran sulfate hybridisation buffer	10 % dextran sulfate
	1 M NaCl
	1 % SDS
low stringency buffer	2x SSC
	0.1 % SDS
high stringency buffer	0.1x SSC
	0.1 % SDS
20x SSC	3 M NaCl
	0.3 M sodium citrate
RNAse free water	0.1 % DEPC in distilled water

3.2.5 Polymerase chain reaction (PCR)

3.2.5.1 Reverse transcription

In order to produce a probe against the gene of mouse CREB-1 and analyze the presence of CREB-1 isoforms total RNA was isolated from C2F3 cells (according to 3.2.4.1). Reverse transcription was made from 1 µg total RNA of myoblasts, confluent cells and myotubes using QuantiTect Reverse Transcription Kit according to the manual of the manufacturer (20 µl final volume).

3.2.5.2 PCR

2 µl of the cDNA samples of growing myoblasts, confluent myoblasts and myotubes were used as a template in the CREB isoform specific PCR reaction with mCREB-103-5´ and mCREB-396-3´ primers. 2 µl cDNA sample of growing myoblasts was used in CREB probe PCR reaction with mCREB 418 5´ and mCREB 962 3´ primers. 10 µl of PCR reactions were run on a 2 % agarose gel to visualize the PCR products.

Usual PCR reaction

2 µl cDNA

1.5 mM $MgCl_2$

0.25 mM dNTP

1 µM primer 1 and 2

1x PCR buffer without $MgCl_2$

2.5-5 U Taq-Polymerase

CREB isoform specific PCR

92°C	2 min	
92°C	30 sec	30x
66°C	1 min	
72°C	1 min	
72°C	10 min	
4°C	∞	

CREB probe PCR

92°C	2 min	
92°C	30 sec	30x
57°C	1 min	
72°C	1 min	
72°C	10 min	
4°C	∞	

3.2.6 Protein

3.2.6.1 Preparation of whole cell extracts

Trypsinesed cells were washed two times in PBS and centrifuged at 200 x g at 4°C for 5 minutes. The cell pellet was resupended in about 2 volumens of Totex buffer, and incubated on ice with frequent vortexing for 10 minutes. The samples were incubated at –80°C for 20 minutes and then thawed on ice with frequent vortexing for 10 minutes. The unsolubilized fraction was centrifuged down at 15,000 x g at 4°C for 10 minutes and the supernatant (containing the solubilized proteins) was stored at –20°C. The protein concentration was determined by Biorad Protein Assay according to Bradford [82] standardized to 0-10 µg/ml BSA solution.

Totex buffer 20 mM Hepes pH 7.9

400 mM NaCl

20 % glycerol

1 % NP-40
1 mM $MgCl_2$
0.5 mM EDTA
0.1 mM EGTA
10 mM β-glycerophosphat
10 mM NaF
5 mM DTT
0.5 mM Na_3VO_4
1 mM PMSF

3.2.6.2 Nuclear and cytoplasmatic protein preparation

Cells were washed with ice cold PBS, scraped in PBS+phosphatase inhibitors and centrifuged at 200 x g at 4°C for 10 minutes. The pellet was resuspended in 1 ml hypotonic buffer (HB) and centrifuged at 200 x g at 4°C for 5 minutes. The pellet was resuspended in 200 µl HB+0.2 % NP-40 buffer, and centrifuged at 17,700 x g at 4°C for 30 seconds. The supernatant was considered the cytoplasmatic fraction and the pellet was considered the nuclear fraction. The cytoplasmatic fraction was stored at –80°C and the nuclear fraction was resuspended in 20-100 µl HB+20 % glycerol buffer. The same volume (20-100 µl) HB+20 % glycerol+0.8 M NaCl buffer was added, the samples were incubated at 4°C for 30 min with constant mixing on a rotating wheel and centrifuged at 17,700 x g at 4°C for 10 minutes. The supernatant (nuclear extract) was aliquoted and stored at –80°C. Protein concentration was determined by Biorad Protein Assay according to Bradford [82].

PBS+phosphatase inhibitors
1 mM Na_3VO_4
5 mM NaF
10 mM nitrophenylphosphate
10 mM β-glycerophosphate
in PBS

Hypotonic buffer (HB)
20 mM Hepes (pH 7.9)
1 mM Na_3VO_4
5 mM NaF
10 mM nitrophenylphosphate
10 mM β-glycerophosphate
1 mM Na_2MO_4
0.1 mM EDTA
1x protease inhibitors cocktail (Boehringer/Roche)

Hypotonic buffer+0.2 % NP-40

Hypotonic buffer+20 % glycerol

Hypotonic buffer+20 % glycerol+0.8 M NaCl

3.2.6.3 Protein gel electrophoresis

Denaturing SDS polyacrylamide gel electrophoresis (SDS-PAGE) was done according to Lämmli [83]. A 4 % SDS stacking gel and a 12.5 % SDS separation gel were cast in a Hoefer Tall Mighty Small SDS-PAGE chamber. Each sample was boiled for 5 minutes in 6x SDS loading dye before loading. Per lane, 6-8 µg nuclear protein or 30 µg total protein was loaded. The size of separated proteins was estimated using the PageRuler Prestained Protein Ladder. The gel was run in running buffer at 10-15 mA with constant current for 3-4 hours.

stacking gel	0.1 % SDS
	125 mM Tris pH 6.8
	4 % acrylamide/bisacrylamide (29:1)
	0.1 % APS
	0.01 % TEMED
separation gel	0.1 % SDS
	375 mM Tris pH 8.8
	12.5 % acrylamide/bisacrylamide (29:1)
	0.1 % APS
	0.01 % TEMED
10x running buffer	250 mM Tris
	2 M glycine
	1 % SDS
6x SDS protein loading dye	125 mM Tris pH 6.8
	3 mM EDTA
	20 % glycerol
	9 % SDS
	0.05 % bromphenolblue
	10 % β-mercaptoethanol

3.2.6.4 Western Blot

After the run, the separation gel was transferred to an Optitran BA-S 85 reinforced nitrocellulose membrane (Whatmann) in western blot transfer buffer by 12.5 V for two and a half hour in a Hoefer transfer chamber. To ensure equal protein loading, Ponceau S staining was done. The membrane was saturated in blocking buffer for 1 hour, probed with the first antibody in blocking

buffer for 1 hour (at room temperature) or overnight (at 4°C). The membrane was washed in TBST three times for 10 minutes, then probed with the secondary antibody conjugated with horseradish peroxidase (HRP) in blocking buffer at room temperature for 1-2 hours and washed in TBST five times for 10 minutes. An Enhanced chemiluminescence (ECL) detection kit was used to visualize the horseradish peroxidase conjugated secondary antibody-first antibody complex and light emission was captured on Fuji medical X-ray film (Super RX) by autoradiography. To reprobe a membrane it was stripped in stripping buffer at 50°C for 30 minutes. Then it was washed 5 times in TBST and blocked again in blocking buffer for 1 hour followed by probing with the new first antibody.

transfer buffer	25 mM Tris
	0.2 M glycine
	0.1% SDS
	20 % methanol
10x TBST	20 mM Tris pH 7.5
	150 mM NaCl
	0.5 % Tween-20
blocking buffer	5 % (w/v) non-fat milk powder
	1x TBST
stripping buffer	50 mM Tris pH 6.8
	2 % SDS
	0.1 M β-mercaptoethanol

3.2.6.5 Immunoprecipitation

In order to determine the kinase activity of endogenous AMPKα1 or the AMPKα1-CA, the kinase was immunoprecipitated with a specific antibody. The cells were washed two times with PBS and dried in air. 0.75 ml lysis buffer was added (per 10 cm dish) and incubated at 4°C for 30 min with constant mixing on a rotating wheel. The cells were scraped and centrifuged at 13,000 x g at 4°C for 20 min. The supernatant was put into a new 1.5 ml tube and protein concentration was measured according to Bradford. 200 µg of protein was taken and the volume was adjusted to 1 ml with lysis buffer. In the preclearing step, 10 µl Protein A-G-beads were given to the lysate and incubated at 4°C for 1 hour with constant mixing on a rotating wheel. The samples were centrifuged at 610 x g for 5 minutes and the supernatant was transferred into a new 1.5 ml tube. AMPKα1-CA was immunoprecipitated by 10 µg anti-c-myc antibody, the endogenous AMPKα was immunoprecipitated by 1:100 anti-AMPKα antibody (Cell Signaling) or by 1:50 anti-AMPKα antibody (gift from Dr. Carling) at 4°C for 1 hour with constant mixing

on a rotating wheel. 40 µl Protein A-G-beads were added to the samples and incubated at 4°C overnight with constant mixing on a rotating wheel. The immunoprecipitated proteins were pelleted by centrifugation at 610 x g at 4°C for 1 minute. The supernatant was kept for western blot. The pelleted complex was washed two times with buffer A and two times with buffer B. One half of the beads was mixed with 6x SDS loading dye for Western blotting, the other half was analyzed in the kinase assay.

Lysis buffer (Buffer A)	50 mM Tris pH 7.5
	1 mM EDTA
	1 mM DTT
	10 % glycerol
	50 mM NaF
	5 mM sodium pyrophosphate
	1 mM benzamidine
	0.1 mM PMSF
	1 % Triton-X 100
Buffer B	50 mM Tris pH 7.5
	1 mM EDTA
	10 % glycerol
	1 mM DTT

3.2.6.6 Kinase assay

In order to measure the kinase activity of endogenous AMPKα1 or the AMPKα1-CA, kinase assay was performed. The AMPK kinase bound beads were resuspended in 30 µl kinase buffer and incubated at 30°C for 30 minutes. The reaction was stopped by centrifugation at 9,000 x g for 30 seconds and the supernatant was transferred into a new 1.5 ml tube. 15 µl supernatant was applied onto a phosphocellulose P81 Whatman cation exchange paper. It was washed with 1 % H_3PO_4 three times for 20 minutes each, then it was finally washed with acetone and dried in air. The immunoprecipitated AMPK enzyme phosphorylates the SAMS peptide (HMRSAMSGLHLVKRR), so the SAMS peptide labelled with radioactive phosphate was measured with scintillation counting.

Kinase buffer	40 mM Na-Hepes pH 7.0
	0.2 mM AMP
	80 mM NaCl
	0.8 mM DTT
	5 mM $MgCl_2$

10 % glycerol
0.2 mM SAMS peptide
0.18 mM ATP (cold)+0.02 mM 2 µCi ^{32}P γATP (hot)

3.2.6.7 Phosphatase treatment of nitrocellulose membrane

In order to analyze the phosphorylation status of the CREB-1 double bands SDS-PAGE was performed and the proteins were transferred to Optitran BA-S 85 reinforced nitrocellulose membrane (Whatman). The membrane was blocked in blocking buffer for one hour and then incubated in phosphatase buffer with constant mixing on a rotating platform at 4°C overnight. The membrane was washed with PBS-0.1 % Tween 20 for 5 minutes, then with TBST three times for 10 minutes each. Afterwards the normal western blot protocol was followed with the first antibody probing and etc.

Phosphatase buffer
1 % BSA
0.1 % Triton X-100
2 mM $MnCl_2$
5 mM DTT
1200 U/ml lambda-phosphatase
in TBS

3.2.7 Reporter gene assay

The promoter activities were determined by luciferase reporter gene assay with two expression vectors. pRL-CMV vector consists of a constitutively active cytomegalovirus promoter (CMV) upstream of the renilla luciferase gene of the sea pansy *Renilla reniformis*. The second plasmid with the promoter of interest had the cytochrome *c* pro moter fragment to be analyzed upstream of the firefly luciferase gene of the firefly *Photinus pyralis*. The plasmids were transfected into logarithmically growing (12-well plate seeded) myoblasts with Metafectene or with Lipofectamine 2000. Usually 3-6 parallel samples were used. Non-confluent myoblasts were analyzed 24 hours after transfection, confluent myoblasts 48-72 hours after transfection, myotubes were analyzed 96-144 hours after transfection. The cells were washed with PBS and lysed in 200 µl Passive lysis buffer per well. After 5 minutes incubation the cells were collected and centrifuged at 20,000 x g at 4°C for 10 minutes. The supernatant was transferred in a new tube and a 50 µl aliquot was used in 400 µl firefly buffer+100 µl injected firefly substrate buffer. A second 50 µl aliquot was used in 400 µl renilla buffer+100 µl injected renilla substrate buffer. Light emission was detected with a Sirius luminometer for 10 seconds. The values from

transfected cells were corrected with the values of untransfected cells and each firefly value was normalized to its renilla value according to the following equation:

$$\frac{RLU^{Firefly}(\text{transfected cells}) - RLU^{Firefly}(\text{untransfected cells})}{RLU^{Renilla}(\text{transfected cells}) - RLU^{Renilla}(\text{untransfected cells})} = \text{Firefly value normalized to Renilla}$$

Firefly buffer	25 mM glycine-glycine pH 7.8
	1 mM DTT
	15 mM KH_2PO_4
	15 mM $MgSO_4$
	4 mM EGTA
Firefly substrate buffer	25 mM glycine-glycine pH 7.8
	15 mM $MgSO_4$
	4 mM EGTA
	2 mM DTT
	0.2 mM D-Luciferine
Renilla buffer	0.5 M NaCl
	0.1 M KH_2PO_4
	1 mM EDTA
	0.02 % BSA
	0.6 mM NaN_3
	pH 7.6
Renilla substrate buffer	renilla buffer+0.2 µM coelenterazine

3.2.8 Microscopy

3.2.8.1 Indirect immunofluorescence

C2C12 cells were grown on a 4 cm cell culture dish and differentiated to myotubes with horse serum for 4-7 days. Cells were washed twice with PBS and fixed with methanol at −80°C for 10 minutes. Then the cells were washed twice with PBS and twice with PBS-0.2 % gelatine. Mouse monoclonal 1F11 anti-MHC antibody was used in a dilution of 1:2 at 37°C for 45 minutes. The cells were washed twice with PBS, two times with PBS-0.2% gelatine and fluorescein-conjugated antibody raised against mouse IgG was added in 1:50 dilution at 37°C for 30 minutes. The cells were washed twice with PBS, twice with PBS-0.2% gelatine and the nuclei were stained with 1 µg/ml Hoechst 33258 diluted in PBS. After two final washing steps with PBS, the treated area of the dish was quickly dried and covered with 10 µl Mowiol buffer and a

cover slip. The fluorescein labelled antibody was visualized with a Zeiss Axiophot immunofluorescence microscope and fusion index was determined with the help of Perfect Image software according to the following equation: Fusion index [%]=(nuclei in myotubes/total nuclei) x 100. Four independent areas were analyzed and an average of them was calculated.

Mowiol buffer
2.4 g Mowiol 4-88
6 g glycerol
6 ml H_2O
12 ml 0.2 M Tris pH 8.5
2.5 % 1,4-diazobicyclo-(2.2.2)-octane DABCO

3.2.8.2 Intracellular calcium measurement

To determine the intracellular calcium concentration of cells, they were raised on cover slips. Before the measurement, the culture medium was aspirated and the cells were washed two times with PSS buffer, then loaded with PSS buffer containing 5 µM Fura-2 AM usually for 30-60 minutes. All measurements and the incubation steps were performed at 37°C. To reduce the background, Fura-2 AM was removed before the measurement by washing the cells with PSS buffer. Dual wavelength measurements of Fura-2 AM fluorescence were performed using a setup based on a Zeiss microscope equipped with a PLAN Neofluar 16x objective. Emission wavelength of 510 nm and excitation wavelength of 340 nm/380 nm were achieved with a multiway wavelength illumination system (POLYCHROME II). Spatiotemporal Ca^{2+} distributions were determined using a CCD-camera with 100 ms exposure time and 2 fold binning. Acquisition and analysis of the fluorescence images was done by TillVision (v4.01) software. All signals were background corrected and the ratio of the excitation at 340 nm/380nm was used for analysis.

PSS buffer
118 mM NaCl
5 mM KCl
1.6 mM $CaCl_2$
1.2 mM $MgCl_2$
24 mM HEPES
10 mM glucose
pH 7.4

3.2.9 Statistical analysis

Calculating the significance between the samples two-tailed, Student´s t-test was performed with unpaired, unequal distribution and p value was illustrated to be significant, when the value was less than or equal with 0.5.

3.2.10 Software tools

AIDA 2.1

TillVision v4.01

Perfect Image

4 Results

4.1 *In vitro* model for muscle differentiation and mitochondrial biogenesis

The mouse skeletal muscle cell lines C2C12 and C2F3 retain their potency to differentiate from mononucleated, growing myoblasts in a "muscle progenitor" stage through a stage of confluent, quiescent myoblasts to multinucleated myotubes in an end-differentiated stage [80]. We chose this model to study mitochondrial biogenesis because the cells are easy to maintain and differentiate and the amount of mitochondria increases during differentiation [2,3].

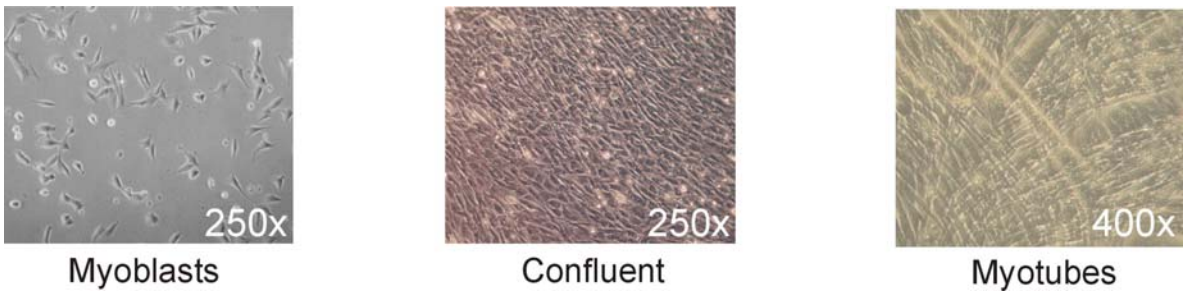

Figure 6. C2F3 cells during differentiation

Growing myoblasts were split every two to three days, but were not allowed to reach confluence since this decreases the differentiation capacity. For differentiation, cells were seeded at 50-80 % confluence. After reaching 100% confluence, growth medium was changed to differentiation medium containing 2 % horse serum and the cells were kept for additional three to five days. The differentiation level increased with time and reached a stationery phase after three to five days. Myotubes were distinguishable from myoblasts under the light microscope, as they were larger and had several nuclei.

4.1.1 Expression of differentiation markers during myogenesis

Since it is not possible to induce a state of 100 % differentiation, every myotube culture contains myoblasts as well. To quantify differentiation, we calculated the fusion index, the ratio of nuclei in myotubes vs. all nuclei by double staining for a differentiation marker (MHC) and nuclei, respectively (Figure 7).

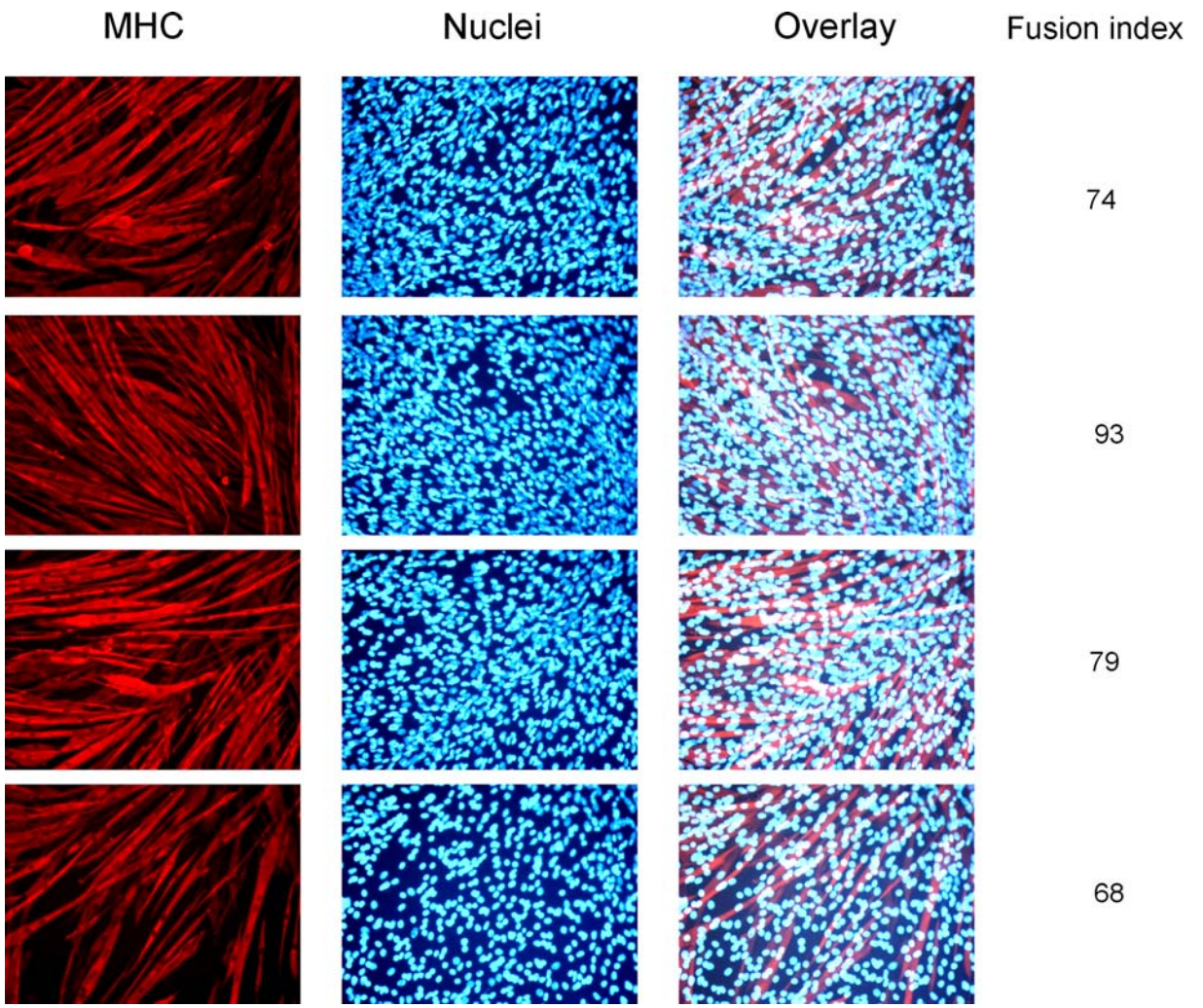

Figure 7. MHC expression of differentiated C2C12 myotubes

After cell fixation the differentiation marker myosin heavy chain (MHC) was stained with an anti-myosin heavy chain antibody (red) while the nuclei were visualized with Hoechst 33258 staining (blue). The right panel shows the overlay of the two staining. The numbers illustrate the calculated fusion indices of the representative areas at the right side.

The number of nuclei in MHC positive myotubes were divided by the total number of nuclei, resulting in the fusion index. Usually the fusion index was between 40-78 %.

During muscle differentiation several other proteins like myogenin, MyoD, myf5 and MRF-4 are also upregulated [84]. Western blot analysis was performed from nuclear extracts of C2F3 cells to visualize the myogenin protein, which is a good marker for the activated muscle differentiation program. Figure 8 shows that myogenin is not present in growing myoblasts, but appears in confluent myoblasts and remains in myotubes. MHC and myogenin expression indicate that by fusion, the muscle differentiation program of C2C12 and C2F3 muscle cells is indeed executed.

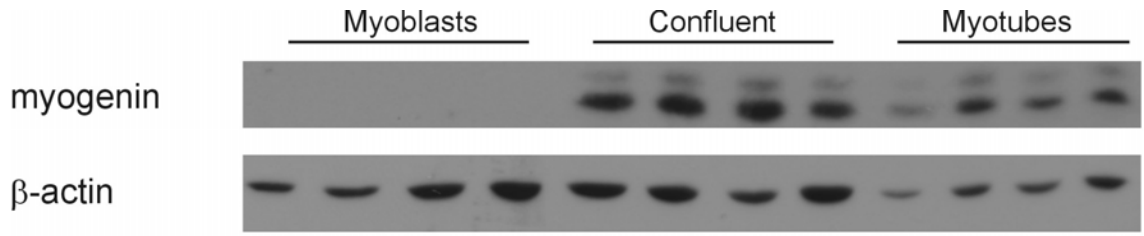

Figure 8. Myogenin expression in differentiating C2F3 cells

Nuclear extracts were prepared from four parallel samples of myoblasts, confluent cells and myotubes and were probed by Western blot with antibodies against myogenin or β-actin, which was used as a loading control.

4.1.2 Intracellular calcium levels in myoblasts and myotubes

As a second messenger, calcium is involved in several physiological pathways and plays an important role in the muscle differentiation process [19]. The elevation of intracellular calcium by the ionophore A23187 was shown to moderately induce transcription of cytochrome *c* and its promoter activity [85] as well as the phosphorylation level of AMPK [22]. Furthermore CaMKIV, which is one of the protein kinases phosphorylating and thus activating CREB-1 and which is also known to be involved in the mediation of mitochondrial proliferation [86], upregulates the expression of mitochondrial enzymes upon increased intracellular calcium concentrations [21]. Thus, we addressed the question whether resting intracellular calcium concentration differs between myoblasts and myotubes. Calcium levels were measured by staining with a fluorescent calcium binding dye, Fura-2 and it was found that the 340/380 ratio, reflecting the calcium concentration, was significantly higher in myoblasts compared to myotubes (Figure 9).

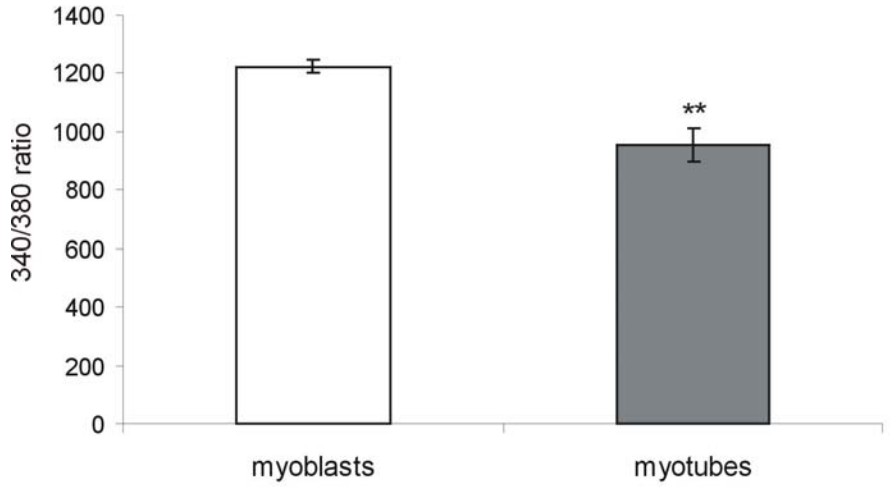

Figure 9. Calcium concentration in C2C12 cells during the differentiation process

Intracellular calcium concentration was determined by fluorescence measurement of the calcium indicator Fura-2 and the 340/380 ratios are illustrated on the y axis. C2C12 myoblasts and myotubes were loaded for 60 minutes with Fura-2 followed by a 5-10 minutes post incubation. Data are mean ± standard deviation obtained from three independent experiments. ** indicates a significant difference ($p<0.01$) between myoblasts and myotubes.

However, time course experiments showed that Fura-2 uptake was higher in myotubes compared to myoblasts (data not shown). Thus, to exclude artifacts according to an unequal concentration of Fura-2 in myoblasts vs. myotubes, fluorescence was determined every 10 minutes during the loading period and five minutes after the loading. We observed a solid increase in the 340 or 380 nm mean fluorescence values during loading reflecting the rising level of Fura-2 in the cytosol (Figure 10A), but the ratio of 340/380 increased only moderately with the loading time (Figure 10B). In every time point, myotubes picked up more Fura-2 than myoblasts, but the ratio of 340/380 of myotubes was always smaller or similar to myoblasts during the whole loading process (Figure 10).

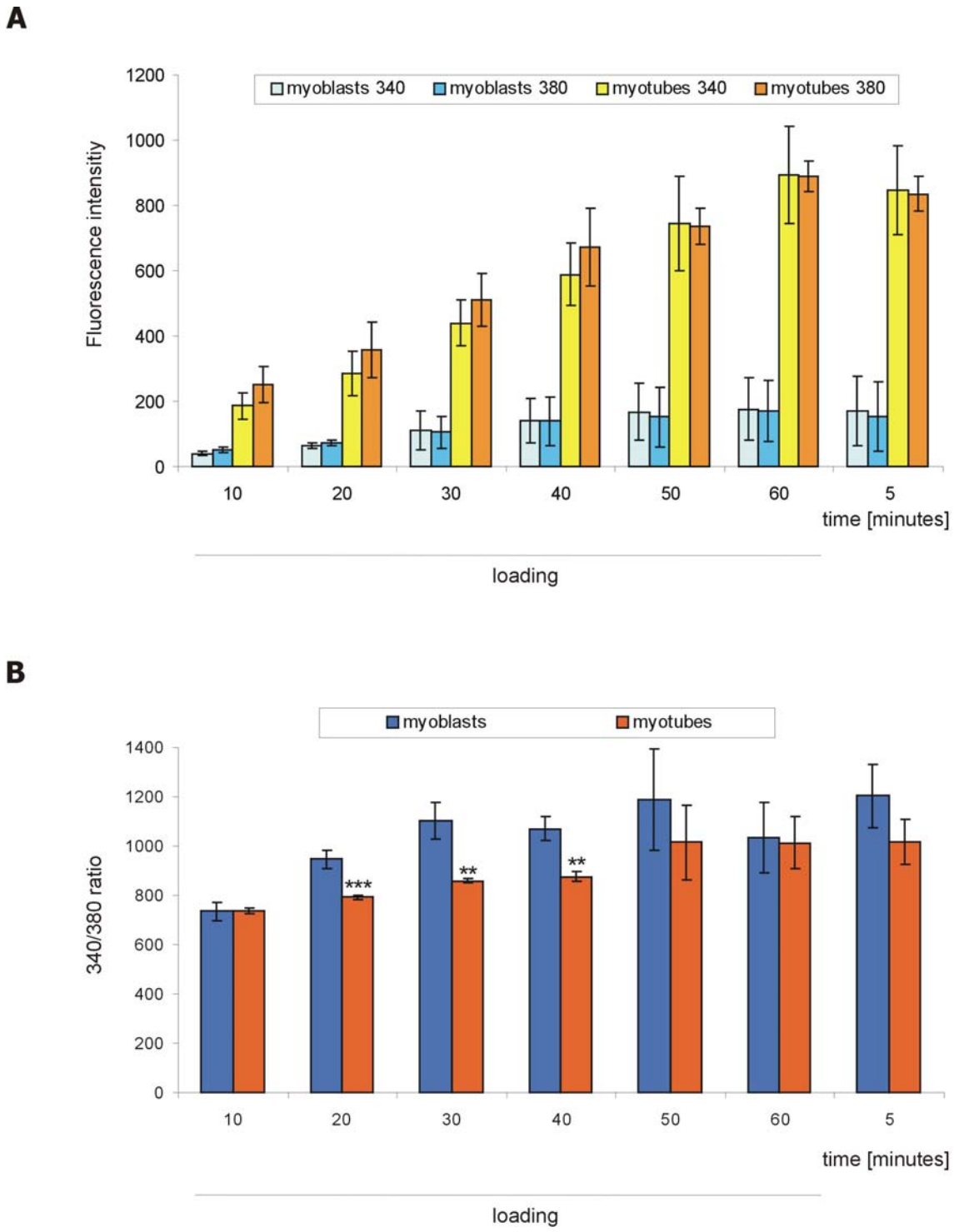

Figure 10. Calcium concentration of C2C12 cells during the loading procedure

Intracellular calcium concentration was determined by fluorescence measurement of the calcium indicator Fura-2. C2C12 myoblasts (blue) and myotubes (orange and red color) were loaded from 10 to 60 minutes with Fura-2 followed by a five minutes post incubation period. Data are mean ± standard deviation obtained from three myoblast and four myotube samples. ***A*** the individual fluorescence intensities at 340 nm, 380 nm as well as ***B*** the ratios of 340/380 are illustrated on the y axis. ** indicates a significant difference ($p<0.01$), *** indicates a significant difference ($p<0.001$) between myoblasts and myotubes. Unless it is not indicated there were no significant differences between myoblasts and myotubes.

Since differentiation and probably mitochondrial biogenesis is initiated at the step of confluence, we measured calcium level in the confluent stage, in which cells were incubated either with differentiation medium containing horse serum or cultivated in fetal calf serum. It was suggested, that 100 % confluence is needed to execute the muscle differentiation program, while horse serum alone is not sufficient to induce differentiation. To study how cell density influences resting calcium, cells were seeded at low to high densities. The calcium concentration was significantly increased in confluent cells seeded at high cell density (95 %) in the presence of horse serum compared to cells cultivated at the same densities in fetal calf serum (Figure 11, right columns). However, cells seeded at low densities (30 and 60 %) did not show elevated calcium concentration upon change to horse serum (Figure 11, first four columns). Surprisingly, the fluorescence intensity of Fura-2 at 340 nm was enhanced about to two-three fold by horse serum, independent of the starting cell concentration (Figure 11, white columns). In conclusion, intracellular calcium levels were found to be higher in myoblasts compared to myotubes, while differentiation medium alone seems to increase calcium concentration in confluent cells, suggesting that calcium elevation occurs after the confluent stage during muscle differentiation.

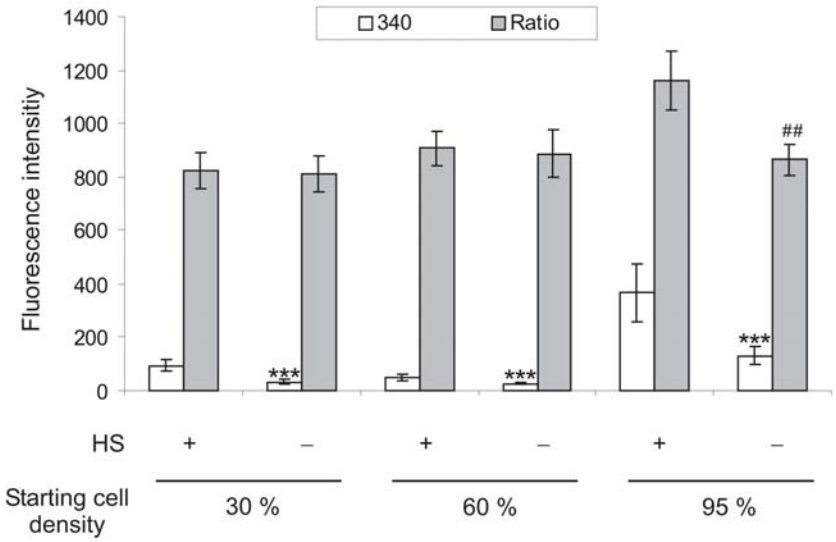

Figure 11. Calcium concentration in confluent C2C12 cells

Intracellular calcium concentration was determined by fluorescence measurement of the calcium indicator Fura-2. The individual fluorescence intensities at 340 nm or the 340/380 ratios are illustrated on the y axis. Cells were seeded at 30, 60, 95 % cell densities two days before the experiment and cultivated in FCS. Cells were then cultivated with (+HS) or without horse serum (–HS) for additional 16 hours. Confluent myoblasts were loaded with Fura-2 for 1 hour followed by a 15 minutes post incubation period. Data are mean ± standard deviation obtained from five samples. *** indicates a significant difference ($p<0.001$) of 340 nm fluorescence values in the presence or absence of HS. ## indicates a significant difference ($p<0.01$) of 340/380 ratios in the presence or absence of HS. Unless it is not indicated there were no significant differences of 340/380 ratios in the presence or absence of HS.

4.1.3 α-actinin4 localization during differentiation

Goffart *et al*. have recently identified a new palindromic sequence, which was found to be common in a large number of nuclear encoded mitochondrial genes. Proteins binding to this sequence were identified by preparative EMSA and MALDI/TOF. One of these *cis*-element binding proteins, α-actinin4, was shown to have an altered binding pattern in EMSA when myoblasts were compared to myotubes [87]. Thus, Western blot analysis from nuclear and cytoplasmic extracts of myoblasts and myotubes were performed to verify possible altered expression of α-actinin4. The levels of α-actinin4 in the cytoplasmic fraction of myoblasts, confluent cells and myotubes were equal (Figure 12A and C). However, compared to myoblasts the nuclei of myotubes and confluent cells showed a significant, two- to threefold higher content of α-actinin4 (Figure 12B and D). In both cellular fractions, two different proteins, β-actin and β-tubulin for cytoplasmic fractions and β-actin and histone H1 for nuclear fractions, respectively were used as loading controls. The expression levels of these loading controls correlated well with each other. The purity of nuclei was confirmed by additional Western blot analysis. β-actin is expressed about equally in cytoplasmic and nuclear fractions, histone H1 was only observed in the nuclei and as expected β-tubulin was found mainly in the cytoplasmic fractions (Figure 12E). The α-actinin4 nuclear translocation occurring during myogenesis indicates that it is a possible transcription factor, which binds the newly identified *cis*-element and may transactivate muscle specific genes.

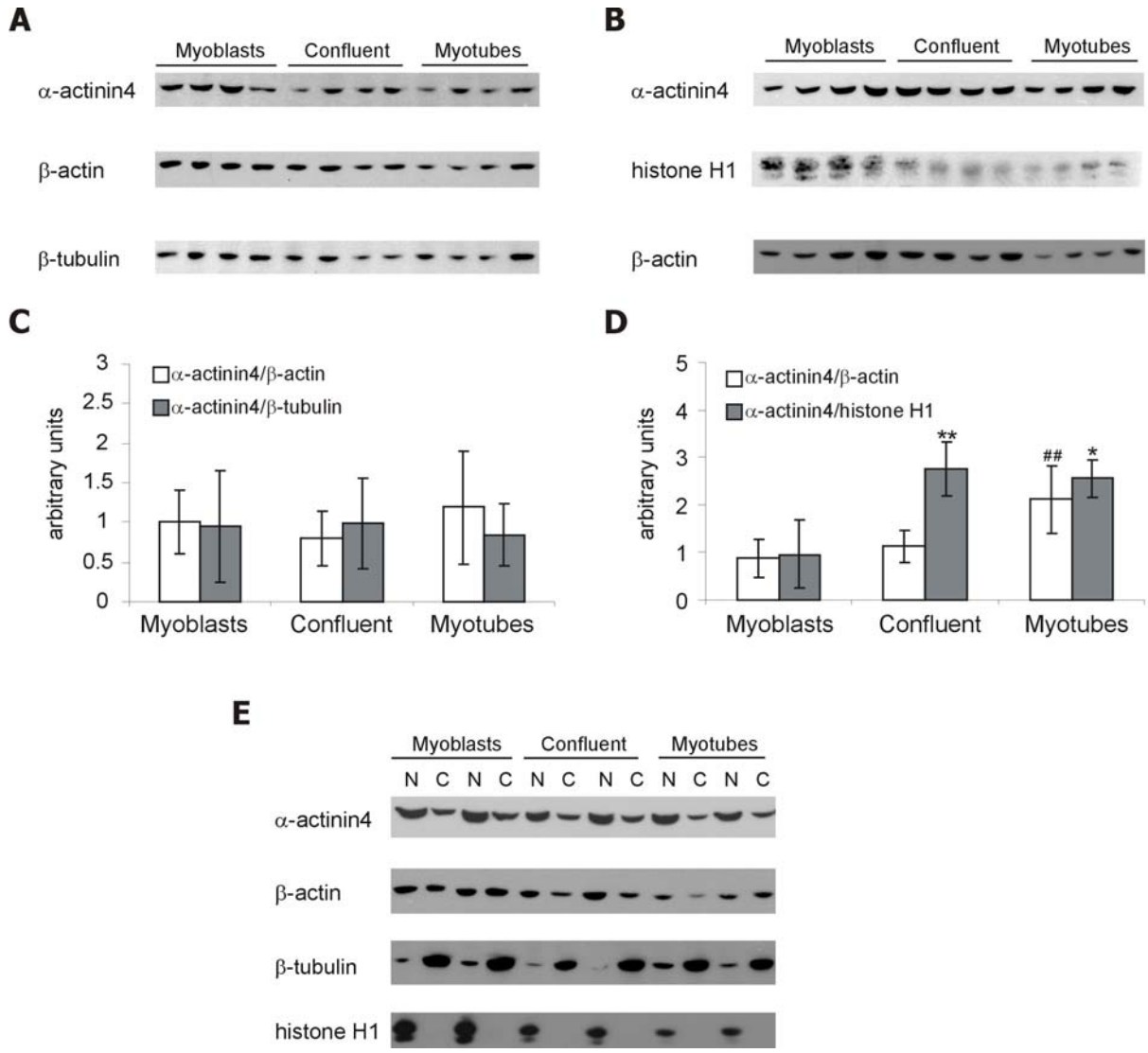

Figure 12. Expression of α-actinin4 in nuclear and cytoplasmic fractions of C2F3 cells

Western blots of ***A*** cytoplasmic and ***B*** nuclear fractions were prepared from myoblasts, confluent cells or myotubes and probed with antibodies as indicated. The intensity of bands was evaluated densitometrically for ***C*** cytoplasmatic and ***D*** nuclear fractions. Data are mean ± standard deviation obtained from four samples normalized to the loading controls. * indicates a significant difference ($p<0.05$), ** indicates a significant difference ($p<0.01$) of the α-actinin4/histone H1 ratio between myoblast values and confluent cells/myotube values. ## indicates a significant difference ($p<0.01$) of the α-actinin4/β-actin ratio between myoblast and myotube values. ***E*** Nuclear (N) and cytoplasmic proteins (C) were analyzed by Western blot side-by-side to control the purity of the nuclear fraction.

4.2 The role of AMPK in cytochrome c promoter regulation

4.2.1 Cloning of AMPKα1-CA into pTRE2Hyg vector

The truncation of the full-length AMPKα1 protein at position 312 creates an AMPK lacking the interaction domain with β and γ subunit, but preserves the kinase domain. This constitutively active AMPKα1-CA was successfully used in former studies [40,41,88] to investigate the effect of the kinase without the need of phosphorylation by the upstream kinase. The pcDNA3-AMPKα1-CA construct contains the sequence of the rat AMPKα1-CA downstream of a viral, constitutively active promoter. Our initial aim was to create a muscle cell line expressing AMPKα1-CA protein in an inducible manner. Therefore, we chose the Tetracycline (Tet) regulated system, in which the expression of the gene of interest is activated by the TRE (Tetracycline response element) promoter in the presence of the transactivator protein producing helper vector. In the presence of Tetracycline or its derivatives Doxycycline (Dox), the transactivator protein binds the ligand resulting in the inhibition of transcription (Tet-Off system).

In order to express the AMPKα1-CA in mammalian cells, its cDNA sequence was cloned from pcDNA3-AMPKα1-CA into the mammalian expression vector pTRE2Hyg.

4.2.2 Generation of stable cell lines expressing tTA transactivator

C2C12 E6 and C2C12 D3 clones were provided by Prof. Brüning (Köln), stably expressing the transactivator from the inserted plasmid pCMV-tTA and were tested for their Dox sensitivity using a pTRE2Hyg-Firefly reporter plasmid, which was transiently transfected to test the inducibility (Figure 13). Both clones expressed the Firefly protein, but D3 gave a higher absolute luciferase activity. In both cases the transcription from the TRE promoter was blocked in the presence of Dox, and 1 μg/ml was enough for at least a 5-fold decrease. However, an enzyme activity still remained with even 5 μg/ml Dox suggesting that the system is leaky. In the following experiments the C2C12 D3 clone was used and transfected with the pTRE2Hyg-AMPKα1-CA plasmid to generate stable clones.

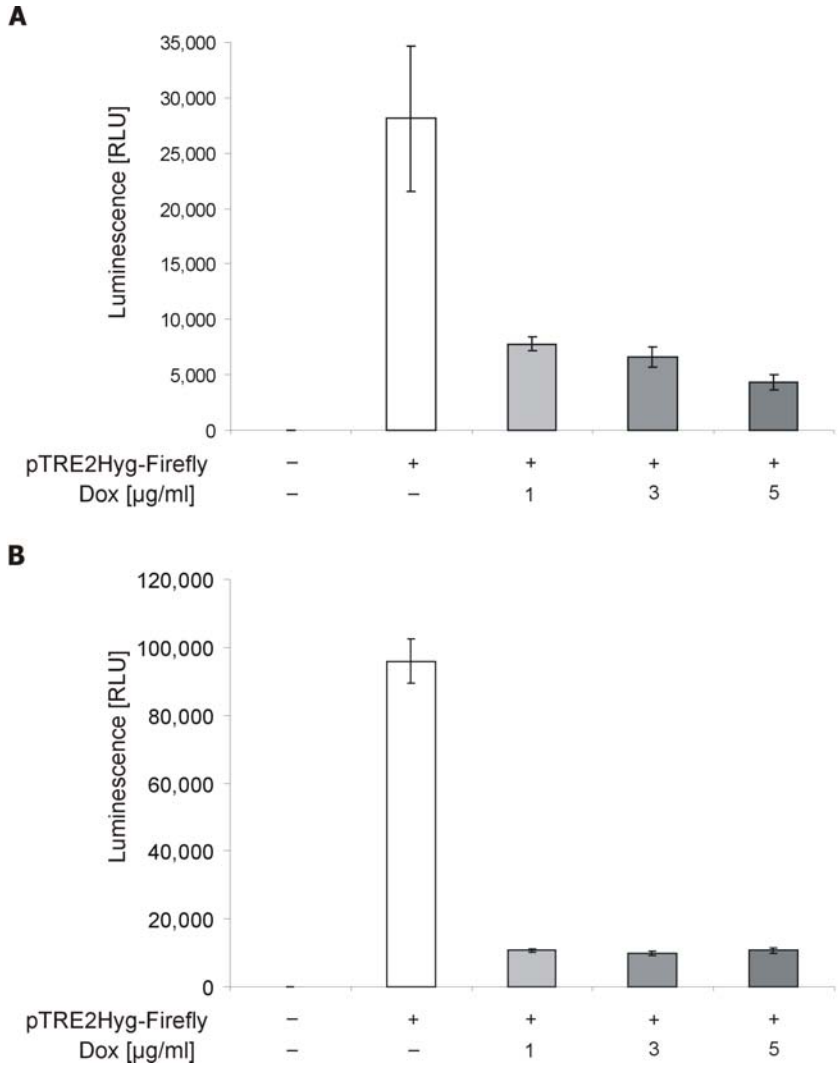

Figure 13. TRE promoter activity in TRE transactivator (tTA) expressing cells

Firefly luciferase activity was measured in (***A***) C2C12 E6 or in (***B***) C2C12 D3 cells driven by the TRE promoter in the presence or absence of Dox. Data are mean ± standard deviation obtained from six samples. RLU: relative light units

C2C12 E6 and D3 cell lines were also tested for the optimal amount of Hygromycin B, the selection antibiotic to eliminate those cells, which did not take the plasmid. 100, 300, 500, 700, 900 µg/ml Hygromycin B concentrations were given to the cell culture medium and the cell viability was monitored for five days. 700 µg/ml was enough to kill all the cells in five days, therefore this concentration was used in further experiments.

4.2.3 Transfection, isolation and selection of AMPKα1-CA clones

The C2C12 D3 cells were transfected with the pTRE2Hyg-AMPKα1-CA construct. The selection was started after two days in the presence of G418 (Neomycin) and Hygromycin B. Dox was also included in the medium to inhibit the expression of AMPKα1-CA. Growing clones were isolated after two weeks and transferred to separate wells. From 300 isolated clones 71

were further cultivated to a high scale. AMPKα1-CA expression was induced by removal of Dox for two days, total protein was extracted and the samples were tested for the expression of AMPKα1-CA by Western blot analysis.

4.2.4 Analysis of AMPKα1-CA clones

The AMPKα1-CA contains an N-terminal c-myc tag, which was used to detect the AMPKα1-CA expression in the transfected cells. Purified Myc-tagged coronin 7 protein was used as positive control while C2C12 D3 untransfected cells served as negative control (Figure 14). The AMPKα1-CA protein has a predicted molecular weight of 37 kDa, but unfortunately in this range an artificial background band also appeared, which was present in the negative control D3 cells as well.

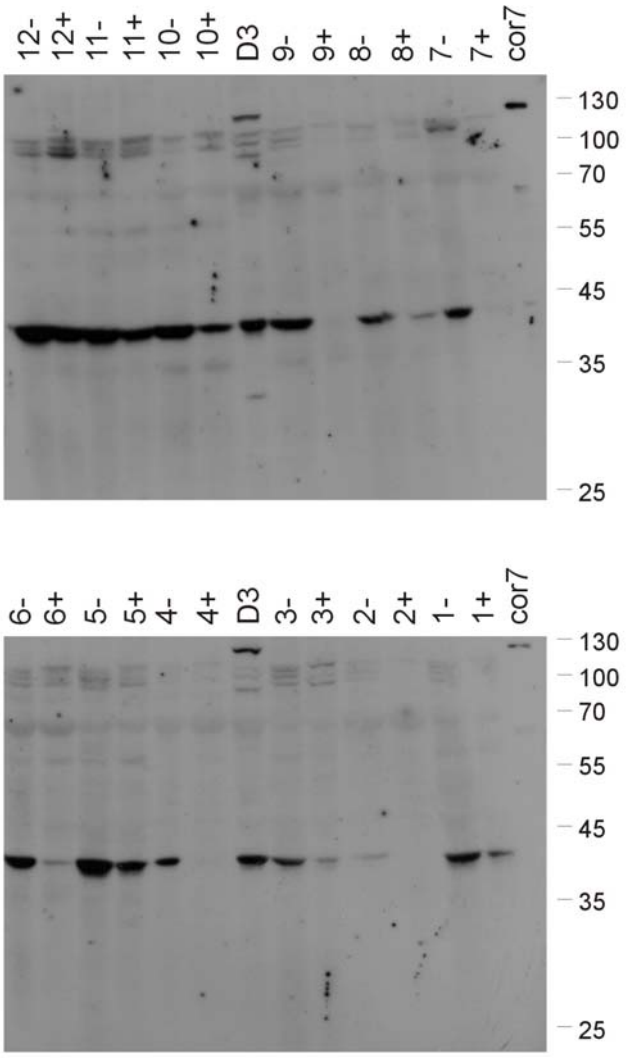

Figure 14. AMPKα1-CA clones using anti-c-myc antibody

Western blot analysis of AMPKα1-CA expressing C2C12 D3 clones in the presence (+) or absence (–) of Dox. C2C12 D3 cells were used as negative control, purified coronin-7 Myc-fusion protein as positive control. The size of molecular weight markers is given in kDa.

To exclude this artifact we changed our strategy and used an AMPKα specific antibody instead of anti-c-myc antibody, which recognizes the endogenous wild-type AMPKα subunits (white arrow, molecular weight 63 kDa) but also well detects the truncated AMPKα1-CA protein (black arrow) at 37 kDa (Figure 15 and Appendix Figure 2).

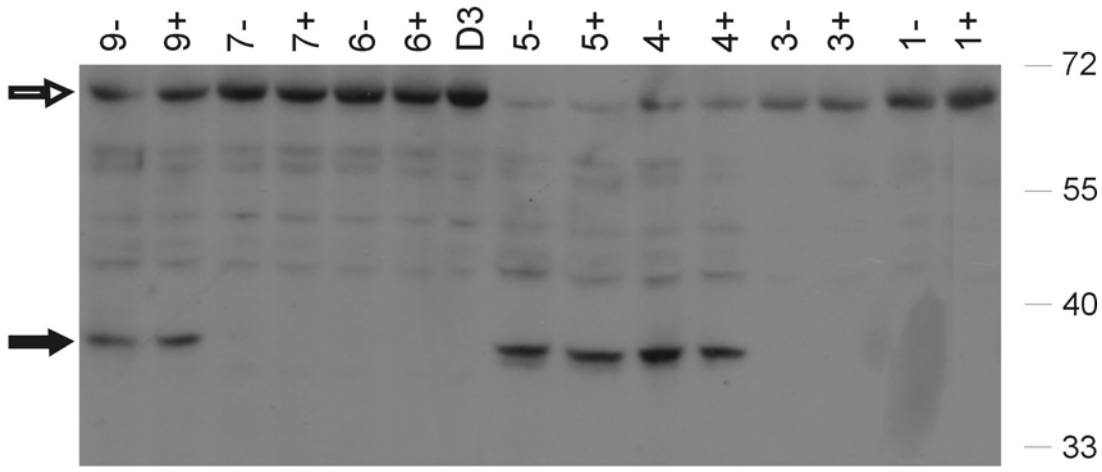

Figure 15. Western blot of AMPKα1-CA clones using anti-AMPKα antibody (showed partially)

Western blot analysis of AMPKα1-CA expressing C2C12 D3 clones in the presence (+) or absence (–) of Dox. C2C12 D3 cells were used as negative control. White arrow shows the endogenous and black arrow the AMPKα1-CA proteins. The complete screening of AMPKα1-CA clones illustrated in the Appendix Figure 2. The size of molecular weight markers is given in kDa.

Table 2 summarizes the results: From 71 clones 68 were analyzed and 49 were found to be positive for AMPKα1-CA expression, but none of them were Dox regulated, as AMPKα1-CA was produced also in the presence of Dox. Some clones seemed to be regulated by Dox, but this was not reproducible in further experiments. Clone 27 was chosen as strong expressor, clone 5 as intermediate and clone 1 as no expressor to analyze the effect of the constitutively active AMPKα1 subunit in latter experiments.

Table 2. Summary of the AMPKα1-CA clones[1]

Name*	Exp.#
CA-1	-
~~CA-2~~	
CA-3	-
CA-4	+
CA-5	**+**
CA-6	-
CA-7	-
CA-8	+
CA-9	+
CA-10	-
CA-11	-
CA-12	-
CA-13	+
CA-14	+
CA-15	-

Name	Exp.
CA-16	+
CA-17	+
CA-18	+
CA-19	+
CA-20	+
CA-21	-
CA-22	+
CA-23	+
CA-24	+
CA-25	+
CA-26	+
CA-27	**+++**
CA-28	+
CA-29	-
CA-30	-

Name	Exp.
CA-31	-
CA-32	-
CA-33	+
CA-34	+
CA-35	+
CA-36	-
CA-37	+
CA-38	+
CA-39	-
CA-40	+
CA-41	+
CA-42	+
CA-43	+
CA-44	+
CA-45	+

Name	Exp.
CA-46	+
CA-47	+
~~CA-48~~	
CA-49	+
~~CA-50~~	
CA-51	+
CA-52	+
CA-53	+
CA-54	+
CA-55	+
CA-56	+
CA-57	-
CA-58	+
CA-59	+
CA-60	-

Name	Exp.
CA-61	+
CA-62	-
CA-63	+
CA-64	+
CA-65	-
CA-66	+
CA-67	+
CA-68	+
CA-69	+
CA-70	+
CA-71	+

[1] The table summarizes the results of Western blot analysis from Figure 15 and Appendix Figure 2 illustrating the induction level of AMPKα1-CA.

* indicates the name of the AMPKα1-CA clones,

illustrates the expression (+) or the lack (-) of AMPKα1-CA protein from whole cell extracts,

+++ indicates strong AMPKα1-CA expression.

4.2.5 Immunoprecipitation of AMPKα1-CA

In order to study whether the AMPKα1-CA expressing cell line has an increased kinase activity, kinase assays were performed. The AMPKα1-CA protein was immunoprecipitated from an extract of the strong expressor CA-27 clone. To test the efficiency of the commercial antibody in immunoprecipitation experiments, different amounts were used and proteins bound to the beads were detected with the same AMPKα antibody. As depicted in Figure 16A, the AMPKα antibody could not completely deplete the expressed AMPKα1-CA protein from the supernatant of CA-27. Therefore, AMPKα1-CA protein was immunoprecipitated with a c-myc antibody. Figure 16B shows that 10 µg c-myc antibody was enough to completely precipitate the AMPKα1-CA protein from the cell lysate, as no protein was visible after immunoprecipitation in the supernatant. The beads specifically bound the AMPKα1-CA protein expressed by clone 27,

while beads incubated with extracts from clone 1, which does not express the fusion protein, showed no specific protein binding. Strong immunoreactivity is present in the molecular range of AMPKα1-CA, but a distinct AMPKα1-CA band is detected in the beads sample of clone 27, while it is missing from the beads sample of clone 1 (Figure 16B, rectangles).

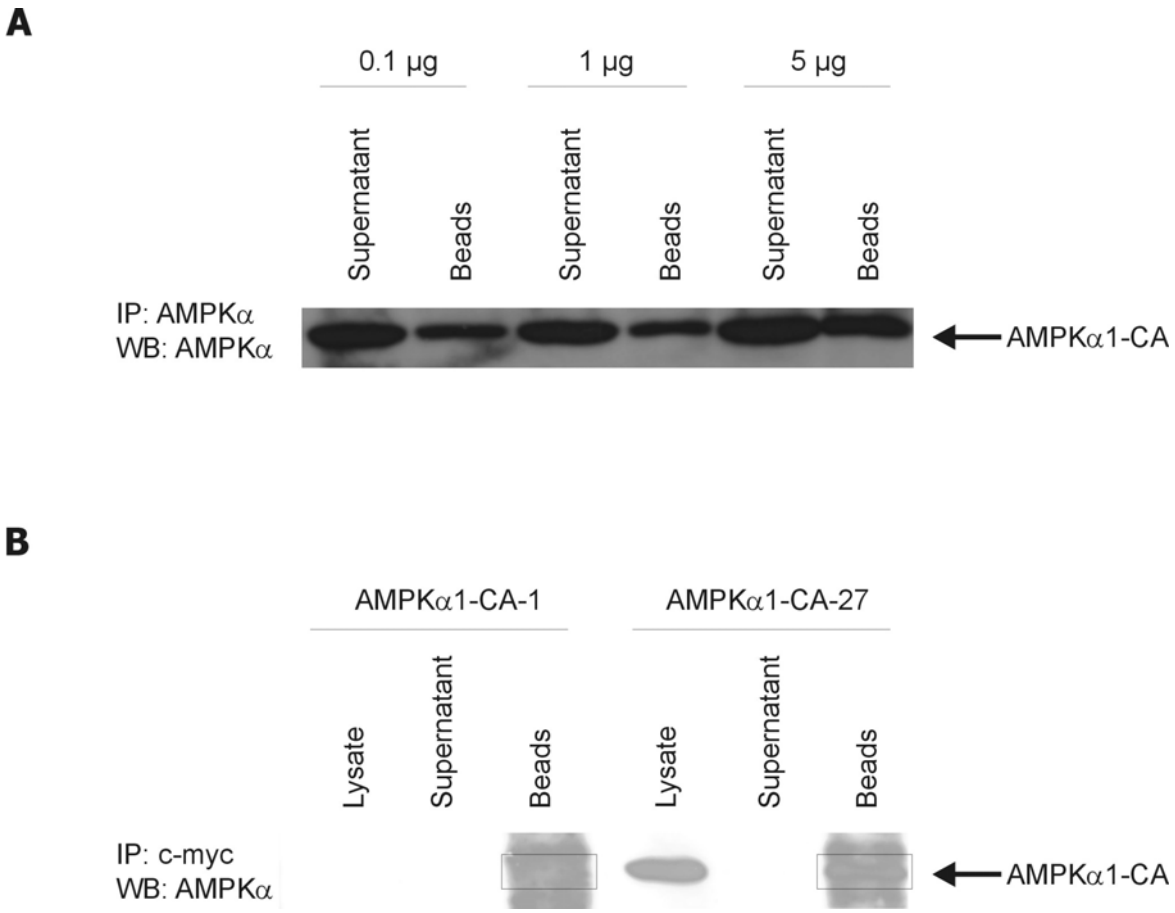

Figure 16. Immunoprecipitation of AMPKα1-CA by AMPKα or c-myc antibodies

Western blot was probed with commercial AMPKα antibody. ***A*** Samples were prepared from AMPKα1-CA-27 (strong expressor) cell lysate with 0.1, 1 or 5 µg AMPKα antibody (Cell Signaling) ***B*** The samples were prepared from AMPKα1-CA-27 and CA-1 (non expressing) cell lysates with 10 µg c-myc antibody. Lysate: cell lysate before immunoprecipitation, Supernatant: cell lysate after immunoprecipitation, Beads: proteins eluted from the beads after immunoprecipitation

4.2.6 AMPKα1 and AMPKα1-CA kinase assay

The kinase activity of AMPKα1-CA was determined from clone 27, clone 1 and C2C12 D3 untransfected cells. The strong expressor cell line clone 27 showed an elevated AMPKα1-CA kinase activity compared to the non-expressing clone 1 and the untransfected control (Figure 17A). The presence of Dox did not influence the kinase activity in agreement with its inability to inhibit the expression of AMPKα1-CA. To compare the constitutively active to the endogenous

AMPKα1 activity, the endogenous kinase was immunoprecipitated with a commercial anti-AMPKα antibody. Interestingly, no or very low kinase activity was obtained (Figure 17B), which could be a consequence of incomplete immunoprecipitation (Figure 16A). Thus, to study the endogenous AMPKα1 kinase activity an antibody provided by Dr. Carling was used to immunoprecipitate the endogenous AMPKα1 (Figure 17B). The basal kinase activity was found to be similar in myoblasts, confluent cells and myotubes (Figure 17C). However, the endogenous kinase activity was about eight times higher as the highest AMPKα1-CA kinase activity (Figure 17A and C).

In conclusion, we established a cell line expressing the AMPKα1-CA continuously, which has an elevated kinase activity. However, comparing AMPKα1-CA to the endogenous kinase activity there is an eight times difference between them.

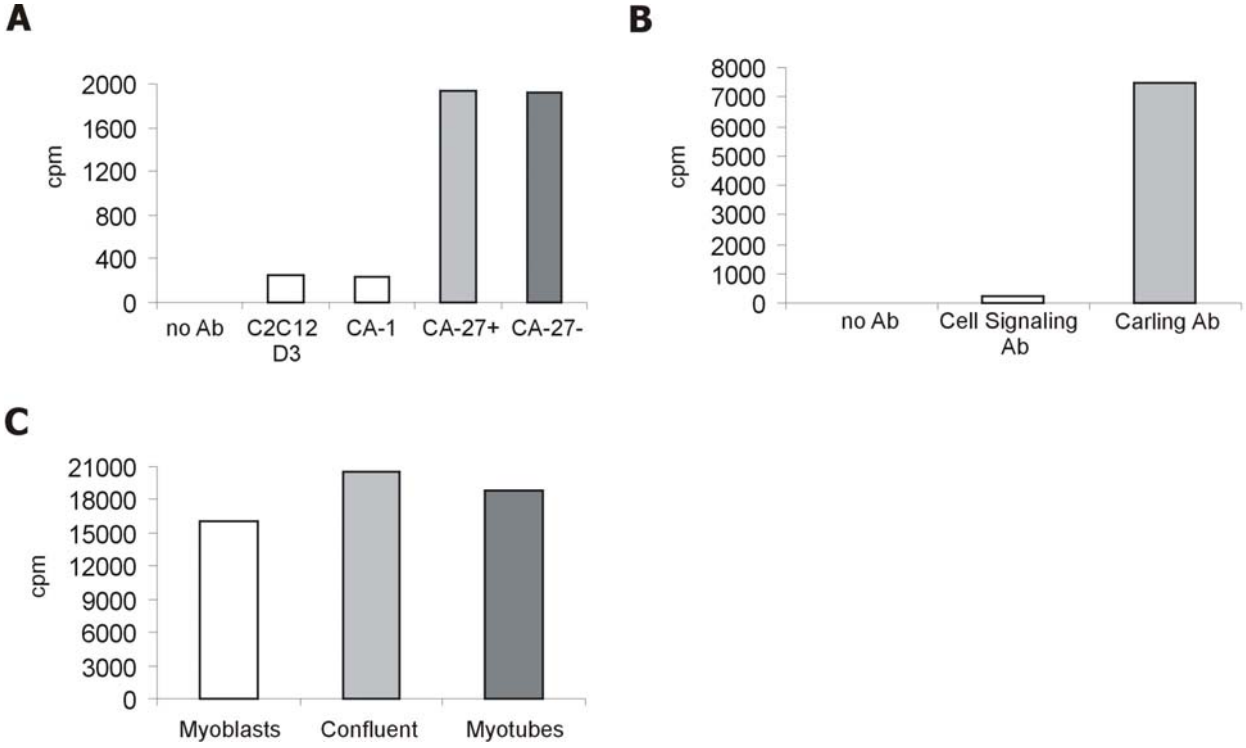

Figure 17. Endogenous AMPKα1 and AMPKα1-CA kinase assays

A Kinase activity of the anti-c-myc Ab immunoprecipitated AMPKα1-CA from myoblasts of C2C12 D3 and AMPKα1-CA-1 (negative control) and CA-27 (strong expressor) cell lines in the presence (+) or absence (–) of Dox. ***B*** Endogenous AMPKα1 activity immunoprecipitated by Cell Signaling anti-AMPKα or anti-AMPKα1 Ab provided by Dr. Carling. ***C*** Endogenous AMPKα1 activity immunoprecipitated by anti-AMPKα1 Ab provided Dr. Carling from C2C12 myoblasts, confluent cells and myotubes. Data are from a single experiment. cpm: counts per minutes

4.2.7 Analysis of cytochrome *c* promoter activity in AMPKα1-CA expressing cells

To investigate whether the constitutively active AMPKα1 activates the cytochrome *c* promoter we transfected stable AMPKα1-CA clones with a cytochrome *c* reporter gene construct containing the full length rat cytochrome *c* promoter upstream a firefly reporter gene and with a control CMV promoter-activated renilla reporter gene. The cell lysate used for luciferase measurement was also tested by Western blot to check the expression level of AMPKα1-CA. These results confirmed the former experiments, namely clone 1 used as negative control does not express the AMPKα1-CA, clone 5 expresses it in a moderate level and clone 27 is a strong expressor of the fusion protein (Figure 18).

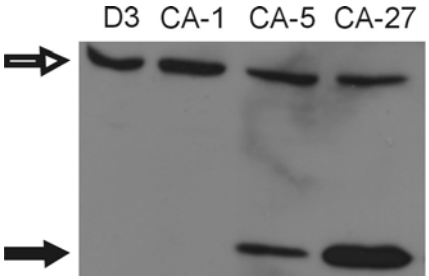

Figure 18. AMPKα1-CA protein expression level in AMPKα1-CA clones

Western blot probed with anti-AMPKα Ab (Cell Signaling) was performed from the lysate of C2C12 D3, clone 1, clone 5 and clone 27 cell lines used for luciferase assays. All cells were maintained in the absence of Dox. White arrow shows the endogenous AMPKα and the black arrow the AMPKα1-CA proteins.

Despite of the expression of AMPKα1-CA the cytochrome *c* promoter activity was neither elevated in the intermediate expressor clone 5 nor in the strong expressor clone 27 (Figure 19A). Confirming earlier experiments, Dox did not change the expression of AMPKα1-CA (Figure 18) hence it did not have any effect on the cytochrome *c* promoter activity (Figure 19A). The approach to transiently overexpress the AMPKα1-CA efficiently enough was not successful (Dr. Carling, personal communication). In order to come to the conclusion, we finally transiently cotransfected two dominant negative constructs, dominant negative AMPKα1 and α2, together with cytochrome *c* firefly and renilla reporter vectors. Cytochrome *c* promoter activity was determined in myoblasts, confluent cells and in myotubes. Overexpression of AMPK dominant negative constructs did not change the cytochrome *c* promoter activity, neither in myoblasts nor in confluent cells nor in myotubes (Figure 19B). However, the activity of cytochrome *c* promoter was increased several fold upon differentiation comparing myoblasts to myotubes, verifying the induction of the promoter upon myogenesis, previously shown [32].

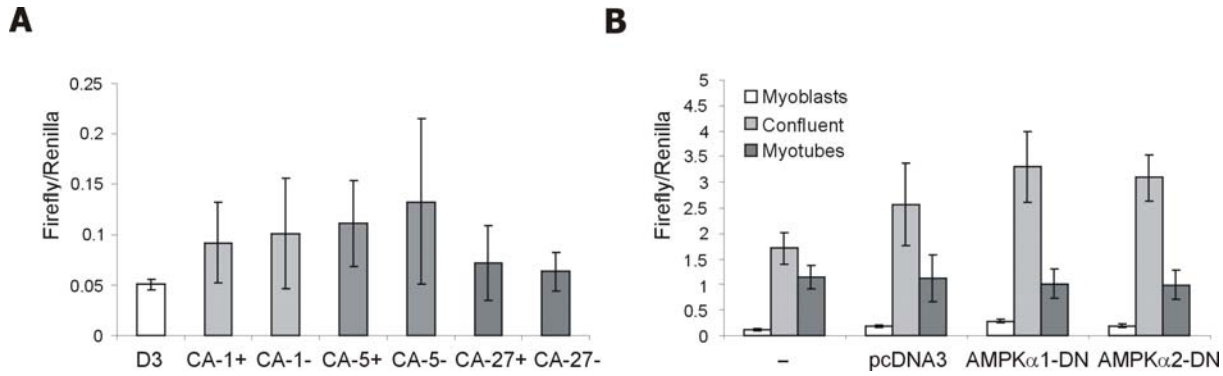

Figure 19. Cytochrome *c* promoter activity in (*A*) AMPKα1-CA stablely transfected cell lines or (*B*) transiently transfected cells

A The promoter activity was measured in C2C12 D3 untransfected myoblasts or in stable myoblasts of clone 1, 5, 27 in the presence (+) or absence (–) of Dox. ***B*** The promoter activity was measured in the presence of pcDNA3 empty vector, AMPKα1-DN or AMPKα2-DN (dominant negative) vectors in myoblasts, confluent cells or myotubes. Data are mean ± standard deviation obtained from (*A*) six or (*B*) nine samples.

4.3 CREB-1 is involved in cytochrome *c* promoter regulation

Former experiments of the laboratory suggested that CREB-1 is necessary for the activation of the cytochrome *c* promoter during muscle differentiation (see 2.3 and [32]).

4.3.1 CREB-1 and ATF-1 during myogenesis

The expression pattern of CREB-1 isoforms was investigated in C2F3 myoblasts, confluent cells and myotubes. The total amount of CREB-1 proteins decreased during the differentiation program (Figure 20A and B) but the level of phosphorylated CREB-1 level remained unchanged (Figure 20C and D). Surprisingly, both the anti-CREB and anti-P133-CREB antibody, which recognizes Ser-133 phosphorylated CREB-1 proteins, detected two CREB-1 immunoreactive bands (Figure 20A and C) with an almost similar molecular weight (42 and 43 kDa). We called them CREB-1α and CREB-1Δ (see below), being the possible products arising from two different alternatively spliced isoforms of the *CREB-1* gene product. The anti-CREB antibody also recognizes the ATF-1 protein with about 37 kDa molecular weight. The amount of ATF-1 decreased during the differentiation as well (Figure 20A and G), while the P-ATF-1 level was highest in myoblasts, significantly decreased in confluent cells and increased again in myotubes (Figure 20C and H). One should note that for visualizing ATF-1 expression, the Western blot had to be exposed for much longer time periods, than for detecting CREB-1. However, this longer exposure time does not mean a lower ATF-1 level in these cells, as the antibody is only 72 % homologous to the ATF-1 protein sequence in contrast to the 100 % homology to the CREB-1 protein. Ratios were calculated from the intensity of the upper (CREB-1α) and the lower CREB immunoreactive band (CREB-1Δ). The CREB-1α/CREB-1Δ ratio increased about threefold during myogenesis (Figure 20A and E), while the P133-CREB-1α/P133-CREB-1Δ ratio was elevated significantly about eightfold in myotubes compared to myoblasts (Figure 20C and F).

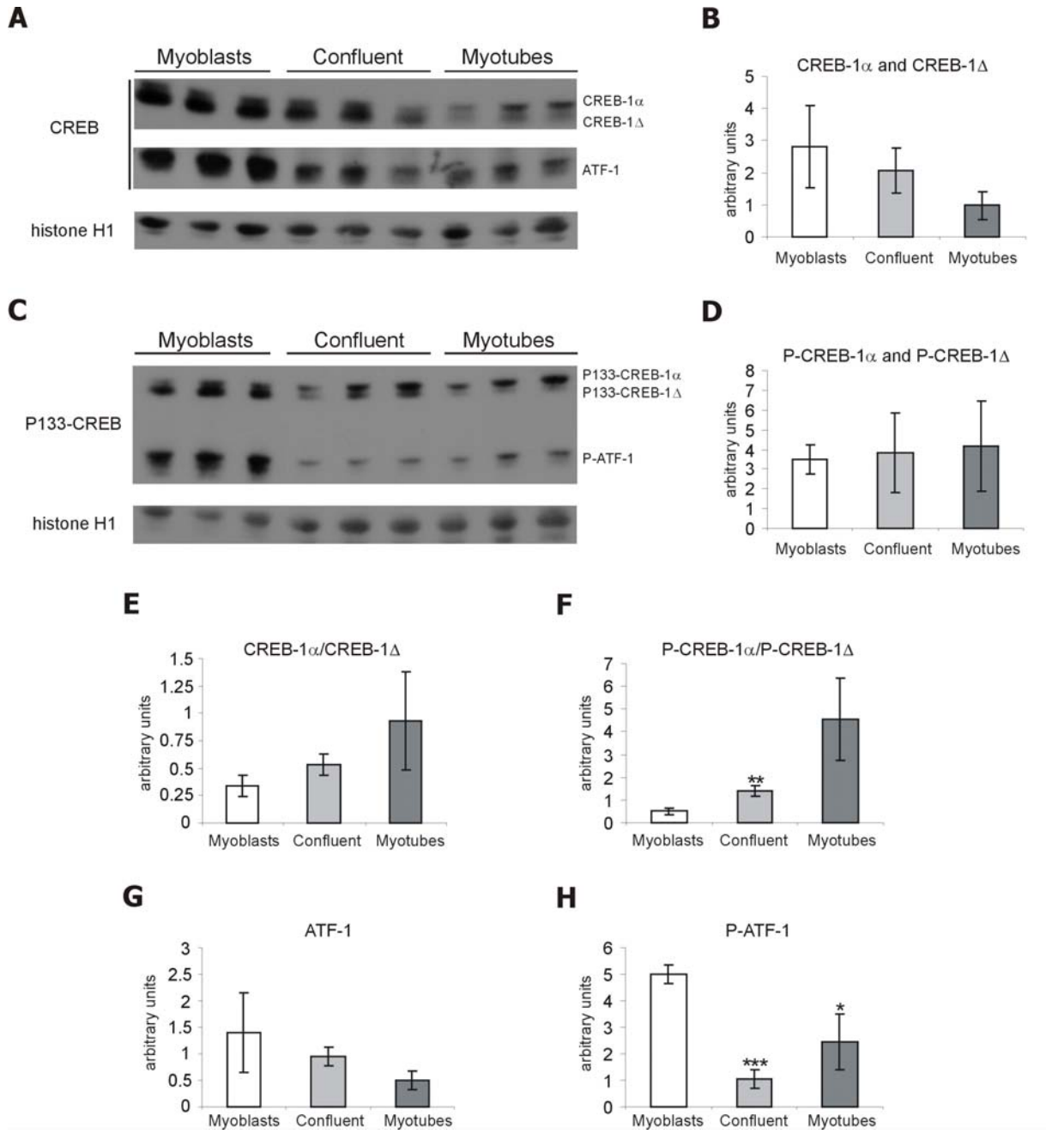

Figure 20. Protein expression of CREB-1 family members during muscle differentiation

Nuclear extracts were made from myoblasts, confluent cells and myotubes. ***A*** CREB-1 and ATF-1, or ***C*** P133-CREB-1 and P-ATF-1 proteins were detected with the antibodies indicated on the left side of the picture. Histone H1 level was used as internal loading control and values were normalized to it. The total ***B*** CREB-1, ***D*** P133-CREB-1 or ***G*** ATF-1 level were densitometrically evaluated as well as the ***E*** CREB-1α/CREB-1Δ, ***F*** P133-CREB-1α/P133-CREB-1Δ ratios or ***H*** P-ATF-1 protein amounts. Data are mean ± standard deviation obtained from three samples. * indicates a significant difference ($p<0.05$), ** indicates a significant difference ($p<0.01$), *** indicates a significant difference ($p<0.001$) between myoblast values and confluent/myotube values. Unless it is not indicated there were no significant differences between myoblast values and confluent/myotube values.

4.3.2 CREB-1 isoforms in C2F3 cells

Western blots showing double CREB-1 immunoreactive bands initially led us to the first hypothesis that they are phosphorylated and unphosphorylated forms of CREB-1. By incubation with phosphatase, both phospho-133 CREB immunoreactive bands however disappeared, while the intensity of the CREB-1 immunoreactive bands remained unchanged (Figure 21), indicating that both bands are phosphorylated.

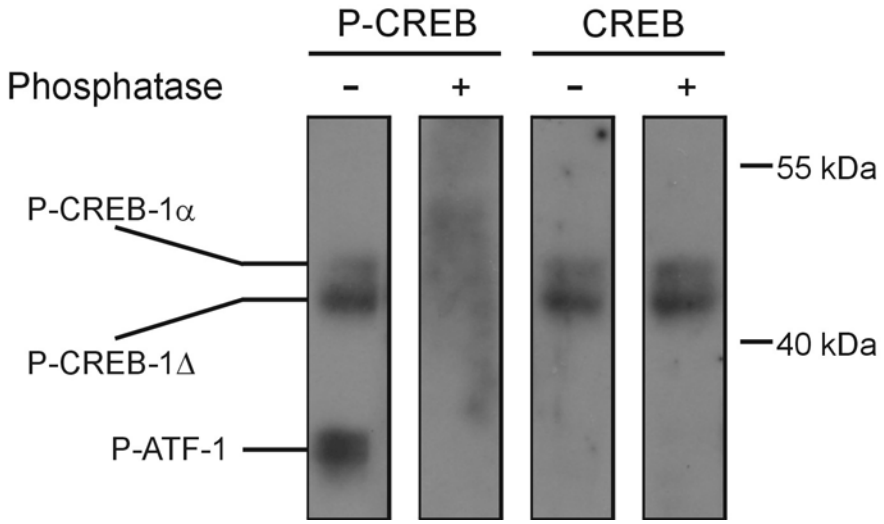

Figure 21. Phosphatase treatment of CREB-1 immunoreactive bands

Nuclear extracts of confluent cells were separated with SDS-PAGE and blotted to a nitrocellulose membrane. The membrane was treated with (+) or without (−) phosphatase followed by antibody probing, as indicated above the picture.

Thus, alternatively, these double bands could be the CREB-1 family members CREB-1 and CREM. To investigate this, specific CREB-1 recognizing antibodies were used in nuclear extracts of C2F3 cells. The anti-CREB antibody from Cell Signaling recognizes every CREB-1 family member: CREB-1, CREM and ATF-1, while the antibody from Upstate recognizes only CREB-1, but not CREM and ATF-1. A specific antibody was used from Santa Cruz directed against the exon 5 domain, which is present in CREB-1α but spliced out from the mRNA of CREB-1Δ.

The results showed that Cell Signaling and Upstate antibodies recognize the same double bands (Figure 22), which exclude the presence of the CREM protein. The Santa Cruz antibody detects only a single immunoreactive band with the same molecular weight as the upper band detected by Cell Signaling and Upstate antibodies. These Western blots thus indicate that these bands are the CREB-1α (upper band) and CREB-1Δ (lower band) isoforms present in C2F3 cell nuclei.

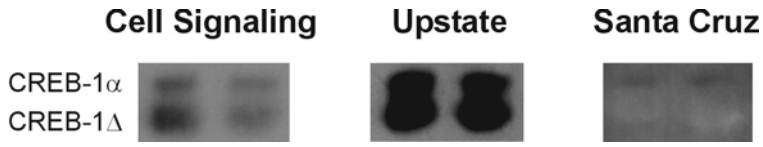

Figure 22. Identification of CREB-1α and CREB-1Δ protein isoforms by Western blot

Nuclear extracts of confluent cells were probed with antibodies recognizing every CREB-1 family member (Cell Signaling), only the CREB-1 isoforms (Upstate) or exclusively the CREB-1α isoform.

To further support the existence of CREB-1 isoforms generated by alternative splicing, semiquantitative RT-PCR reverse transcription was performed from mRNA of C2F3 cells. The primer pairs used for the PCR reaction were chosen to be specific for the two isoforms. PCR products for both isoforms were detected in myoblasts, confluent cells and myotubes as well (Figure 23A). Samples were taken from 22 to 36 cycles to determine the logarithmic phase of the PCR reaction for semiquantitative measurements. At 30 cycles the reaction was not in the exponential phase anymore, while 27 cycles were found to be still in the log phase (Figure 23A and B).

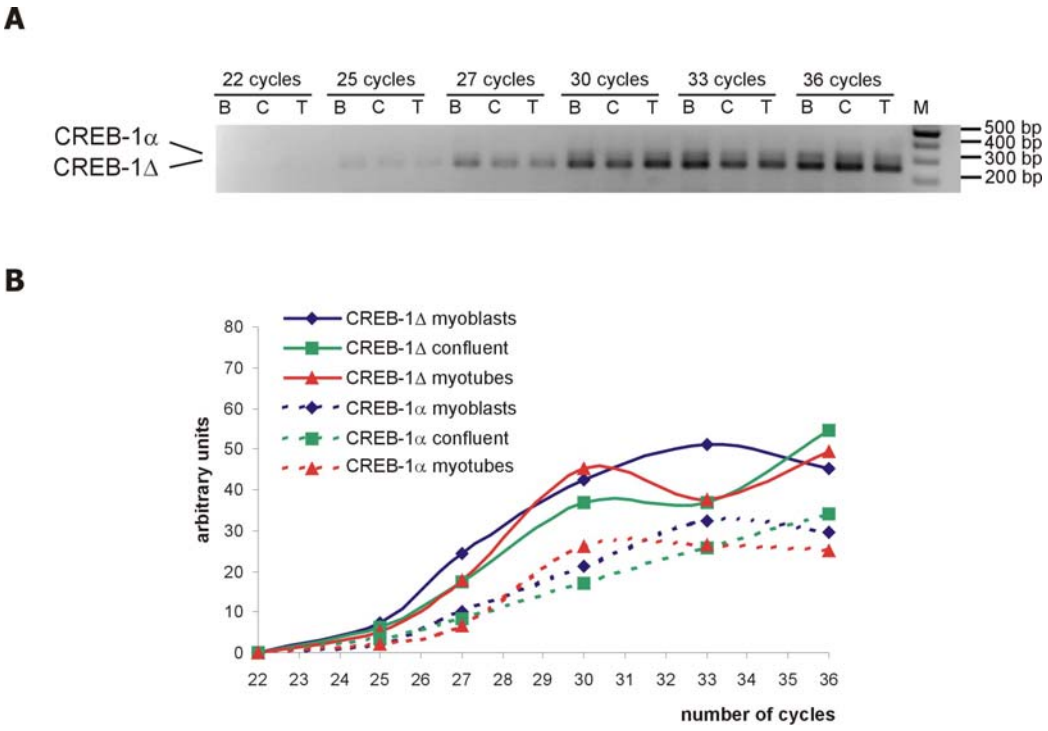

Figure 23. Determining the log phase for semiquantitative RT-PCR

A Reverse transcription was performed from mRNA of myoblasts (B), confluent cells (C) and myotubes (T). CREB-1 PCR, using primers specific for both isoforms was performed from 22 to 36 cycles. ***B*** Densitometrical evaluation of the intensity of CREB-1α and CREB-1Δ PCR products.

27 cycles were used to amplify cDNA samples of myoblasts, confluent cells and myotubes. However, no difference was found in the intensity of the CREB-1α and CREB-1Δ PCR products during muscle differentiation (Figure 24).

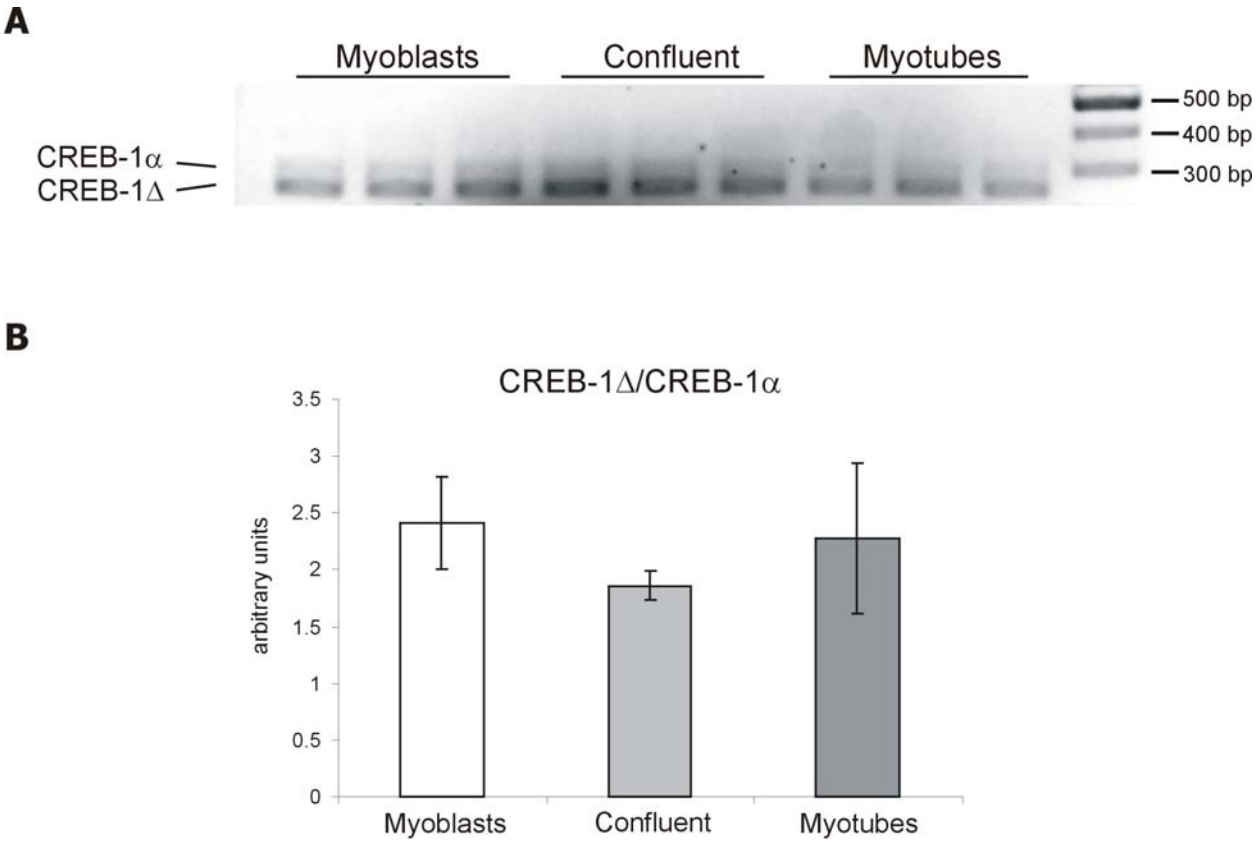

Figure 24. Distribution of CREB-1α and CREB-1Δ mRNA isoforms during myogenesis

A Reverse transcription was performed from mRNA of myoblasts, confluent cells and myotubes and CREB-1 PCR using primers specific for both isoforms was performed for 27 cycles. ***B*** Densitometrical evaluation of the intensity of CREB-1Δ/CREB-1α PCR products. Data are mean ± standard deviation obtained from three samples. There were no significant differences between myoblast values and confluent/myotube values.

To further analyze the transcription products of the CREB-1 gene, Northern blot analysis was performed from mRNA samples of C2F3 cells (Figure 25). However, in contrast to previous NCBI database information, the mRNA of mouse CREB-1α is 8431 nucleotides, of CREB-1Δ is 8389 nucleotides long according to most recent data. Since, the only difference between the two sequences is the 42 bp exon 5 coding 14 amino acid, it was impossible to separate the 8.4 and 8.3 kb sequences from each other with Northern blot technique. In these muscle cells, beside CREB-1α and Δ, CREB-1β was also present at mRNA level and further experiments suggested that the double bands showed by Figure 23 and 24 correspond to CREB-1α and Δ (data not shown).

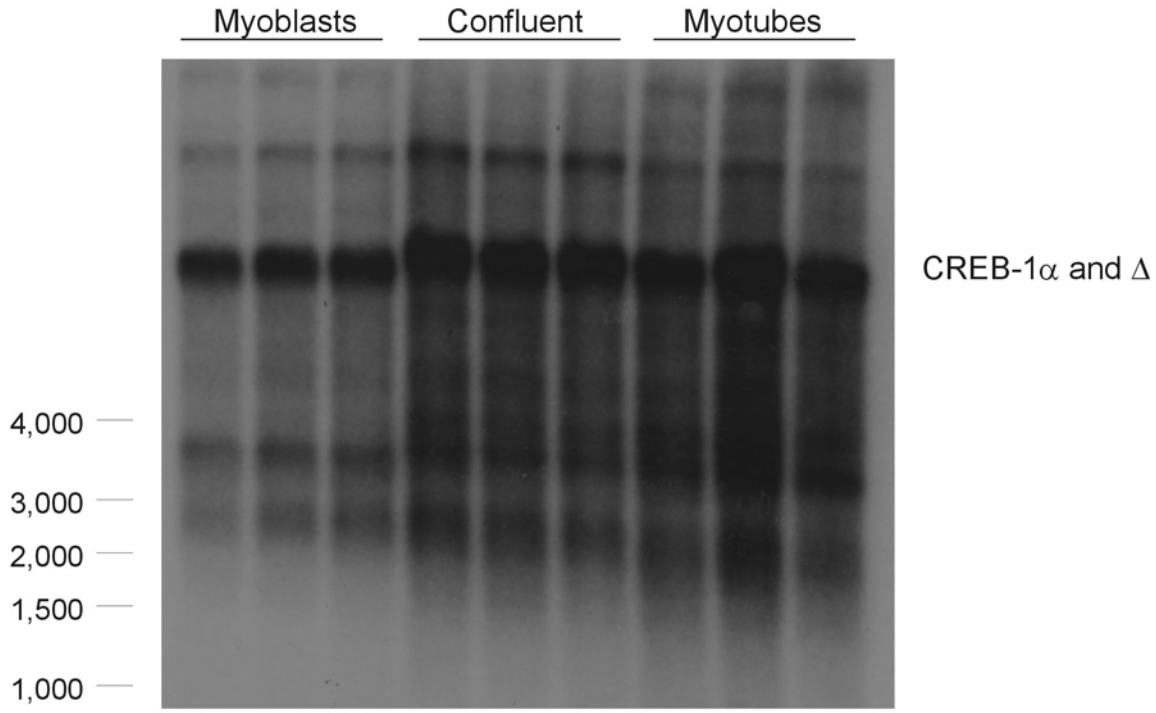

Figure 25. CREB-1 gene expression detected by Northern hybridization

PolyA-mRNA was prepared from myoblasts, confluent cells and myotubes and hybridized to a probe against a mouse CREB-1 sequence, which is common in both isoforms. At the left, sizes of RNA molecular weight marker are given in bp.

4.3.3 Knock-down of CREB-1 by siRNA technology

In order to further analyze whether CREB-1 regulates the cytochrome *c* promoter, we wanted to specifically inhibit its expression by siRNA directed against the mRNA of CREB-1. Four different siRNA sequences were used in a pool and they were able to decrease the protein level after one to three days. The highest knock-down effect was reached 24 hours after transfection, thus this time point was used in latter experiments (Figure 26A and B). However, the negative pool siRNA used as a negative control also inhibited CREB-1 protein expression, although the difference was not as strong as in the case of CREB-1 siRNA (Figure 26A and B). To exclude such off-target effects caused by high amounts (100 nM) of siRNA, in the next experiment 25-100 nM siRNA were tested. However, each concentration of negative controls (negative #1 and negative pool) interacted with the endogenous CREB-1 protein expression, and even in the presence of the transfection reagent Lipofectamine 2000 alone, a similar effect was detected (Figure 26C and D).

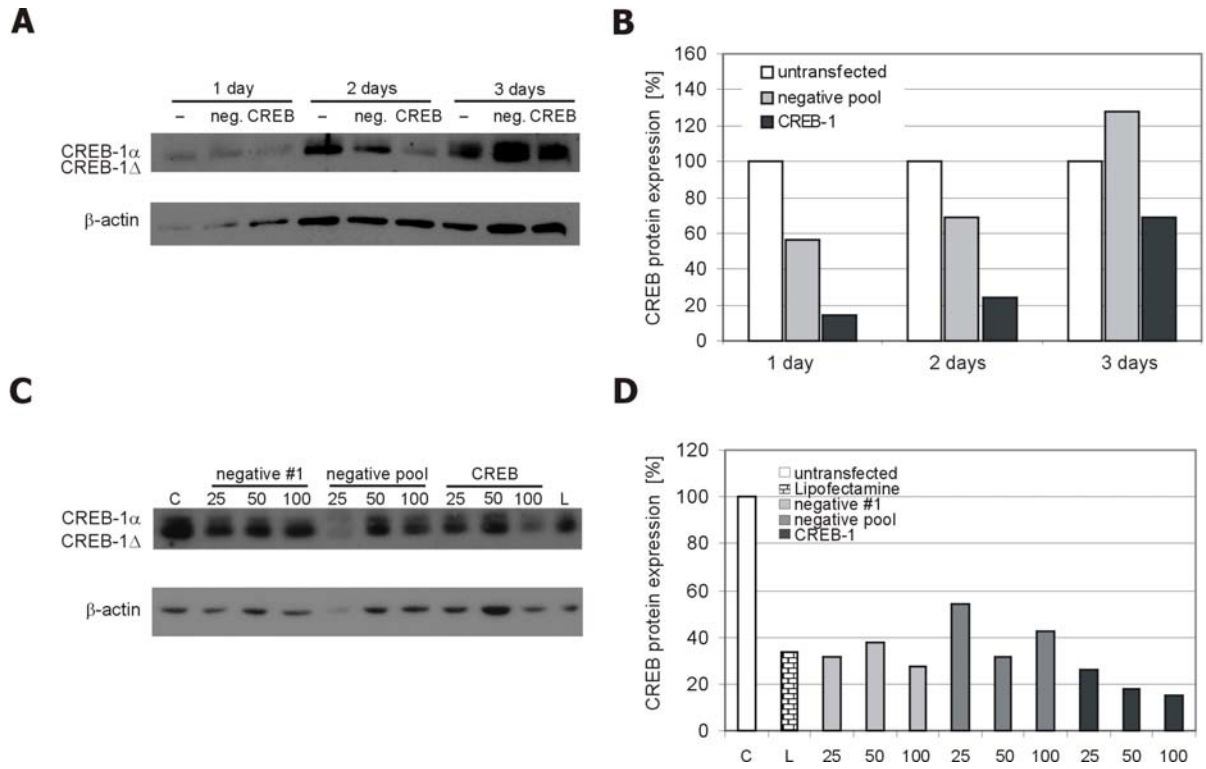

Figure 26. siRNA against CREB-1 decreases CREB-1 protein

A C2F3 cells were transfected with 100 nM negative pool (neg.) control siRNA or with 100 nM siRNA against CREB-1 for 1-3 days, nuclei were extracted and CREB-1 protein amount was checked by Western blot. ***B*** Densitometrical evaluation of the intensity of the CREB-1 protein bands normalized to β-actin given in % of untransfected control. ***C*** 25-100 nM negative #1 or negative pool siRNA were used as siRNA control and 25-100 nM siRNA against CREB-1 was transfected to knock-down CREB-1 protein expression. The nucleus preparation was performed 24 hours after transfection and CREB-1 protein amount was checked by Western blot. ***D*** Densitometrical evaluation of the intensity of the CREB-1 protein bands normalized to β-actin given in % of untransfected control. C: untransfected control, L: Lipofectamine 2000 alone.

This means that the transfection procedure itself unspecifically counteracted with the endogenous CREB-1 protein expression, although the specific siRNA decreased CREB-1 expression according to the siRNA concentration (25 nM, 50 nM, 100 nM siRNA caused 74 %, 82 %, 85 % knock-down of CREB-1 protein level, respectively) (Figure 26C and D).

Nevertheless, we cotransfected the CREB-1 siRNA with a cytochrome *c* reporter construct to see whether knock-down of CREB-1 could interact with the promoter activity. Different concentration of siRNA against CREB-1 decreased the cytochrome *c* promoter activity as did the negative control #1 or negative pool control (Figure 27). This experiment and the Western blots showed again that the transfection itself could cause an unspecific off-target effect counteracting with the CREB-1 protein expression and/or with the cytochrome *c* promoter activity. Thus, the siRNA approach was not suitable to answer the question whether CREB-1 interacts with the

cytochrome *c* promoter. Therefore, to solve this problem we changed our strategy using a constitutively active and dominant negative form of CREB-1, respectively.

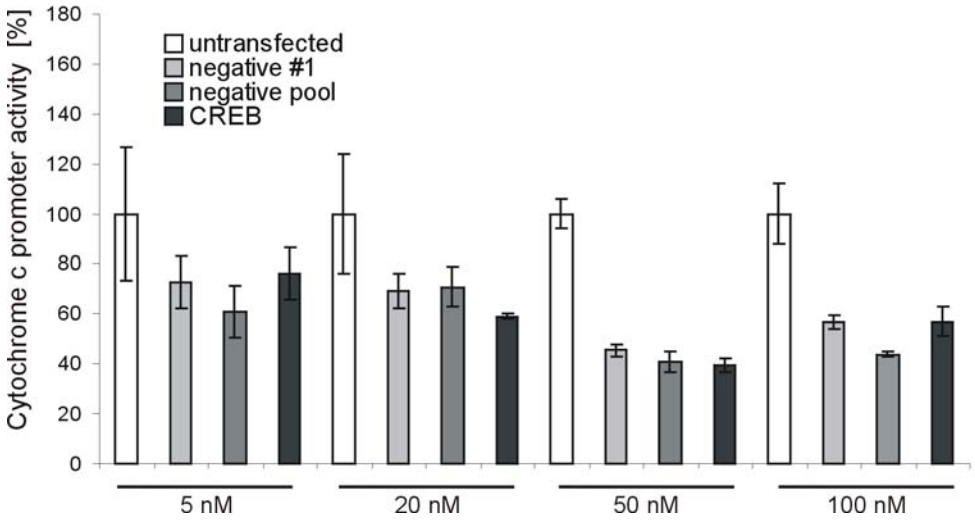

Figure 27. Cytochrome *c* promoter activity upon siRNA cotransfections

5-100 nM control siRNA (negative #1 and negative pool) or 5-100 nM siRNA against CREB-1 were cotransfected with cytochrome *c* promoter-firefly and renilla reporter vectors. The cytochrome *c* promoter activity was measured 24 hours after transfections, normalized to renilla values and given in % of untransfected control. Data are mean ± standard deviation obtained from three samples.

4.3.4 The effect of CREB-1 constructs on the cytochrome *c* promoter

C2/CREB is a constitutively active form of CREB-1, which contains the activation domain of CREB-2 fused to the basic DNA binding/Leucine zipper dimerization domain (bZIP) of CREB-1 and acts as a CREB-1 transcriptional activator, independently of the phosphorylation state. It was cotransfected with cytochrome *c* promoter-firefly and renilla reporter vectors in the presence or absence of a dominant negative CREB construct called A-CREB (plasmids were kind gifts of Prof. Thiel, Homburg). A-CREB consists of only the basic DNA binding/Leucine zipper dimerization domain (bZIP) but lacks the N-terminal activation domain. Therefore it serves as a specific repressor by dimerizating with the endogenous CREB-1 and thus forming an inactive CREB-1/A-CREB dimer. The α-inhibin promoter was used as a positive control as it contains well-described CRE sequences [88]. Cytochrome *c* and α-inhibin promoters were upregulated four and twelve times, respectively in confluent cells compared to myoblasts (Figure 28A and B). The C2/CREB construct significantly activates the cytochrome *c* and α-inhibin promoters in myoblasts as well as in confluent cells (Figure 28A and B). Cotransfecting the dominant negative A-CREB significantly diminished the C2/CREB overactivated promoter

activity, in myoblasts and also in confluent cells (Figure 28A and B). This suggests that CREB-1 directly regulates the cytochrome *c* promoter.

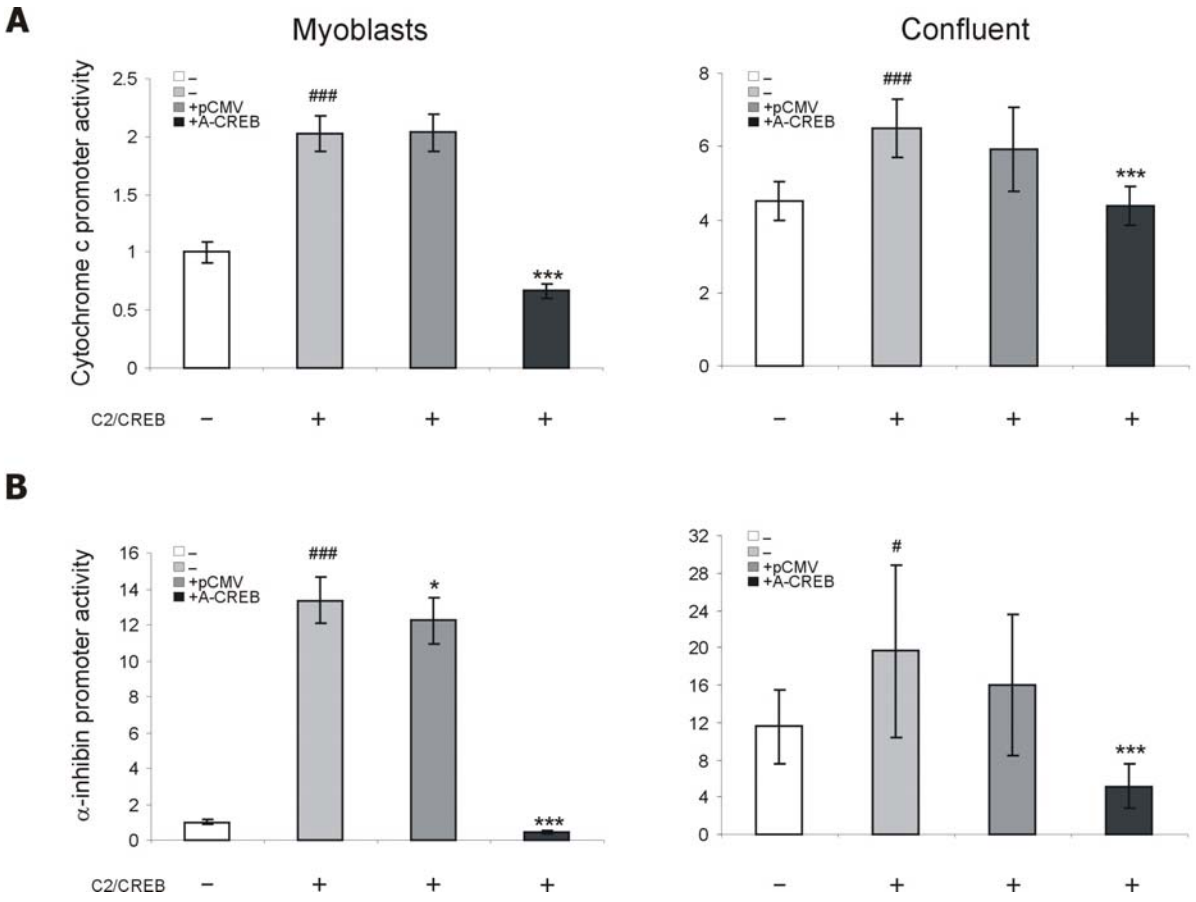

Figure 28. Cytochrome *c* and α-inhibin promoter activities modulated by CREB-1

Cytochrome *c* or α-inhibin promoters were cotransfected with renilla control and with C2/CREB constitutively active (light grey column) or with pCMV empty (dark grey column) or with A-CREB dominant negative vector (black column). ***A*** Cytochrome *c* or ***B*** α-inhibin promoter activities were measured from myoblasts or confluent cells and normalized to the basal promoter activities of myoblasts. Data are mean ± standard deviation obtained from 12 samples and normalized to the transfected cells lacking the C2/CREB plasmid. # indicates a significant difference ($p<0.05$), ### indicates a significant difference ($p<0.001$) in the presence or absence of C2/CREB construct (white and light grey columns). * indicates a significant difference ($p<0.05$), *** indicates a significant difference ($p<0.001$) between C2/CREB construct alone (light grey column) and C2/CREB+pCMV (dark grey column) or C2/CREB construct alone (light grey column) and C2/CREB+A-CREB constructs (black column). Unless it is not indicated there were no significant differences among the samples.

4.3.5 Modulating the activity of PKA and PP2 phosphatases

Since Ser-133 phosphorylation of CREB-1 is necessary for its transcriptional activity, we finally addressed the question, which kinase(s) or phosphatases modulate its phosphorylation in

muscle cells. The activity of protein kinase A (PKA) and PP2 phosphatases were blocked or activated by a specific activator or inhibitors, respectively. PP2A phosphatase was blocked with okadaic acid, while PP2B (calcineurin) was inhibited by Cyclosporin A. PKA was activated with a specific activator called Sp-5,6-DCI-cBIMPS and inhibited with the inhibitor Rp-8-CPT-cAMPS. The toxicity of the applied chemicals was monitored for 4-5 days (data not shown) and concentrations, which were not toxic, were used in the latter experiments. The phosphorylation of CREB-1 was analyzed by Western blot with the phosphoserine-133 specific antibody in C2F3 myoblasts. Okadaic acid and Cyclosporin A phosphatase inhibitors increased the phosphorylation of CREB-1 (Figure 29A, B and 30A, B). Sp-5,6-DCI-cBIMPS activated and Rp-8-CPT-cAMPS blocked the phosphorylation of CREB-1 as they are supposed to activate or inhibit the activity of PKA, respectively (Figure 29C, D and 30C, D). However, 5 nM Okadaic acid seemed to modify the cell shape of differentiated C2F3 myotubes, since in contrast to long myotubes in untreated or with 50 pM or 500 pM Okadaic acid treated wells, round myotubes appeared on the 5 nM Okadaic acid treated wells (data not shown).

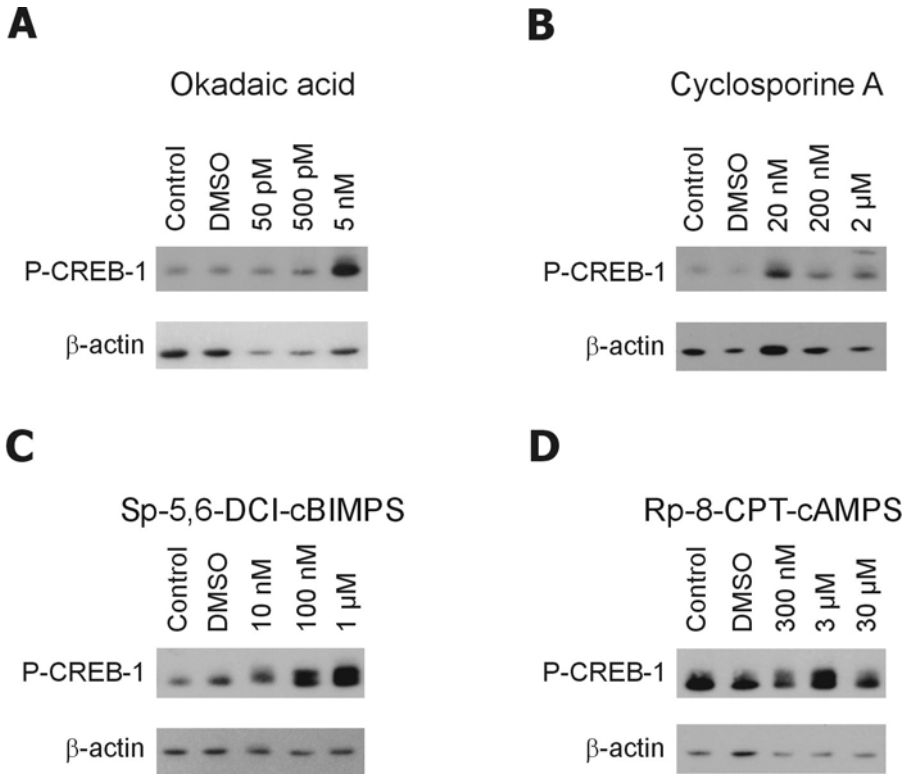

Figure 29. PKA and PP2 phosphatases influences the phosphorylation status of CREB-1

Myoblasts were treated for 24 hours in the presence of phosphatase and PKA inhibitors or PKA activator. Western blots of isolated cell nuclei were probed with P133-CREB antibody and representative pictures are shown. ***A*** PP2A was inhibited with Okadaic acid ***B*** PP2B (calcineurin) with Cyclosporin A, ***C*** PKA was activated with Sp-5,6-DCI-cBIMPS ***D*** and inhibited with Rp-8-CPT-cAMPS with the given concentrations. Cells were treated with DMSO as negative control.

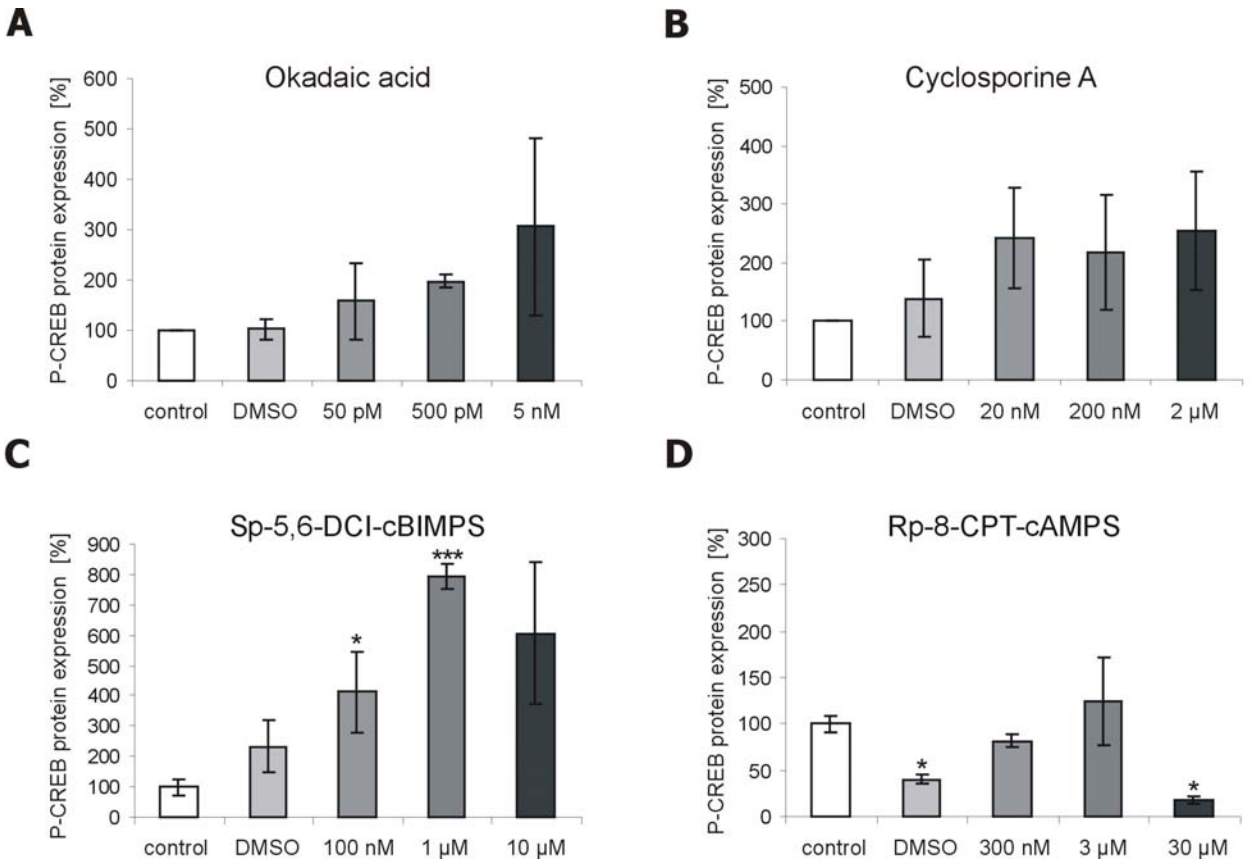

Figure 30. Quantitation of phospho133-CREB-1 intensities upon treatment with phosphatase and PKA inhibitor or PKA activator

Myoblasts were treated for 24 hours in the presence of phosphatase and PKA inhibitors or PKA activator. Western blots of isolated cell nuclei were probed with P133-CREB antibody and evaluated densitometrically, normalized to β-actin and given as the % of untransfected control. Cells were treated with DMSO as negative control. ***A*** PP2A was inhibited with Okadaic acid ***B*** PP2B (calcineurin) with Cyclosporin A, ***C*** PKA was activated with Sp-5,6-DCI-cBIMPS ***D*** and inhibited with Rp-8-CPT-cAMPS with the given concentrations. ***A-B*** data are mean ± standard error obtained from 2-3 independent experiments ***C-D*** data are mean ± standard deviation obtained from 2-3 samples. * indicates a significant difference ($p<0.05$), *** indicates a significant difference ($p<0.001$) between chemical treated and untreated samples. Unless it is not indicated there were no significant differences among the samples.

These activator and inhibitors were also included in cytochrome *c* promoter assays to evaluate whether alterations of Ser-133 phosphorylation of CREB-1 could change the activity of the promoter. Only Cyclosporin A increased moderately the cytochrome *c* promoter activity in C2F3 myoblasts, while other chemicals did not interact with our model promoter (Figure 31A). In differentiated myotubes none of the chemicals were able to change the cytochrome *c* promoter driven luciferase activity (Figure 31B). In summary, Cyclosporin A increased the Ser-133 phosphorylation of CREB-1 as well as the cytochrome *c* promoter activity suggesting a possible role of PP2B (calcineurin) regulating the function of CREB-1 in muscle cells.

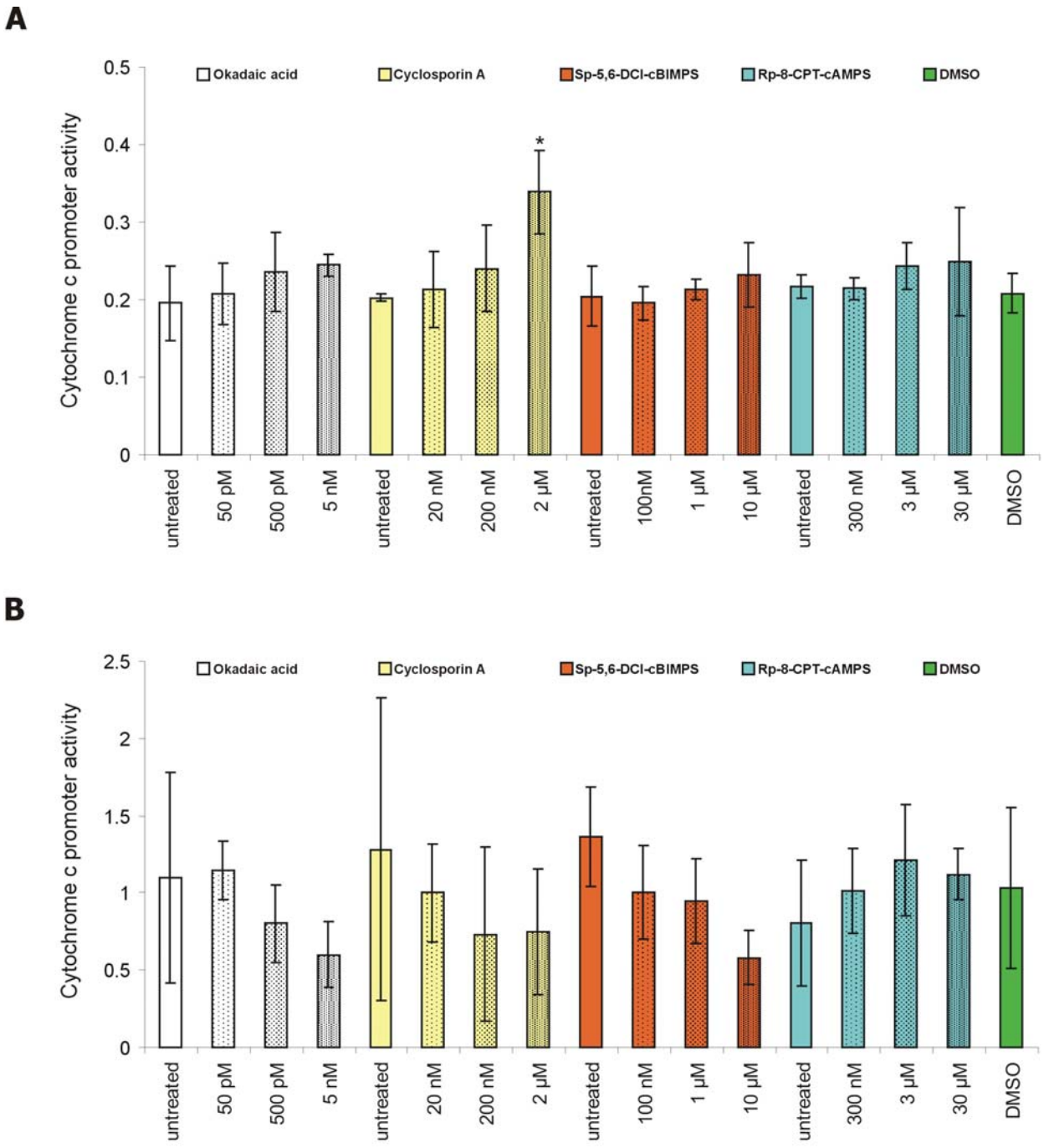

Figure 31. Cytochrome *c* promoter activity in the presence of phosphatase and PKA inhibitors or PKA activator

Cells were treated for ***A*** 24 or ***B*** 120 hours with the indicated kinase or phosphatase inhibitors or activator. PP2A was inhibited with Okadaic acid, PP2B (calcineurin) with Cyclosporin A and PKA was activated with Sp-5,6-DCI-cBIMPS and inhibited with Rp-8-CPT-cAMPS with the given concentrations. Cytochrome *c* promoter activity was determined ***A*** in myoblasts or ***B*** in differentiated myotubes. Data are mean ± standard deviation obtained from three samples. ***** indicates a significant difference ($p<0.05$) between untreated control and 2 µM Cyclosporin A treated cells.

5 Discussion

Mitochondrial biogenesis is a well controlled and complex process. The pathways responsible for transmitting the signals for an increased amount of mitochondria are not well understood. To investigate candidates involved in this process, regulation of cytochrome c promoter during skeletal muscle differentiation was used as a representative model. Specifically, we asked the question whether the AMP activated kinase (AMPK) or the cyclic AMP-response element binding protein 1 (CREB-1) are responsible for regulating mitochondrial biogenesis in this situation.

5.1 Comparison of undifferentiated and differentiated muscle cells

5.1.1 Enhanced myogenic marker gene expression in differentiating muscle cells

C2F3 or C2C12 mouse skeletal muscle cell lines were used to study mitochondrial biogenesis upon muscle differentiation *in vitro*. During this process, the mitochondrial amount as well as mitochondrial enzyme activities are elevated comparing multinucleated myotubes with precursor myoblasts [2]. The differentiation program of skeletal muscle is mediated by the family of myogenic regulatory factor (MRFs) proteins. The primary MRFs, MyoD and Myf-5 determine the cell faith, while the secondary MRFs, myogenin and MRF-4 induce myoblasts to fuse with each other to myotubes. MRFs heterodimerize through their basic helix-loop-helix domain (bHLH) with other bHLH transcription factors and bind the E-box *cis*-element of muscle specific gene promoters [89]. Myosin heavy chain (MHC) can be also used to determine the differentiation state of muscle cells, as its expression can be detected first at the time of myoblast fusion and remains high in muscle fibers, but is missing in growing myoblasts [90].

Skeletal muscle cell lines were induced to differentiate by fusion of growing myoblasts to quiescent myotubes. Myogenin was detected by Western blot in confluent cells and myotubes but not in growing subconfluent C2F3 myoblasts (Figure 8). In parallel, MHC protein was exclusively expressed in differentiated C2C12 myotubes investigated by indirect immunofluorescence, showing that these cells were successfully differentiated.

5.1.2 Altered intracellular calcium levels during differentiation

Calcium is an intracellular messenger involved in many cellular functions. In muscle cells after membrane depolarization calcium channels open in the sarcoplasmatic reticulum (SR) and the increase of intracellular calcium concentration is a prerequisite for actin-myosin interaction. Furthermore, calcium activates several calcium dependent protein kinases and phosphatases and

is essential for the ordered sequence of muscle differentiation. It has been shown that cell commitment, phenotypic differentiation as well as cell fusion need an increase of the intracellular calcium concentration [91]. In the presence of EGTA, an extracellular calcium chelator, myoblast differentiation was diminished, while the calcium ionophor A23187 promotes muscle differentiation, increasing the number of fused myotubes [92]. Upon chelating the intracellular calcium with the membrane permeable BAPTA-AM, the number of differentiated myotubes detected by immunofluorescence was suppressed in a dose dependent manner. Additionally, BAPTA-AM not only decreased the resting calcium level of treated myoblasts, but also the activated calcium influx mediated by storage activated calcium channels [93]. L-type calcium channels were found to contribute to the elevation of the intracellular calcium level in cultivated muscle cells, and inhibiting this calcium channel with specific inhibitors decreased expression of myogenin and disturbed myoblast fusion. At the same time, suppressing the rise of intracellular calcium by inhibiting the sarcoplamatic reticulum calcium channels, also diminished the number of differentiated myoblasts [19]. In muscle cells NMDA glutamate receptors were also found to be responsible for the calcium influx upon muscle differentiation, since glutamate treatment elevated the number of fused myoblasts, while a specific NMDA inhibitor suppressed this effect [94]. Recent detailed analyses indicate that post-natal myoblasts can use three alternative mechanisms to elevate their intracellular calcium level: the release from internal stores, the influx through storage and through voltage operated channels [93]. Mitochondria are also involved in the maintenance of intracellular calcium level mediated by its Na^+/Ca^{2+} exchanger and Ca^{2+} uniporters. Challet *et al.* indicated a ryanodine receptor (RyR) dependent oscillation in mitochondrial calcium, suggesting that mitochondria communicate very tightly with the SR in myotubes [95].

The ratios of 340 and 380 nm fluorescence intensities suggest that myoblasts have significantly higher calcium concentrations compared to myotubes (Figure 9). Enhanced intracellular calcium is involved in muscle fiber type fast-to-slow twitch transformation [96], since chronic low-frequency stimulation (CLFS) of fast-twitch muscle fibers generates a long-term, two to three-fold time higher calcium concentration as in unstimulated muscle fibers and cause massive upregulation of mitochondria *in vivo* [97]. Kubis *et al.* also reported an elevated calcium level upon electrostimulation of cultured cells, which in contrast with the repetitive peaks of short calcium transients seemed not to be involved in the activation of calcineurin-NFATc1 pathway. This signal pathway contributes to the fast-to-slow fiber type transition in skeletal muscle cells via upregulating slow myosin heavy chain gene expression [24]. CLFS suppressed the SR Ca^{2+}-ATPase activity [97] and it was suggested that decreased ATP levels may reduce the calcium flux into the SR producing an increased intracellular calcium

concentration. Indeed an elevated cytosolic calcium concentration was found in fibroblasts of MELAS (mitochondrial encephalomyopathy, lactic acidosis and stroke-like episodes) patients, harboring a point mutation of mtDNA in the gene coding for the mitochondrial leucine-tRNA. The fibroblasts of affected patients showed normal levels of ATP, but an impaired mitochondrial membrane potential, suggesting that not the mitochondrial ATP production rather than its calcium sequestering capacity may contribute to this increased calcium level [98]. Depleting mtDNA by ethidium bromide or poisoning the mitochondrial respiration with different inhibitors also invoke a higher resting calcium concentration in C2C12 cells. These interventions decreased the cellular ATP level and enhanced the ryanodine receptor 1 mRNA and protein levels, which is thought to play a role in the contraction triggered calcium influx [99]. Thus, calcium may be an important initial trigger for mitochondrial biogenesis and an insufficient ATP production by mitochondria may be a retrograde signal for transmitting the need for an increased mitochondrial mass. Indeed, initial differentiation by high confluence and serum withdrawal leads to a significant rise in intracellular calcium (Figure 11, 95 % starting cell density). This was not observed under suboptimal condition of cell confluence (Figure 11, 30 and 60 % starting cell densities).

However, muscle differentiation is a slow, genetically determined process, hence the changes of activating pathways and the resulting biological answers happen during a different time scales. Several calcium activated processes invoke spatially and temporally distinct calcium waves such as single spikes, sustained low plateaus or repeating oscillations [99]. Our calcium imaging microscopic tool was not suitable to monitor intracellular calcium concentration over several days so an important calcium peak during initiation of differentiation may have been missed, which may crucial to trigger the following events.

In conclusion, we observed that in the beginning of differentiation at the myoblast stage, C2C12 cells have an increased level of calcium when comparing them to the end-stage differentiated myotubes (Figure 9), and the intracellular calcium is elevated during the differentiation process upon serum withdrawal (Figure 11). Thus calcium may be important for muscle differentiation and therefore calcium activated phosphatases were studied later.

5.1.3 α-actinin4 translocates to the nuclei of myotubes

In our laboratory, a new sequence motif was detected, which was found in the promoter sequence of cytochrome c, TFAM, COXIV as well as many other nuclear encoded mitochondrial gene promoters. This sequence was shown by EMSA experiments to bind a protein complex and the abundance and binding affinity of these DNA binding proteins were different in myoblasts compared to myotubes. The complexes isolated from nuclear extracts of myotubes contained

several proteins and one of them was α-actinin4, identified by mass spectrometry. Immunofluorescence experiments showed that myoblasts contain α-actinin4 in a diffuse pattern but the protein is localized mainly in the nucleus in myotubes [87].

Western blots verified the results of the immunofluorescence staining, since nuclear levels of α-actinin4 were enhanced two to three times in myotubes compared to myoblasts, although the cytoplasmic level of the protein remained unchanged (Figure 12). α-actinin4 is usually localized outside of the nucleus and it is thought to regulate the interaction of plasma membrane and cytoskeleton, since it is involved in several endo- and exocytosis processes [100,101]. However, in distinct cancer cell lines a nuclear localization of α-actinin4 was also shown [102] and in podocytes it is present at the plasma membrane, while in transformed kidney cells (HEK) it is found in the perinuclear cytosol [103]. Thus, the localization of this protein strongly depends on the cell type or physiological conditions. The presence of α-actinin4 in the nucleus suggests its possible involvement in transcription processes, and one of its isoforms, α-actinin2 was recently shown to function as a coactivator [104]. Thus α-actinin4 could also be involved in DNA binding or may act as a coactivator in the formation of a transcriptional complex at the promoter of nuclear genes encoding mitochondrial proteins.

5.2 Overexpression of AMPKα1-CA in C2C12 cells

To investigate whether AMPK mediates mitochondrial biogenesis in muscle cells, we chose the Tet-Off system, which is a method to suppress the expression of the gene of interest in the presence of Tet or Dox and to switch on its expression by withdrawal of the antibiotics. The cDNA of the constitutively active AMPKα1 was cloned into the vector pTRE and this construct was transfected into C2C12 D3 cells, which express the TRE transactivator. Clones were isolated and were analyzed by Western blot for expression of AMPKα1-CA. However, Dox did not regulate the levels of the AMPKα1-CA protein at all (Figure 15 and Appendix Figure 2). The D3 transactivator expressing cell line had been tested for Dox suppression of the TRE promoter and a ten times decreased, but not silent promoter activity was obtained in the presence of 1 μg/ml Dox (Figure 13B). These results suggest that there are other factors, which impair in these cells the ability of Dox to inhibit the transactivator protein. Obviously, a low level of transcription was enough to produce similar amounts of AMPKα1-CA protein as in activated cells in the absence of Dox (Figure 15 and Appendix Figure 2). Other results of our laboratory confirm this phenomenon, since C2C12 E6 cells expressing EGFP driven by the TRE are also unable to inhibit its expression in the presence of Dox (Franko and Darvas, unpublished data). Indeed, Sommer e*t al.* reported that the Tet-Off system was leaky in C2C12 cells, since they also

obtained transgene expression in the non-activated state [105]. To overcome this limitation, these authors generated an autoregulatory Tet-Off system, which provided higher induction factors with low basal expression in the non-induced state [106]. The Tet-Off system was recently compared with other inducible expression systems and the results indicate that this system although reaching the highest maximum expression level, is comparably leaky and has only a small induction capacity [107]. Personal communications with the company providing the vectors (Becton Dickinson) also indicated that this Tet-Off system is not universally suitable for every cell line. To confirm this, the TRE promoter containing a firefly luciferase reporter plasmid was transfected into C2F3 and C2C12 cells. Interestingly, we achieved a high amount of luciferase activity driven by the TRE promoter and Dox did not affect this expression (Figure 32). This unwanted expression from the TRE promoter denotes that there are transcription factors in these cells, which could bind and induce the transcription from the TRE promoter even in the absence of the specific transactivator protein. An alternative explanation for this constitutive expression could be that the chromosomal environment triggers the activation of the transgene even in the presence of Dox due to the presence of activator or enhancer sequences. However, Dox was able to inhibit the expression of the transgene in C2C12 D3 cells, which have the TRE transactivator, but its suppressing capacity was lower as in previous experiments, compare Figure 32 and 13B. Altogether, cell lines were established, which constitutively express the AMPKα1-CA protein, but with no possibility of regulation.

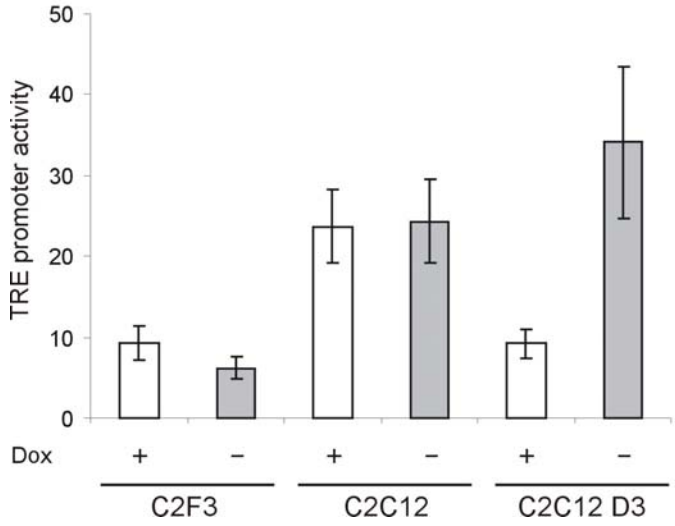

Figure 32. TRE promoter activity in muscle cell lines

A TRE promoter driven firefly luciferase reporter plasmid was cotransfected with an SV-40 promoter driven renilla luciferase control vector into C2F2, C2C12 cells or C2C12 D3 (TRE transactivator expressing) cell lines. Luciferase activity was determined 24 hours after transfection in the presence (+) or absence (−) of doxycycline (Dox). The firefly luciferase values were normalized to renilla values and data are mean ± standard deviation obtained from 5 samples.

The activity of AMPKα1-CA was confirmed by kinase assays, and accordingly Dox did not affect the kinase activity (Figure 17A). The endogenous AMPKα1 kinase activity was also determined and was found to be about nine times higher as the maximal activity of AMPKα1-CA (Figure 17B). Calculating the phosphate amount incorporated into the SAMS peptide, AMPKα1-CA phosphorylated 1.8 pmol/min/mg phosphate, while the endogenous kinase phosphorylated 15.7 pmol/min/mg phosphate (calculated from the dark grey column of Figure 17A and the light grey column of Figure 17B). The difference between the endogenous α1 and AMPKα1-CA kinase activity is in line with data obtained by Stein *et al.*, who also found a much higher endogenous compared to the AMPKα1-CA activity obtained after transfection [40]. They suggested that due to the inability to bind the regulatory β and γ subunits, the truncated AMPKα1-CA may not localize normally and that this may explain the low kinase activity [40]. Only when using an adenoviral system, the AMPKα1-CA kinase activity was higher as the endogenous [108], meaning that a high transfection efficiency is also a prerequisite for an appropriately high activity. However, this does not fully explain the low kinase activity in stable clones, where every cell expresses the construct.

Nevertheless, cytochrome c promoter expression was not different in clone 27 or clone 5, which express AMPKα1-CA at high or intermediate levels, respectively (Figure 18 and 19A). Also, in transient transfection experiments the cytochrome c promoter activity remained the same upon cotransfection of dominant negative forms of AMPKα1 or AMPKα2 proteins, confirming that AMPK does not regulate the cytochrome *c* promoter (Figure 19B). In addition, the endogenous kinase activity was measured but no difference was detected among myoblasts, confluent cells and myotubes (Figure 17C).

In conclusion, we generated cell lines expressing AMPKα1-CA, which despite of its constitutive kinase activity was not able to alter the expression of the cytochrome c promoter, indicating that either AMPKα1 itself is not involved in this process or that the total AMPK activity we achieved was not high enough to trigger an appropriate answer.

5.3 CREB-1 regulates the cytochrome *c* promoter

Former studies of our laboratory and other results suggested that CREB-1 is important for regulating nuclear encoded mitochondrial genes [32] and a model of a CREB-1 transcriptosome was built according to these results (Figure 33).

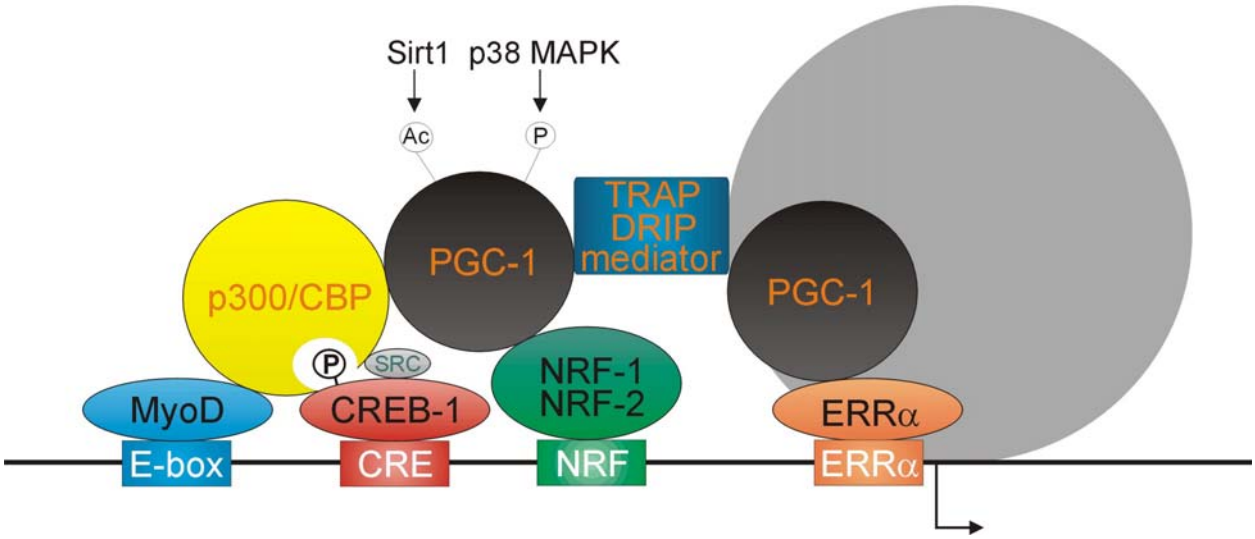

Figure 33. A model for a transcriptosomal complex on mitochondrial genes

The black line illustrates the DNA sequence of a model promoter with chosen *cis*-elements thought to play a role during the process of muscle differentiation. The grey circle represents the RNA II polymerase and the broken arrow shows the transcriptional start site.

To investigate this hypothesis in more detail, the expression level of CREB-1 was analyzed by Western blot. We found a decrease in the overall CREB-1 amount without changing the overall Ser-133 phosphorylation status of the protein (Figure 20A-D). Thus, the overall Ser-133 phosphorylated CREB-1 compared to the total CREB-1 protein is elevated upon muscle differentiation suggesting a role of phosphorylated CREB-1 in this process. The transcription factor ATF-1, which also belongs to the CREB-1 family, dropped during differentiation and phospho-ATF-1 levels reduced (Figure 20A, C, G and H) denoting that ATF-1 could be important in the first stage of muscle differentiation. Surprisingly, Western blot analysis showed that in the 42-43 kDa molecular weight range, two CREB-1 reactive bands were detected, which reacted with anti-CREB as well as with anti-Ser-133 phospho-CREB antibodies (Figure 20A and C). In further experiments we identified these double bands as the CREB-1α and CREB-1Δ products of the same gene generated probably by alternative splicing (Figure 21 and 22). The presence of the isoforms was also proven at the mRNA level and CREB-1Δ was found to be the predominant mRNA, and the ratio of CREB-1α and CREB-1Δ mRNA remained the same during the differentiation process (Figure 23 and 24).

5.3.1 CREB-1 isoforms are present in different tissues

Although the presence of CREB-1α and Δ isoforms was discovered already in 1990, the function of them still remains obscure. Yamamoto *et al.* showed that in rat brain the predominant isoform is the CREB-1Δ on the mRNA as well as the protein level as well. They found that *in*

vitro, the capacity for transactivation of the rat CREB-1α isoform is approximately 10 times higher as CREB-1Δ [109]. However, another study indicated that the two human CREB-1 isoforms bind to their DNA target with similar strength [110]. Also, the mouse CREB-1α and Δ transcriptional activities were found to be equal, but the mRNA ratio showed, as in the former studies, that CREB-1Δ is the mainly expressed isoform [111]. The discrepancy of the α domain causing different transcriptional activity *in vitro* in the three species were explained by minor amino acid variations among them [111]. In addition to the α- and Δ-isoforms, other CREB-1 isoforms were detected, namely CREB-1αγ, γ, Ω, Ψ. They differ by the presence or absence of further domains derived from alternatively spliced exons, but all originate from the same gene. All of them are truncated proteins lacking the bZIP domain, thus they have been suggested to rather function as repressors counteracting CREB-1α or Δ. Expression of CREB-1 γ and αγ was strongly induced upon spermatogenesis, indicating a role in this process [111]. Also, the nuclear localization signal of CREB-1Δ was determined to be at the amino acid positions 287-295, which is situated in the bZIP domain, suggesting a cytoplasmatic localization of all shorter isoforms lacking this domain [112]. Two other mouse CREB-1 isoforms were discovered latter and named CREB-1Δ-14 and CREB-1Δ-35, due to the absence of 14 nucleotides of exon 9 or 35 nucleotides of exon 8. Since they lack the bZIP domain, they were indeed localized in the cytosol but still had a capacity for blocking the transcriptional activity of CREB-1α in CRE reporter gene assays. As these isoforms are cytoplasmic and the full length CREB-1 is located in the nucleus, the hypothesized role for their action is that they act as pseudosubstrates of PKA and thereby decrease the phosphorylation of endogenous CREB-1. Both of them were shown to be widely expressed in several tissues but they were enriched in brain, thymus and testis [113]. Homologues of these CREB-1 isoforms were observed in *Aplysia* brain as well. While the full length CREB-1a serves as an activator of long term facilitation in this organism, CREB-1b is a repressor and CREB-1c is thought to be an activator of long term memory dependent on CREB-1a [114].

Disrupting the second exon of CREB-1 in mice caused a complete loss of CREB-1α and Δ expression, but CREM, which belongs to the classical CREB-1 family and a new CREB-1 isoform, called CREB-1β, were upregulated and compensated the loss of CREB-1α and Δ in these animals [115,116]. In wild-type tissues CREB-1β and CREB-1α mRNA are expressed to about the same level, and both contribute to about 1/3, while CREB-1Δ is thought to contribute to about 2/3 of the overall CREB-1 mRNA pool. CREB-1β was able to transactivate CRE-sequence containing model promoters, so it was considered to be a transcriptional activator as well [116]. Analyzing their performance, these KO mice showed an impaired long term memory

in the hippocampus, although CREB-1β was expressed there [117]. When the CREB-1α/Δ deficient mice were further investigated, it was found that although they were highly expressed, CREB-1β and CREM were unable to bind to and transactivate other nuclear transcription factors in the absence of CREB-1α and Δ [118]. This was in contradiction to the initial study of Blendy *et al.* [116], which showed that CREB-1β does have transcriptional activity. However, these authors transfected a CREB-1β plasmid into cells, in which the wild-type CREB-1α and Δ isoforms were probably also present. In contrast, in the latter study [118] there was no expression of CREB-1α or Δ at all, which dissolves the apparent inconsistency between the two studies. In conclusion, CREB-1β probably has transcriptional activity, but only in the presence of the CREB-1α and Δ isoforms.

The presence of CREB-1α and Δ isoforms was verified in more recent studies: For example, both isoforms were equally upregulated in hippocampus and cortex of depressive transgenic mice model with impaired glucocorticoid receptor function upon antidepressant treatment, although the predominant isoform at the mRNA level remained CREB-1Δ, consistent with the earlier studies [119]. In CREB-1α overexpressing transgenic mice, CREB-1α was observed to enhance its own transcription as well. Furthermore, in these animals the expression of CREB-1β as well as CREB-1Δ were also increased [120].

Our results revealed that in C2F3 muscle cells, CREB-1Δ is the predominant isoform at the mRNA level, both in myoblasts as well as in myotubes, in accordance with these previous studies. However, at the protein level there was a marked shift in the CREB-1α/CREB-1Δ ratio: While myoblasts expressed high amounts of CREB-1Δ, myotubes switched to the CREB-1α isoform (Figure 20A and E). This indicates that in myotubes, in spite of the higher level of CREB-1Δ mRNA, an unknown mechanism elevates CREB-1α protein. Hoeffler *et al.* and recently Sato *et al.* suggested that the regulation of CREB-1 function may take place predominantly at the level of translation or by posttranslational modifications [121,122]. Irrespective of the isoform, the phosphorylation status was maintained, indicating that the isoforms are functionally phosphorylated at Ser-133 as soon as they are available for the kinase(s) (Figure 20C and F).

What is the functional difference between CREB-1α and Δ, why do cells express two isoforms and what does a shift mean for CREB-1 function? These questions have not been answered yet in spite of 17 years of intensive research. The exon 5 encoded α-domain has a proposed α-helical, basic, hydrophobic structure. Disrupting this domain caused a strongly decreased activity in driving promoters with CRE sequences and inserting the α-domain into the sequence of CREB-1Δ elevates promoter activity compared to the Δ isoform [109]. The authors

hypothesized that the α-domain, due to its basic residues, is able to bind to the phosphorylated Ser-133 KID (kinase inducible) domain in the same molecule and thus elevates the transcriptional activity of the protein. However, it can function autonomously as well in the absence of KID domain through its postulated interaction with other proteins of the transcriptional complex [109]. Analyzing the potential posttranslational modifications of the mouse CREB-1 protein domain encoded by exon 5 using bioinformatic tools [123], we observed two possible serine phosphorylation sites at position 89 and 98, a likely lysine glycosylation site at position 94 and one probable YinOYang (O-ß-GlcNAc glycosylation on cytoplasmic/nuclear proteins) modification site at position 88. Although the two latter observed modifications are not referred yet, CREB-1 was shown to be phosphorylated by many kinases in addition to PKA, such as PKC, Akt, Msk, Rsk, p38, CaMKII, CaMKIV and dephosphorylated by multiple phosphatases, for example calcineurin (PP2B), PP2A and PP1 (Figure 4). Besides the Ser-133 phosphorylation, which is essential for the recruitment to CBP/p300, other phosphorylation sites are also known, e.g. Ser-142, which was indicated to play a role in entrainment of the mammalian circadian clock [124]. Therefore, unique phosphorylation and other modification sites of the α domain could play a role in CREB-1α activation, for example by providing new docking sites for other transcriptional coactivators.

5.3.2 CREB-1 activates the cytochrome *c* promoter

To modulate the endogenous level of CREB-1 we used first an siRNA approach. However, transfecting any siRNA into C2F3 cells induced an unspecific drop of CREB-1 levels as well as a drop in cytochrome *c* promoter activity (Figure 26 and 27). This phenomenon was caused probably by the transfection reagent itself (Figure 26C and D), thus in further experiments, constitutive active and dominant negative constructs of CREB-1 were applied to promote or inhibit the endogenous CREB-1 activity, respectively. Transfecting the constitutively active C2/CREB enhanced promoter activity and the dominant negative A-CREB suppressed this upregulation (Figure 28). These results indicate that CREB-1 indeed activates the cytochrome *c* promoter. To verify that CREB-1 directly binds the promoter, the downstream CRE sequence had been analyzed in EMSA experiments on nuclear extracts of C2F3 myoblasts and myotubes. A specific DNA binding protein-CRE element complex was visible in myoblasts as well as in myotubes [32]. Antibodies against CREB-1 or Ser-133 phosphorylated CREB-1 caused a further retardation of the DNA binding protein-CRE element complex, suggesting that CREB-1 and P-CREB-1 binds to the CRE element of cytochrome *c* promoter *in vitro*. In addition, chromatin immunoprecipitation experiments detected a direct interaction between a fragment of mouse cytochrome *c* promoter containing both CRE elements and CREB-1 and Ser-133 phospho-

CREB-1 in myoblasts, confluent cells and myotubes. CREB-1α was also observed to bind to this promoter sequence in confluent cells and myotubes but was completely missing in myoblasts [32]. This observation is in agreement with the results of the Western blot analysis, where CREB-1α/CREB-1Δ ratio as well as the P133-CREB-1α/P133-CREB-1Δ ratio was the lowest in myoblasts but increased in confluent cells and myotubes (Figure 20). According to the results mentioned above we set up a model for the interaction of CREB-1 and the cytochrome *c* promoter (Figure 34). In myoblasts, CREB-1Δ is the predominant isoform and binds to the downstream CRE element. During myogenesis the level of CREB-1Δ drops in parallel with an increase of CREB-1α, which ends up in a situation, where CREB-1α and not CREB-1Δ binds to the downstream CRE sequence. We hypothesize that upon different isoform binding different transcriptional responses are invoked via CREB-1α or CREB-1Δ, respectively.

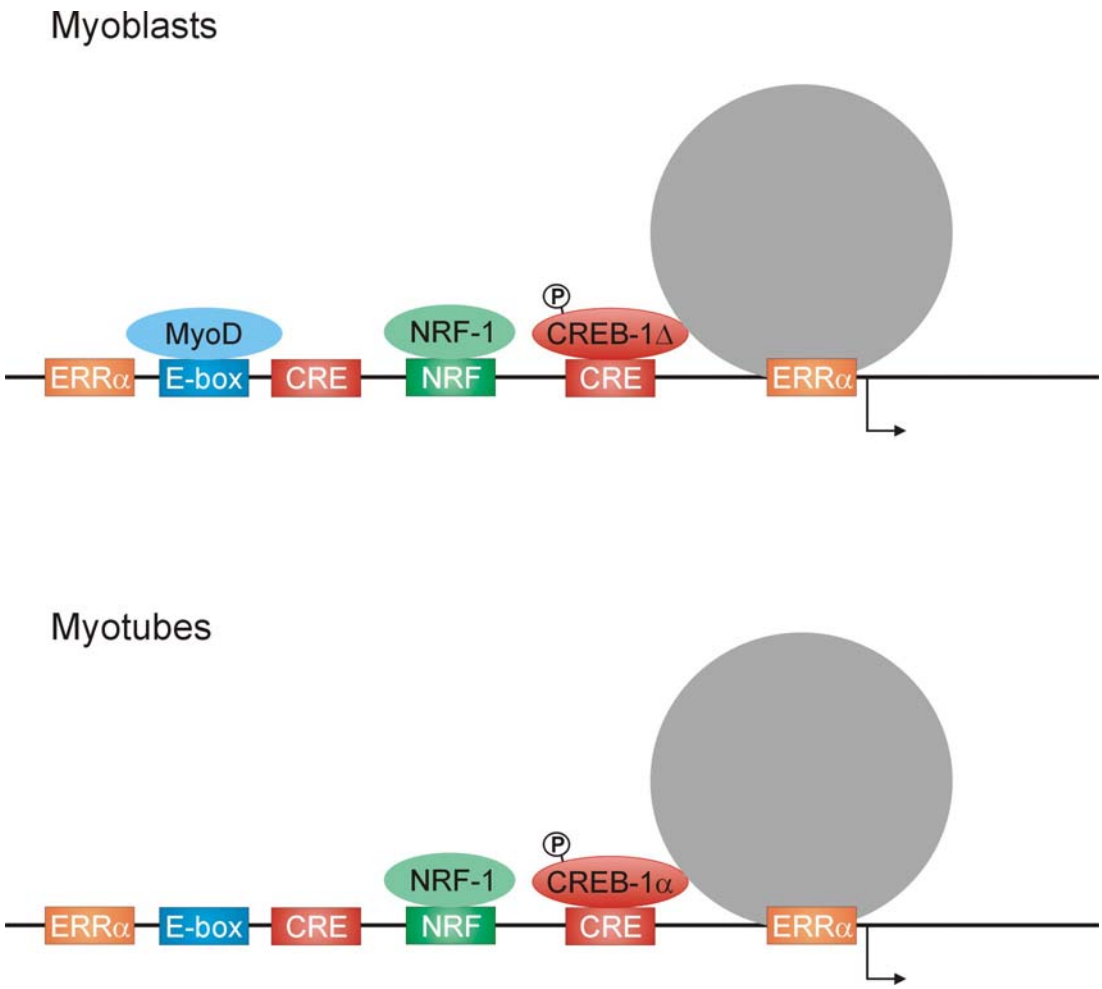

Figure 34. An interaction model of CREB-1 and cytochrome *c* promoter

The black line illustrates the DNA sequence of the cytochrome *c* promoter with chosen *cis*-elements thought to play a role during the process of muscle differentiation. The grey circle represents the RNA II polymerase and the arrow shows the transcriptional start site. PGC-1α protein was found to be absent in these cells ([125] and data not shown).

In conclusion, these results suggest that CREB-1 binds *in vitro* as well as *in vivo* to the cytochrome *c* promoter and enhances its activity and that through these effects CREB-1 is involved in the regulation of mitochondrial biogenesis during myogenesis. This conclusion correlates well with the recently discovered role of the TORCs (transducer of regulated CREB) activating PGC-1α upon muscle differentiation [73], and the role of CREB-1 in mitochondrial biogenesis induced by mitochondrial dysfunction [67,68,69].

5.3.3 CREB-1 regulating upstream signals

In order to study the enzymes, which may modify the activity of CREB-1 by phosphorylation or dephosphorylation of Ser-133, PKA activators and inhibitors as well as protein phosphatase inhibitors were applied to C2F3 muscle cells. 24 hours treatment with Okadaic acid or Cyclosporin A, inhibiting the PP2A or PP2B phosphatases, respectively, elevated CREB-1 phosphorylation at Ser-133 (Figure 29 and 30A and B). A specific PKA activator, Sp-5,6-DCI-cBIMPS enhanced CREB-1 Ser-133 phosphorylation and Rp-8-CPT-cAMPS, which is a selective PKA inhibitor, suppressed it (Figure 29 and 30C and D). These chemicals were then used in cells transfected with a reporter plasmid to analyze whether these interventions could alter the expression of the cytochrome *c* promoter. Cyclosporin A activated the promoter in myoblasts, but the PKA modulating chemicals as well as the PP2A inhibitor Okadaic acid did not change significantly the promoter activity, neither in myoblasts nor in myotubes (Figure 31). These results indicate that PKA, PP2A and PP2B (calcineurin) are able to modify the phosphorylation status of CREB-1 in muscle cells, but reducing the calcineurin dephosphorylating step was the only signal, which slightly induced the cytochrome *c* promoter activity, probably via increased CREB-1 phosphorylation. It is known that PP2A, PP2B and PKA have several other substrates beside CREB-1, thus for changing the activity of the cytochrome *c* promoter other transcription factors may be needed, which could be regulated as well via posttranslational modifications such as phosphorylation.

Protein kinase A was the first identified enzyme mediating CREB-1 phosphorylation triggered by the increase of cAMP [48]. Later on, new observations suggested that not just kinases but also phosphatases are involved in regulating CREB-1 phosphorylation and transcriptional activity independently of the level of cAMP. Besides mediating CREB-1 phosphorylation, these proteins participate in the regulation of myogenesis as well. Initially Okadaic acid treatment was shown to block the differentiation of C2C12 cells, when applied in a concentration of 62 nM, which is thought to decrease the activity of PP1 phosphatase. A lower concentration (6 nM) only counteracting with the activity of PP2A did not affect the

differentiation status of the cells [126]. The 5 nM maximum concentration, which was used in our study is thus thought to alter only the activity of PP2A, leaving PP1 unaffected [126]. In contrast to the altered cell morphology and the increased Ser-133 phosphorylation, 5 nM Okadaic acid did not modify the expression of cytochrome *c* promoter indicating that PP2A dephosphorylation of CREB-1 does not play a crucial role in the transcriptional activity of CREB-1 in these muscle cells. This idea correlates with the results of Alberts *et al.* who showed that in the NIH3T3 cell line PP1, but not PP2A is the main phosphatase, which alters the phosphorylation status and transcriptional activity of CREB-1 [127]. In contrast, another study indicated that in liver nuclear extracts PP2A is responsible for the dephosphorylation of CREB-1 and that it has 30 times higher activity than PP1 [128]. Zákány *et al.* also showed that 20 nM Okadaic acid treatment, which is supposed to block PP2A activity, increased the Ser-133 phosphorylation of CREB-1 in chicken limb bud cell cultures [129]. Recently, a new proteosomal targeting motif was identified in the amino acid sequence of CREB-1 and was shown to regulate CREB-1 degradation via serine phosphorylation and ubiquitination. 1 nM Okadaic acid was detected to increase the overall serine phosphorylation of CREB-1 contributing to the phosphorylation status of Ser-133, the proteosomal targeting motif and other motifs. These authors postulated that PP1 is the phosphatase responsible for CREB-1 dephosphorylation [130].

In conclusion, both PP1 and PP2A phosphatases are able to dephosphorylate the Ser-133 phosphate group of CREB-1 in distinct tissues and through this dephosphorylation they change the gene regulation activity of CREB-1. At the concentration of Okadaic acid, which was applied in the present work, the activity of PP2A was inhibited and since this inhibition increased the Ser-133 phosphorylation of CREB-1, this phosphatase seems to be mainly involved in this process in our cells.

Calcineurin (PP2B) was also shown to be able to dephosphorylate CREB-1. It was observed to regulate Ser phosphorylation of the NMDA glutamate receptor, and via this pathway increased phosphorylation of Erk1/2 and CREB-1 was detected in the presence of the calcineurin inhibitor Cyclosporin A in neurons of rat striatum [131]. In C2C12 cells, 5 μM Cyclosporin A enhanced the level of Ser-133 phosphorylated CREB-1 indicating that calcineurin could be an upstream CREB-1 modifier in muscle cells as well [132]. Calcineurin not only regulates the phosphorylation status of CREB-1 but is also involved in the muscle differentiation program. Calcineurin phosphatase activity was demonstrated to be temporally induced at the onset of muscle differentiation in C2C12 cells. Overexpression of calcineurin enhanced the number as well as the myosin heavy chain expression of differentiated myotubes. [133]. In other studies, calcineurin was demonstrated to induce myogenin and myosin heavy chain expression of C2C12

cells [134]. This effect of calcineurin was also detected in primary myoblast cultures and L6 myoblasts investigated by Friday *et al.* [91]. Nuclear factor of activated T cells (NFATc3) and myocyte enhancer factor (MEF2) are other transcription factors regulated by calcineurin [133,135]. In C2C12 cells, MEF2 was demonstrated to be activated by calcineurin and by this mechanism calcineurin also induced the promoter of PGC-1α, a transcriptional coactivator, postulated to participate in the transcriptional complex of the cytochrome *c* promoter as well. However, in this cell line PGC-1α is absent and is thus not a good candidate to be involved in transcriptional regulation [125]. A conservative CRE sequence was also found in the promoter of PGC-1α and the result of this study indicates that CaMKIV regulates the promoter upon activation of CREB-1 [135]. These observations suggest that during enhanced intracellular calcium concentration both CaMKIV and calcineurin are activated and work synergistically and/or additively together causing elevated PGC-1α promoter activity via CREB-1 and MEF2, respectively. A-CREB transfection of C2C12 cells showed a decreased PGC-1α promoter activation through CaMKIV and calcineurin, which indicates that CREB-1 is indeed a crucial factor for the transactivation of the PGC-1α promoter [135]. In addition, calcineurin was shown to regulate the expression of PGC-1α promoter constructs transfected into rat *tibialis anterior* muscle as well. However, overexpression of a constitutive form of calcineurin did not enhance the expression of the cytochrome *c* promoter fragment –326 to +863 [136], which is shorter upstream but longer downstream than the promoter sequence used in our study (–631 to +135) (Figure 2A). These results suggest that PGC-1α is a good candidate as a transcriptional mediator regulated by calcineurin, although the cytochrome *c* promoter construct analyzed in this study [136] lacks possible *cis*-elements, which could participate in the PGC-1α controlled mechanisms. The rat cytochrome *c* promoter, used in our study, was investigated by a transcription factor binding site analysis software (Genomatix, MatInspector) [31] and Figure 2A illustrates the *cis*-elements, which are thought to be involved in muscle specific transcription. According to this analysis, a MEF3 binding site is identified in the cytochrome *c* promoter at –355 to –344, which is missing from the promoter sequence studied by Guerfali *et al.* [136]. Since calcineurin modulates the transcriptional activity of MEF2 it could be possible that MEF3 is also a substrate for calcineurin and in the absence of a MEF3 *cis*-element, calcineurin is not able to modify the cytochrome *c* promoter activity. Xu *et al.* demonstrated that calcineurin indeed transactivates an artificial promoter containing a MEF3 binding site, although it activated the myogenin promoter in the absence of a MEF3 *cis*-element as well [134]. This shows that CREB-1 is not the only transcription factor regulated by calcineurin, and transcription factors binding to MEF3 site could be also crucial in the transactivation of the cytochrome *c* promoter.

The fact that the cytochrome *c* promoter does not contain any MEF2 *cis*-element consolidates the possible importance of MEF3 sequence.

In conclusion, CREB-1 is definitely involved in the regulation of the cytochrome *c* promoter. The enzymes, which modulate the phosphorylation status of CREB-1, are not completely identified, but PKA, PP2A and calcineurin are good candidates since they are able to alter the phosphorylation of CREB-1. As blocking the activity of PP2B increases the phosphorylation of CREB-1 (Figure 29 and 30B) and the cytochrome *c* promoter activity (Figure 31A), as well as the fact that calcineurin is postulated to regulate muscle differentiation, this phosphatase could be a possible key enzyme modulating the effect of CREB-1 in the process of mitochondrial biogenesis in myogenic cells.

6 Appendix

Appendix Figure 1. Cloning procedures of AMPKα1-CA into pTRE2Hyg vector

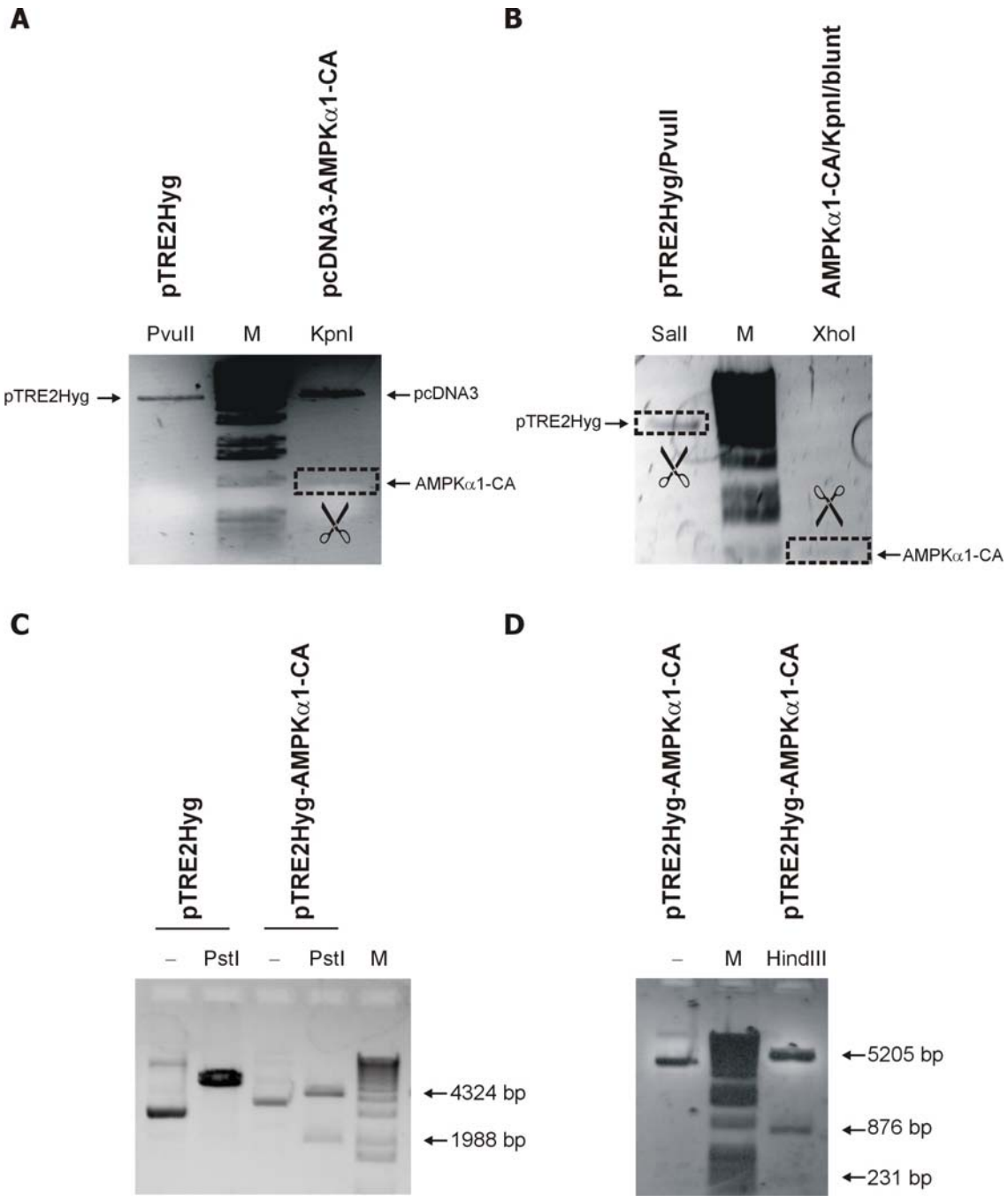

A and ***B*** pTRE2Hyg and pcDNA3-AMPKα1-CA constructs were digested with the illustrated restriction enzymes, and the digested DNA fragments were isolated from the gel (dashed rectangles and scissors). ***C*** and ***D*** Test digestions of the pTRE2Hyg-AMPKα1-CA construct verify the presence of AMPKα1-CA insert. The pTRE2Hyg-AMPKα1-CA construct or the empty vector was incubated with the illustrated restriction enzymes or in their absence (–). M: Molecular weight marker.

Appendix Figure 2. Western blot analysis of AMPKα1-CA clones

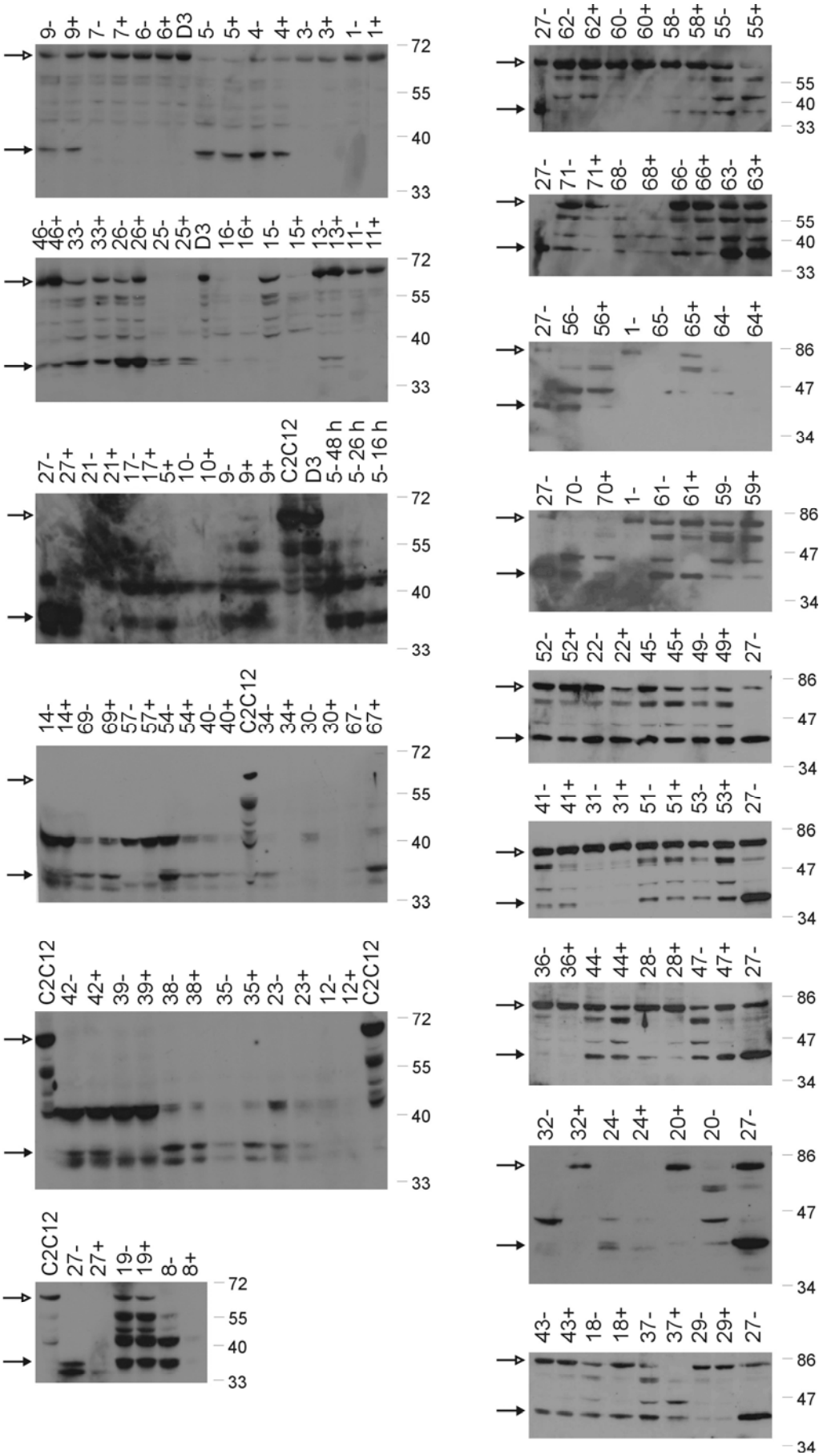

Western blot analysis was performed from protein extracts of AMPKα1-CA expressing C2C12 D3 clones in the presence (+) or absence (–) of doxycycline. C2C12, C2C12 D3 or the CA-1 clone, which turned out to be not expressing the protein of interest and served as negative controls, CA-27 clone as positive (AMPKα1-CA expressing) control. Whitehead arrow shows the endogenous AMPKα and blackhead arrow the AMPKα1-CA proteins. The size of molecular weight markers is given in kDa.

7 References

1. Millar, AH; Day, D; Whelan, J (**2004**) Mitochondrial Biogenesis and Function in Arabidopsis *The Arabidopsis Book* eds. C.R. Somerville and E.M. Meyerowitz, American Society of Plant Biologists, Rockville, MD doi/10.1199/tab.0105, http://www.aspb.org/publications/arabidopsis/

2. Moyes, CD; Mathieu-Costello, OA; Tsuchiya, N; Filburn, C; Hansford, RG (**1997**) Mitochondrial biogenesis during cellular differentiation *Am.J.Physiol.* **272** C1345-C1351

3. Goffart, S (**2002**) Regulation kernlokalisierter mitochondrialer Gene bei der Muskeldifferenzierung *Dissertation*

4. Putman, CT; Kiricsi, M; Pearcey, J; MacLean, IM; Bamford, JA; Murdoch, GK; Dixon, WT; Pette, D (**2003**) AMPK activation increases uncoupling protein-3 expression and mitochondrial enzyme activities in rat muscle without fibre type transitions *J.Physiol.* **551** 169-178

5. Herzig, RP; Scacco, S; Scarpulla, RC (**2000**) Sequential serum-dependent activation of CREB and NRF-1 leads to enhanced mitochondrial respiration through the induction of cytochrome c *J.Biol.Chem.* **275** 13134-13141

6. Dyall, SD; Brown, MT; Johnson, PJ (**2004**) Ancient invasions: from endosymbionts to organelles *Science* **304** 253-257

7. Margulis, L (**1976**) Genetic and evolutionary consequences of symbiosis *Exp.Parasitol.* **39** 277-349

8. Chan, DC (**2006**) Mitochondria: dynamic organelles in disease, aging, and development *Cell* **125** 1241-1252

9. Ryan, MT and Hoogenraad, NJ (**2007**) Mitochondrial-Nuclear Communications *Annu.Rev.Biochem.*

10. Fernandez-Moreno, MA; Bornstein, B; Petit, N; Garesse, R (**2000**) The pathophysiology of mitochondrial biogenesis: towards four decades of mitochondrial DNA research *Mol.Genet.Metab.* **71** 481-495

11. McBride, HM; Neuspiel, M; Wasiak, S (**2006**) Mitochondria: more than just a powerhouse *Curr.Biol.* **16** R551-R560

12. Cereghetti, GM and Scorrano, L (**2006**) The many shapes of mitochondrial death *Oncogene* **25** 4717-4724

13. Timmis, JN; Ayliffe, MA; Huang, CY; Martin, W (**2004**) Endosymbiotic gene transfer: organelle genomes forge eukaryotic chromosomes *Nat.Rev.Genet.* **5** 123-135

14. Villena, JA; Carmona, MC; Rodriguez, dlC; Rossmeisl, M; Vinas, O; Mampel, T; Iglesias, R; Giralt, M; Villarroya, F (**2002**) Mitochondrial biogenesis in brown adipose tissue is associated with differential expression of transcription regulatory factors *Cell Mol.Life Sci.* **59** 1934-1944

15. Klingenspor, M; Ivemeyer, M; Wiesinger, H; Haas, K; Heldmaier, G; Wiesner, RJ (**1996**) Biogenesis of thermogenic mitochondria in brown adipose tissue of Djungarian hamsters during cold adaptation *Biochem.J.* **316** 607-613

16. Hood, DA (**2001**) Invited Review: contractile activity-induced mitochondrial biogenesis in skeletal muscle *J.Appl.Physiol.* **90** 1137-1157

17. Schultz, J and Wiesner, RJ (**2000**) Proliferation of mitochondria in chronically stimulated rabbit skeletal muscle-transcription of mitochondrial genes and copy number of mitochondrial DNA *J.Bioenerg.Biomembr.* **32** 627-634

18. Hood, DA; Irrcher, I; Ljubicic, V; Joseph, AM (**2006**) Coordination of metabolic plasticity in skeletal muscle *J.Exp.Biol.* **209** 2265-2275

19. Porter, GA, Jr.; Makuck, RF; Rivkees, SA (**2002**) Reduction in intracellular calcium levels inhibits myoblast differentiation *J.Biol.Chem.* **277** 28942-28947

20. Ojuka, EO; Jones, TE; Han, DH; Chen, M; Wamhoff, BR; Sturek, M; Holloszy, JO (**2002**) Intermittent increases in cytosolic Ca2+ stimulate mitochondrial biogenesis in muscle cells *Am.J.Physiol Endocrinol.Metab.* **283** E1040-E1045

21. Ojuka, EO; Jones, TE; Han, DH; Chen, M; Holloszy, JO (**2003**) Raising Ca2+ in L6 myotubes mimics effects of exercise on mitochondrial biogenesis in muscle *FASEB J.* **17** 675-681

22. Freyssenet, D; Irrcher, I; Connor, MK; Di Carlo, M; Hood, DA (**2004**) Calcium-regulated changes in mitochondrial phenotype in skeletal muscle cells *Am.J.Physiol Cell Physiol.* **286** C1053-C1061

23. Kubis, HP; Haller, EA; Wetzel, P; Gros, G (**1997**) Adult fast myosin pattern and Ca2+-induced slow myosin pattern in primary skeletal muscle culture *Proc.Natl.Acad.Sci.U.S.A* **94** 4205-4210

24. Kubis, HP; Hanke, N; Scheibe, RJ; Meissner, JD; Gros, G (**2003**) Ca2+ transients activate calcineurin/NFATc1 and initiate fast-to-slow transformation in a primary skeletal muscle culture *Am.J.Physiol.Cell Physiol.* **285** C56-C63

25. Maniura-Weber, K; Goffart, S; Garstka, HL; Montoya, J; Wiesner, RJ (**2004**) Transient overexpression of mitochondrial transcription factor A (TFAM) is sufficient to stimulate mitochondrial DNA transcription, but not sufficient to increase mtDNA copy number in cultured cells *Nucleic Acids Res.* **32** 6015-6027

26. Hickson, RC; Hammons, GT; Holoszy, JO (**1979**) Development and regression of exercise-induced cardiac hypertrophy in rats *Am.J.Physiol.* **236** H268-H272

27. Booth, FW (**1991**) Cytochrome c protein synthesis rate in rat skeletal muscle *J.Appl.Physiol.* **71** 1225-1230

28. Winder, WW; Baldwin, KM; Holloszy, JO (**1974**) Enzymes involved in ketone utilization in different types of muscle: adaptation to exercise *Eur.J.Biochem.* **47** 461-467

29. Evans, MJ and Scarpulla, RC (**1989**) Interaction of nuclear factors with multiple sites in the somatic cytochrome c promoter. Characterization of upstream NRF-1, ATF, and intron Sp1 recognition sequences *J.Biol.Chem.* **264** 14361-14368

30. Gopalakrishnan, L and Scarpulla, RC (**1994**) Differential regulation of respiratory chain subunits by a CREB-dependent signal transduction pathway. Role of cyclic AMP in cytochrome c and COXIV gene expression *J.Biol.Chem.* **269** 105-113

31. Cartharius, K; Frech, K; Grote, K; Klocke, B; Haltmeier, M; Klingenhoff, A; Frisch, M; Bayerlein, M; Werner, T (**2005**) MatInspector and beyond: promoter analysis based on transcription factor binding sites *Bioinformatics* **21** 2933-2942

32. Franko, A; Mercy, L; Arnould, T; Mayer, S; Thiel, G; Wiesner, RJ; Goffart, S (**2007**) CREB-1 binds to and mediates upregulation of the cytochrome c promoter during mitochondrial biogenesis accompanying skeletal muscle differentiation *in preparation*

33. Hardie, DG; Carling, D; Carlson, M (**1998**) The AMP-activated/SNF1 protein kinase subfamily: metabolic sensors of the eukaryotic cell? *Annu.Rev.Biochem.* **67** 821-855

34. Kahn, BB; Alquier, T; Carling, D; Hardie, DG (**2005**) AMP-activated protein kinase: ancient energy gauge provides clues to modern understanding of metabolism *Cell Metab.* **1** 15-25

35. Zhou, M; Lin, BZ; Coughlin, S; Vallega, G; Pilch, PF (**2000**) UCP-3 expression in skeletal muscle: effects of exercise, hypoxia, and AMP-activated protein kinase *Am.J.Physiol.Endocrinol.Metab.* **279** E622-E629

36. Winder, WW; Holmes, BF; Rubink, DS; Jensen, EB; Chen, M; Holloszy, JO (**2000**) Activation of AMP-activated protein kinase increases mitochondrial enzymes in skeletal muscle *J.Appl.Physiol.* **88** 2219-2226

37. Bergeron, R; Ren, JM; Cadman, KS; Moore, IK; Perret, P; Pypaert, M; Young, LH; Semenkovich, CF; Shulman, GI (**2001**) Chronic activation of AMP kinase results in NRF-1 activation and mitochondrial biogenesis *Am.J.Physiol.Endocrinol.Metab.* **281** E1340-E1346

38. Corton, JM; Gillespie, JG; Hardie, DG (**1994**) Role of the AMP-activated protein kinase in the cellular stress response *Curr.Biol.* **4** 315-324

39. Young, ME; Radda, GK; Leighton, B (**1996**) Activation of glycogen phosphorylase and glycogenolysis in rat skeletal muscle by AICAR--an activator of AMP-activated protein kinase *FEBS Lett.* **382** 43-47

40. Stein, SC; Woods, A; Jones, NA; Davison, MD; Carling, D (**2000**) The regulation of AMP-activated protein kinase by phosphorylation *Biochem.J.* **345** 437-443

41. Barnes, K; Ingram, JC; Porras, OH; Barros, LF; Hudson, ER; Fryer, LG; Foufelle, F; Carling, D; Hardie, DG; Baldwin, SA (**2002**) Activation of GLUT1 by metabolic and osmotic stress: potential involvement of AMP-activated protein kinase (AMPK) *J.Cell Sci.* **115** 2433-2442

42. Fryer, LG; Foufelle, F; Barnes, K; Baldwin, SA; Woods, A; Carling, D (**2002**) Characterization of the role of the AMP-activated protein kinase in the stimulation of glucose transport in skeletal muscle cells *Biochem.J.* **363** 167-174

43. Cidad, P; Almeida, A; Bolanos, JP (**2004**) Inhibition of mitochondrial respiration by nitric oxide rapidly stimulates cytoprotective GLUT3-mediated glucose uptake through 5'-AMP-activated protein kinase *Biochem.J.* **384** 629-636

44. Mu, J; Brozinick, JT, Jr.; Valladares, O; Bucan, M; Birnbaum, MJ (**2001**) A role for AMP-activated protein kinase in contraction- and hypoxia-regulated glucose transport in skeletal muscle *Mol.Cell* **7** 1085-1094

45. Zong, H; Ren, JM; Young, LH; Pypaert, M; Mu, J; Birnbaum, MJ; Shulman, GI (**2002**) AMP kinase is required for mitochondrial biogenesis in skeletal muscle in response to chronic energy deprivation *Proc.Natl.Acad.Sci.U.S.A* **99** 15983-15987

46. Viollet, B; Andreelli, F; Jorgensen, SB; Perrin, C; Flamez, D; Mu, J; Wojtaszewski, JF; Schuit, FC; Birnbaum, M; Richter, E; Burcelin, R; Vaulont, S (**2003**) Physiological role of AMP-activated protein kinase (AMPK): insights from knockout mouse models *Biochem.Soc.Trans.* **31** 216-219

47. Jorgensen, SB; Viollet, B; Andreelli, F; Frosig, C; Birk, JB; Schjerling, P; Vaulont, S; Richter, EA; Wojtaszewski, JF (**2004**) Knockout of the alpha2 but not alpha1 5'-AMP-activated protein kinase isoform abolishes 5-aminoimidazole-4-carboxamide-1-beta-4-ribofuranosidebut not contraction-induced glucose uptake in skeletal muscle *J.Biol.Chem.* **279** 1070-1079

48. Shaywitz, AJ and Greenberg, ME (**1999**) CREB: a stimulus-induced transcription factor activated by a diverse array of extracellular signals *Annu.Rev.Biochem.* **68** 821-861

49. Karpinski, BA; Morle, GD; Huggenvik, J; Uhler, MD; Leiden, JM (**1992**) Molecular cloning of human CREB-2: an ATF/CREB transcription factor that can negatively regulate transcription from the cAMP response element *Proc.Natl.Acad.Sci.U.S.A* **89** 4820-4824

50. Lu, R and Misra, V (**2000**) Potential role for luman, the cellular homologue of herpes simplex virus VP16 (alpha gene trans-inducing factor), in herpesvirus latency *J.Virol.* **74** 934-943

51. Stirling, J and O'hare, P (**2006**) CREB4, a transmembrane bZip transcription factor and potential new substrate for regulation and cleavage by S1P *Mol.Biol.Cell* **17** 413-426

52. Nomura, N; Zu, YL; Maekawa, T; Tabata, S; Akiyama, T; Ishii, S (**1993**) Isolation and characterization of a novel member of the gene family encoding the cAMP response element-binding protein CRE-BP1 *J.Biol.Chem.* **268** 4259-4266

53. Cha-Molstad, H; Keller, DM; Yochum, GS; Impey, S; Goodman, RH (**2004**) Cell-type-specific binding of the transcription factor CREB to the cAMP-response element *Proc.Natl.Acad.Sci.U.S.A* **101** 13572-13577

54. Lonze, BE and Ginty, DD (**2002**) Function and regulation of CREB family transcription factors in the nervous system *Neuron* **35** 605-623

55. Carlezon, WA, Jr.; Duman, RS; Nestler, EJ (**2005**) The many faces of CREB *Trends Neurosci.* **28** 436-445

56. Dwivedi, Y; Rao, JS; Rizavi, HS; Kotowski, J; Conley, RR; Roberts, RC; Tamminga, CA; Pandey, GN (**2003**) Abnormal expression and functional characteristics of cyclic adenosine monophosphate response element binding protein in postmortem brain of suicide subjects *Arch.Gen.Psychiatry* **60** 273-282

57. Rudolph, D; Tafuri, A; Gass, P; Hammerling, GJ; Arnold, B; Schutz, G (**1998**) Impaired fetal T cell development and perinatal lethality in mice lacking the cAMP response element binding protein *Proc.Natl.Acad.Sci.U.S.A* **95** 4481-4486

58. Mantamadiotis, T; Lemberger, T; Bleckmann, SC; Kern, H; Kretz, O; Martin, VA; Tronche, F; Kellendonk, C; Gau, D; Kapfhammer, J; Otto, C; Schmid, W; Schutz, G (**2002**) Disruption of CREB function in brain leads to neurodegeneration *Nat.Genet.* **31** 47-54

59. Reusch, JE; Colton, LA; Klemm, DJ (**2000**) CREB activation induces adipogenesis in 3T3-L1 cells *Mol.Cell Biol.* **20** 1008-1020

60. Klemm, DJ; Leitner, JW; Watson, P; Nesterova, A; Reusch, JE; Goalstone, ML; Draznin, B (**2001**) Insulin-induced adipocyte differentiation. Activation of CREB rescues adipogenesis from the arrest caused by inhibition of prenylation *J.Biol.Chem.* **276** 28430-28435

61. Reusch, JE and Klemm, DJ (**2002**) Inhibition of cAMP-response element-binding protein activity decreases protein kinase B/Akt expression in 3T3-L1 adipocytes and induces apoptosis *J.Biol.Chem.* **277** 1426-1432

62. Herzig, S; Long, F; Jhala, US; Hedrick, S; Quinn, R; Bauer, A; Rudolph, D; Schutz, G; Yoon, C; Puigserver, P; Spiegelman, B; Montminy, M (**2001**) CREB regulates hepatic gluconeogenesis through the coactivator PGC-1 *Nature* **413** 179-183

63. Herzig, S; Hedrick, S; Morantte, I; Koo, SH; Galimi, F; Montminy, M (**2003**) CREB controls hepatic lipid metabolism through nuclear hormone receptor PPAR-gamma *Nature* **426** 190-193

64. Magenta, A; Cenciarelli, C; De Santa, F; Fuschi, P; Martelli, F; Caruso, M; Felsani, A (**2003**) MyoD stimulates RB promoter activity via the CREB/p300 nuclear transduction pathway *Mol.Cell Biol.* **23** 2893-2906

65. Chen, AE; Ginty, DD; Fan, CM (**2005**) Protein kinase A signalling via CREB controls myogenesis induced by Wnt proteins *Nature* **433** 317-322

66. Wrutniak-Cabello, C; Casas, F; Cabello, G (**2001**) Thyroid hormone action in mitochondria *J.Mol.Endocrinol.* **26** 67-77

67. Arnould, T; Vankoningsloo, S; Renard, P; Houbion, A; Ninane, N; Demazy, C; Remacle, J; Raes, M (**2002**) CREB activation induced by mitochondrial dysfunction is a new signaling pathway that impairs cell proliferation *EMBO J.* **21** 53-63

68. Mercy, L; Pauw, A; Payen, L; Tejerina, S; Houbion, A; Demazy, C; Raes, M; Renard, P; Arnould, T (**2005**) Mitochondrial biogenesis in mtDNA-depleted cells involves a Ca2+-dependent pathway and a reduced mitochondrial protein import *FEBS J.* **272** 5031-5055

69. Vankoningsloo, S; De Pauw, A; Houbion, A; Tejerina, S; Demazy, C; de Longueville, F; Bertholet, V; Renard, P; Remacle, J; Holvoet, P; Raes, M; Arnould, T (**2006**) CREB activation induced by mitochondrial dysfunction triggers triglyceride accumulation in 3T3-L1 preadipocytes *J.Cell Sci.* **119** 1266-1282

70. Louet, JF; Hayhurst, G; Gonzalez, FJ; Girard, J; Decaux, JF (**2002**) The coactivator PGC-1 is involved in the regulation of the liver carnitine palmitoyltransferase I gene

expression by cAMP in combination with HNF4 alpha and cAMP-response element-binding protein (CREB) *J.Biol.Chem.* **277** 37991-38000

71. Conkright, MD; Canettieri, G; Screaton, R; Guzman, E; Miraglia, L; Hogenesch, JB; Montminy, M (**2003**) TORCs: transducers of regulated CREB activity *Mol.Cell* **12** 413-423

72. Bittinger, MA; McWhinnie, E; Meltzer, J; Iourgenko, V; Latario, B; Liu, X; Chen, CH; Song, C; Garza, D; Labow, M (**2004**) Activation of cAMP response element-mediated gene expression by regulated nuclear transport of TORC proteins *Curr.Biol.* **14** 2156-2161

73. Wu, Z; Huang, X; Feng, Y; Handschin, C; Feng, Y; Gullicksen, PS; Bare, O; Labow, M; Spiegelman, B; Stevenson, SC (**2006**) Transducer of regulated CREB-binding proteins (TORCs) induce PGC-1alpha transcription and mitochondrial biogenesis in muscle cells *Proc.Natl.Acad.Sci.U.S.A* **103** 14379-14384

74. Andersson, U and Scarpulla, RC (**2001**) Pgc-1-related coactivator, a novel, serum-inducible coactivator of nuclear respiratory factor 1-dependent transcription in mammalian cells *Mol.Cell Biol.* **21** 3738-3749

75. Vercauteren, K; Pasko, RA; Gleyzer, N; Marino, VM; Scarpulla, RC (**2006**) PGC-1-related coactivator: immediate early expression and characterization of a CREB/NRF-1 binding domain associated with cytochrome c promoter occupancy and respiratory growth *Mol.Cell Biol.* **26** 7409-7419

76. Schuh, RA; Kristian, T; Fiskum, G (**2005**) Calcium-dependent dephosphorylation of brain mitochondrial calcium/cAMP response element binding protein (CREB) *J.Neurochem.* **92** 388-394

77. Lee, J; Kim, CH; Simon, DK; Aminova, LR; Andreyev, AY; Kushnareva, YE; Murphy, AN; Lonze, BE; Kim, KS; Ginty, DD; Ferrante, RJ; Ryu, H; Ratan, RR (**2005**) Mitochondrial cyclic AMP response element-binding protein (CREB) mediates mitochondrial gene expression and neuronal survival *J.Biol.Chem.* **280** 40398-40401

78. Platenik, J; Balcar, VJ; Yoneda, Y; Mioduszewska, B; Buchal, R; Hynek, R; Kilianek, L; Kuramoto, N; Wilczynski, G; Ogita, K; Nakamura, Y; Kaczmarek, L (**2005**) Apparent presence of Ser133-phosphorylated cyclic AMP response element binding protein (pCREB) in brain mitochondria is due to cross-reactivity of pCREB antibodies with pyruvate dehydrogenase *J.Neurochem.* **95** 1446-1460

79. Woodcock, DM; Crowther, PJ; Doherty, J; Jefferson, S; DeCruz, E; Noyer-Weidner, M; Smith, SS; Michael, MZ; Graham, MW (**1989**) Quantitative evaluation of Escherichia coli host strains for tolerance to cytosine methylation in plasmid and phage recombinants *Nucleic Acids Res.* **17** 3469-3478

80. Yaffe, D and Saxel, O (**1977**) Serial passaging and differentiation of myogenic cells isolated from dystrophic mouse muscle *Nature* **270** 725-727

81. Gossen, M and Bujard, H (**1992**) Tight control of gene expression in mammalian cells by tetracycline-responsive promoters *Proc.Natl.Acad.Sci.U.S.A* **89** 5547-5551

82. Bradford, MM (**1976**) A rapid and sensitive method for the quantitation of microgram quantities of protein utilizing the principle of protein-dye binding *Anal.Biochem.* **72** 248-254

83. Laemmli, UK (**1970**) Cleavage of structural proteins during the assembly of the head of bacteriophage T4 *Nature* **227** 680-685

84. Berkes, CA and Tapscott, SJ (**2005**) MyoD and the transcriptional control of myogenesis *Semin.Cell Dev.Biol.* **16** 585-595

85. Freyssenet, D; Di Carlo, M; Hood, DA (**1999**) Calcium-dependent regulation of cytochrome c gene expression in skeletal muscle cells. Identification of a protein kinase c-dependent pathway *J.Biol.Chem.* **274** 9305-9311

86. Wu, H; Kanatous, SB; Thurmond, FA; Gallardo, T; Isotani, E; Bassel-Duby, R; Williams, RS (**2002**) Regulation of mitochondrial biogenesis in skeletal muscle by CaMK *Science* **296** 349-352

87. Goffart, S; Franko, A; Clemen, CS; Wiesner, RJ (**2006**) alpha-Actinin 4 and BAT1 interaction with the Cytochrome c promoter upon skeletal muscle differentiation *Curr.Genet.* **49** 125-135

88. Pei, L; Dodson, R; Schoderbek, WE; Maurer, RA; Mayo, KE (**1991**) Regulation of the alpha inhibin gene by cyclic adenosine 3',5'-monophosphate after transfection into rat granulosa cells *Mol.Endocrinol.* **5** 521-534

89. Sabourin, LA and Rudnicki, MA (**2000**) The molecular regulation of myogenesis *Clin.Genet.* **57** 16-25

90. Devlin, RB and Emerson, CP, Jr. (**1978**) Coordinate regulation of contractile protein synthesis during myoblast differentiation *Cell* **13** 599-611

91. Friday, BB; Horsley, V; Pavlath, GK (**2000**) Calcineurin activity is required for the initiation of skeletal muscle differentiation *J.Cell Biol.* **149** 657-666

92. Schollmeyer, JE (**1986**) Role of Ca2+ and Ca2+-activated protease in myoblast fusion *Exp.Cell Res.* **162** 411-422

93. Arnaudeau, S; Holzer, N; Konig, S; Bader, CR; Bernheim, L (**2006**) Calcium sources used by post-natal human myoblasts during initial differentiation *J.Cell Physiol.* **208** 435-445

94. Lee, KH; Park, JY; Kim, K (**2004**) NMDA receptor-mediated calcium influx plays an essential role in myoblast fusion *FEBS Lett.* **578** 47-52

95. Challet, C; Maechler, P; Wollheim, CB; Ruegg, UT (**2001**) Mitochondrial calcium oscillations in C2C12 myotubes *J.Biol.Chem.* **276** 3791-3797

96. Sreter, FA; Lopez, JR; Alamo, L; Mabuchi, K; Gergely, J (**1987**) Changes in intracellular ionized Ca concentration associated with muscle fiber type transformation *Am.J.Physiol.* **253** C296-C300

97. Carroll, S; Nicotera, P; Pette, D (**1999**) Calcium transients in single fibers of low-frequency stimulated fast-twitch muscle of rat *Am.J.Physiol.* **277** C1122-C1129

98. Moudy, AM; Handran, SD; Goldberg, MP; Ruffin, N; Karl, I; Kranz-Eble, P; DeVivo, DC; Rothman, SM (**1995**) Abnormal calcium homeostasis and mitochondrial polarization in a human encephalomyopathy *Proc.Natl.Acad.Sci.U.S.A* **92** 729-733

99. Biswas, G; Adebanjo, OA; Freedman, BD; Anandatheerthavarada, HK; Vijayasarathy, C; Zaidi, M; Kotlikoff, M; Avadhani, NG (**1999**) Retrograde Ca2+ signaling in C2C12 skeletal myocytes in response to mitochondrial genetic and metabolic stress: a novel mode of inter-organelle crosstalk *EMBO J.* **18** 522-533

100. Araki, N; Hatae, T; Yamada, T; Hirohashi, S (**2000**) Actinin-4 is preferentially involved in circular ruffling and macropinocytosis in mouse macrophages: analysis by fluorescence ratio imaging *J.Cell Sci.* **113** 3329-3340

101. Hegmans, JP; Bard, MP; Hemmes, A; Luider, TM; Kleijmeer, MJ; Prins, JB; Zitvogel, L; Burgers, SA; Hoogsteden, HC; Lambrecht, BN (**2004**) Proteomic analysis of exosomes secreted by human mesothelioma cells *Am.J.Pathol.* **164** 1807-1815

102. Honda, K; Yamada, T; Endo, R; Ino, Y; Gotoh, M; Tsuda, H; Yamada, Y; Chiba, H; Hirohashi, S (**1998**) Actinin-4, a novel actin-bundling protein associated with cell motility and cancer invasion *J.Cell Biol.* **140** 1383-1393

103. Kigawa, A; Wakui, H; Maki, N; Okuyama, S; Masai, R; Ohtani, H; Komatsuda, A; Suzuki, D; Toyoda, M; Kobayashi, R; Sawada, K (**2004**) Interaction of the spectrin-like repeats of alpha-actinin-4 with humanin peptide *Clin.Exp.Nephrol.* **8** 331-338

104. Huang, SM; Huang, CJ; Wang, WM; Kang, JC; Hsu, WC (**2004**) The enhancement of nuclear receptor transcriptional activation by a mouse actin-binding protein, alpha actinin 2 *J.Mol.Endocrinol.* **32** 481-496

105. Sommer B; Dalle B; Rinsch C; Beuzard Y; Deglon N; Aebischer P (**1999**) Tightly regulated long-term delivery of erythropoietin *in vivo* using encapsulated C2C12 cells *NFP37 Somatic Gene Therapy Annual Meeting*

106. Sommer, B; Rinsch, C; Payen, E; Dalle, B; Schneider, B; Deglon, N; Henri, A; Beuzard, Y; Aebischer, P (**2002**) Long-term doxycycline-regulated secretion of erythropoietin by encapsulated myoblasts *Mol.Ther.* **6** 155-161

107. Meyer-Ficca, ML; Meyer, RG; Kaiser, H; Brack, AR; Kandolf, R; Kupper, JH (**2004**) Comparative analysis of inducible expression systems in transient transfection studies *Anal.Biochem.* **334** 9-19

108. Woods, A; Azzout-Marniche, D; Foretz, M; Stein, SC; Lemarchand, P; Ferre, P; Foufelle, F; Carling, D (**2000**) Characterization of the role of AMP-activated protein kinase in the regulation of glucose-activated gene expression using constitutively active and dominant negative forms of the kinase *Mol.Cell Biol.* **20** 6704-6711

109. Yamamoto, KK; Gonzalez, GA; Menzel, P; Rivier, J; Montminy, MR (**1990**) Characterization of a bipartite activator domain in transcription factor CREB *Cell* **60** 611-617

110. Berkowitz, LA and Gilman, MZ (**1990**) Two distinct forms of active transcription factor CREB (cAMP response element binding protein) *Proc.Natl.Acad.Sci.U.S.A* **87** 5258-5262

111. Ruppert, S; Cole, TJ; Boshart, M; Schmid, E; Schutz, G (**1992**) Multiple mRNA isoforms of the transcription activator protein CREB: generation by alternative splicing and specific expression in primary spermatocytes *EMBO J.* **11** 1503-1512

112. Waeber, G and Habener, JF (**1991**) Nuclear translocation and DNA recognition signals colocalized within the bZIP domain of cyclic adenosine 3',5'-monophosphate response element-binding protein CREB *Mol.Endocrinol.* **5** 1431-1438

113. Sakai, N; Tolbert, LM; Duman, RS (**1999**) Identification and functional analysis of novel cAMP response element binding protein splice variants lacking the basic/leucine zipper domain *Mol.Pharmacol.* **56** 917-925

114. Bartsch, D; Casadio, A; Karl, KA; Serodio, P; Kandel, ER (**1998**) CREB1 encodes a nuclear activator, a repressor, and a cytoplasmic modulator that form a regulatory unit critical for long-term facilitation *Cell* **95** 211-223

115. Hummler, E; Cole, TJ; Blendy, JA; Ganss, R; Aguzzi, A; Schmid, W; Beermann, F; Schutz, G (**1994**) Targeted mutation of the CREB gene: compensation within the CREB/ATF family of transcription factors *Proc.Natl.Acad.Sci.U.S.A* **91** 5647-5651

116. Blendy, JA; Kaestner, KH; Schmid, W; Gass, P; Schutz, G (**1996**) Targeting of the CREB gene leads to up-regulation of a novel CREB mRNA isoform *EMBO J.* **15** 1098-1106

117. Glazewski, S; Barth, AL; Wallace, H; McKenna, M; Silva, A; Fox, K (**1999**) Impaired experience-dependent plasticity in barrel cortex of mice lacking the alpha and delta isoforms of CREB *Cereb.Cortex* **9** 249-256

118. Pandey, SC; Mittal, N; Silva, AJ (**2000**) Blockade of cyclic AMP-responsive element DNA binding in the brain of CREB delta/alpha mutant mice *Neuroreport* **11** 2577-2580

119. Blom, JM; Tascedda, F; Carra, S; Ferraguti, C; Barden, N; Brunello, N (**2002**) Altered regulation of CREB by chronic antidepressant administration in the brain of transgenic mice with impaired glucocorticoid receptor function *Neuropsychopharmacology* **26** 605-614

120. Sakai, N; Thome, J; Newton, SS; Chen, J; Kelz, MB; Steffen, C; Nestler, EJ; Duman, RS (**2002**) Inducible and brain region-specific CREB transgenic mice *Mol.Pharmacol.* **61** 1453-1464

121. Hoeffler, JP; Meyer, TE; Waeber, G; Habener, JF (**1990**) Multiple adenosine 3',5'-cyclic [corrected] monophosphate response element DNA-binding proteins generated by gene diversification and alternative exon splicing *Mol.Endocrinol.* **4** 920-930

122. Sato, K; Suematsu, A; Nakashima, T; Takemoto-Kimura, S; Aoki, K; Morishita, Y; Asahara, H; Ohya, K; Yamaguchi, A; Takai, T; Kodama, T; Chatila, TA; Bito, H; Takayanagi, H (**2006**) Regulation of osteoclast differentiation and function by the CaMK-CREB pathway *Nat.Med.* **12** 1410-1416

123. Blom, N; Sicheritz-Ponten, T; Gupta, R; Gammeltoft, S; Brunak, S (**2004**) Prediction of post-translational glycosylation and phosphorylation of proteins from the amino acid sequence *Proteomics* **4** 1633-1649

124. Gau, D; Lemberger, T; von Gall, C; Kretz, O; Le Minh, N; Gass, P; Schmid, W; Schibler, U; Korf, HW; Schutz, G (**2002**) Phosphorylation of CREB Ser142 regulates light-induced phase shifts of the circadian clock *Neuron* **34** 245-253

125. Lagouge, M; Argmann, C; Gerhart-Hines, Z; Meziane, H; Lerin, C; Daussin, F; Messadeq, N; Milne, J; Lambert, P; Elliott, P; Geny, B; Laakso, M; Puigserver, P; Auwerx, J (**2006**) Resveratrol improves mitochondrial function and protects against metabolic disease by activating SIRT1 and PGC-1alpha *Cell* **127** 1109-1122

126. Park, K; Chung, M; Kim, SJ (**1992**) Inhibition of myogenesis by okadaic acid, an inhibitor of protein phosphatases, 1 and 2A, correlates with the induction of AP1 *J.Biol.Chem.* **267** 10810-10815

127. Alberts, AS; Montminy, M; Shenolikar, S; Feramisco, JR (**1994**) Expression of a peptide inhibitor of protein phosphatase 1 increases phosphorylation and activity of CREB in NIH 3T3 fibroblasts *Mol.Cell Biol.* **14** 4398-4407

128. Wadzinski, BE; Wheat, WH; Jaspers, S; Peruski, LF, Jr.; Lickteig, RL; Johnson, GL; Klemm, DJ (**1993**) Nuclear protein phosphatase 2A dephosphorylates protein kinase A-phosphorylated CREB and regulates CREB transcriptional stimulation *Mol.Cell Biol.* **13** 2822-2834

129. Zakany, R; Szucs, K; Bako, E; Felszeghy, S; Czifra, G; Biro, T; Modis, L; Gergely, P (**2002**) Protein phosphatase 2A is involved in the regulation of protein kinase A signaling pathway during in vitro chondrogenesis *Exp.Cell Res.* **275** 1-8

130. Taylor, CT; Furuta, GT; Synnestvedt, K; Colgan, SP (**2000**) Phosphorylation-dependent targeting of cAMP response element binding protein to the ubiquitin/proteasome pathway in hypoxia *Proc.Natl.Acad.Sci.U.S.A* **97** 12091-12096

131. Choe, ES; Shin, EH; Wang, JQ (**2005**) Inhibition of protein phosphatase 2B upregulates serine phosphorylation of N-methyl-D-aspartate receptor NR1 subunits in striatal neurons in vivo *Neurosci.Lett.* **384** 38-43

132. Zheng, Z; Wang, ZM; Delbono, O (**2004**) Ca(2+) calmodulin kinase and calcineurin mediate IGF-1-induced skeletal muscle dihydropyridine receptor alpha(1S) transcription *J.Membr.Biol.* **197** 101-112

133. Delling, U; Tureckova, J; Lim, HW; De Windt, LJ; Rotwein, P; Molkentin, JD (**2000**) A calcineurin-NFATc3-dependent pathway regulates skeletal muscle differentiation and slow myosin heavy-chain expression *Mol.Cell Biol.* **20** 6600-6611

134. Xu, Q; Yu, L; Liu, L; Cheung, CF; Li, X; Yee, SP; Yang, XJ; Wu, Z (**2002**) p38 Mitogen-activated protein kinase-, calcium-calmodulin-dependent protein kinase-, and calcineurin-mediated signaling pathways transcriptionally regulate myogenin expression *Mol.Biol.Cell* **13** 1940-1952

135. Handschin, C; Rhee, J; Lin, J; Tarr, PT; Spiegelman, BM (**2003**) An autoregulatory loop controls peroxisome proliferator-activated receptor gamma coactivator 1alpha expression in muscle *Proc.Natl.Acad.Sci.U.S.A* **100** 7111-7116

136. Guerfali, I; Manissolle, C; Durieux, AC; Bonnefoy, R; Bartegi, A; Freyssenet, D (**2007**) Calcineurin A and CaMKIV transactivate PGC-1alpha promoter, but differentially regulate cytochrome c promoter in rat skeletal muscle *Pflugers Arch.* **454** 297-305

Erklärung

Ich versichere, dass ich die von mir vorgelegte Dissertation selbständig angefertigt, die benutzten Quellen und Hilfsmittel vollständig angegeben und die Stellen der Arbeit − einschließlich Tabellen, Karten und Abbildungen −, die anderen Werken im Wortlaut oder dem Sinn nach entnommen sind, in jedem Einzelfall als Entlehnung kenntlich gemacht habe; dass diese Dissertation noch keiner anderen Fakultät oder Universität zur Prüfung vorgelegen hat; dass sie − abgesehen von unten angegebenen Teilpublikationen − noch nicht veröffentlicht worden ist sowie, dass ich eine solche Veröffentlichung vor Abschluss des Promotionsverfahrens nicht vornehmen werde.

Die Bestimmungen der Promotionsordnung sind mir bekannt. Die von mir vorgelegte Dissertation ist von Prof. Dr. Rudolf J. Wiesner betreut worden.

Köln den 12. April 2007

8 Acknowledgements

Curriculum vitae